

**Structure and evolution of the northern  
part of the Northeast German Basin  
revealed from seismic interpretation  
and 3D structural modelling**

Dissertation

zur Erlangung des Doktorgrades  
der Naturwissenschaften im Fachbereich  
Geowissenschaften  
der Universität Hamburg

vorgelegt von

**Martin Bak Hansen**

aus

Silkeborg, Dänemark

Hamburg, 2006

Als Dissertation angenommen vom Department für Geowissenschaften  
der Universität Hamburg

Auf Grund der Gutachten von Prof. Dr. Dirk Gajewski  
und Dr. Christian Hübscher

Hamburg, den 24. Januar 2006

Prof. Dr. Kay-Christian Emeis  
Leiter des Departments für Geowissenschaften

# Contents

<b>1. Introduction</b>	<b>1</b>
<b>2. Data Acquisition and Processing</b>	<b>5</b>
2.1 Study Area	5
2.2 Gravimetric Data	6
2.3 Magnetic Data	6
2.4 Multichannel Seismic Data	7
2.4.1 Seismic Sources	8
2.4.2 Seismic Recording System	9
2.4.3 Navigation	10
2.4.4 Data Processing	13
<b>3. The Zechstein Evaporites of the Central European Basin System</b>	<b>19</b>
3.1 Primary Evaporite Deposition	19
3.2 Composition and Physical Properties of Rock Salt	21
3.3 The Late Permian Zechstein Basins	22
<b>4. The Mesozoic – Cenozoic structural framework of the Bay of Kiel area, western Baltic Sea</b>	<b>23</b>
<i>by M. B. Hansen, H. Lykke-Andersen, A. Dehghani, D. Gajewski, C. Hübscher, M. Olesen and K. Reicherter</i>	
<i>Published in International Journal of Earth Sciences, vol. 94, 2005</i>	
4.1 Abstract	23
4.2 Introduction	24
4.3 Geological framework	24
4.4 Database	27
4.4.1 High-resolution multichannel seismic data	27
4.4.2 Well data	29
4.5 Stratigraphic interpretation	29
4.5.1 Sedimentary sequences	29
4.5.2 Seismic stratigraphy	33
4.6 Geological evolution	34
4.6.1 Methods	34
4.6.2 Present day structures	34
4.6.3 Early Triassic (Buntsandstein)	37
4.6.4 Middle Triassic (Muschelkalk)	38
4.6.5 Late Triassic (Keuper)	39
4.6.6 Early Jurassic	41

4.6.7 Middle Jurassic – Early Cretaceous	43
4.6.8 Cretaceous	43
4.6.9 Cenozoic	45
4.7 Discussion and conclusions	48
4.8 Acknowledgements	49
<b>5. Structure and evolution of the northern part of the Northeast German Basin</b>	<b>51</b>
<i>by M. B. Hansen, S. P. Triñanes, H. Lykke-Andersen, C. Hübscher, A. Dehghani and D. Gajewski</i>	
<i>Submitted to Marine and Petroleum Geology, 01/2006</i>	
5.1 Abstract	51
5.2 Introduction	52
5.3 Geological settings	54
5.4 Database	56
5.4.1 High-resolution multichannel seismic data	56
5.4.2 Well data	56
5.4.3 Stratigraphic interpretation	57
5.4.4 Sedimentary sequences	57
5.4.5 Seismic stratigraphy	63
5.5 Structural evolution	64
5.5.1 Methods	64
5.5.2 Structural framework	66
5.5.3 Early – Middle Triassic (Buntsandstein – Muschelkalk)	67
5.5.4 Late Triassic (Keuper)	67
5.5.5 Jurassic	70
5.5.6 Cretaceous	72
5.5.7 Cenozoic	72
5.6 Discussion and Conclusions	77
5.7 Acknowledgements	81
<b>6. Basin evolution of the northern part of the Northeast German Basin – insights from a 3D structural model</b>	<b>83</b>
<i>by M. B. Hansen, M. Scheck-Wenderoth, C. Hübscher, H. Lykke-Andersen, A. Dehghani, B. Hell and D. Gajewski</i>	
<i>Submitted to Tectonophysics, 01/2006</i>	
6.1 Abstract	83
6.2 Introduction	84
6.3 Geological settings	85
6.4 Methods	87

6.5 3D structure of the northern part of the Northeast German Basin	91
6.5.1 Cenozoic	91
6.5.2 Cretaceous	91
6.5.3 Jurassic and Upper Triassic	92
6.5.4 Middle Triassic	92
6.5.5 Lower Triassic	93
6.5.6 Zechstein	93
6.6 Backstripping method	94
6.6.1 Basic assumptions	94
6.6.2 Modelling concept	95
6.7 Backstripping	96
6.7.1 Subsidence and uplift patterns	100
6.7.2 Neotectonic modelling	100
6.8 Discussion and conclusions	102
6.8.1 Late Permian (Zechstein) to Early Triassic	102
6.8.2 Middle Triassic	102
6.8.3 Late Triassic and Jurassic	103
6.8.4 Cretaceous	103
6.8.5 Cenozoic	104
6.8.6 Neotectonic	104
6.8.7 Modelling errors	104
6.8.8 Concluding remarks	105
6.8 Acknowledgements	106
<b>7. Summary and conclusions</b>	<b>107</b>
<b>References</b>	<b>113</b>
<b>Acknowledgements</b>	<b>121</b>



# 1. Introduction

The North German Basin is the largest of a series of Carboniferous-Permian intracontinental basins covering most of the present-day central and northwestern Europe, known as the Central European Basin Systems (CEBS). Other major basins in the CEBS are the Norwegian-Danish Basin and the Polish Basin (Fig. 1.1) (Scheck-Wenderoth and Lamarche, 2005). These basins developed on the continental crust southwest of the Sorgenfrei-Tornquist and Teisseyre-Tornquist zones and north of the Variscan domains. A set of E-W orientated basement highs is located in the middle of the CEBS. These are known as the Mid North Sea High and the Ringkøbing-Fyn High. In all three major basins, initial rifting in Early Permian times was accompanied by widespread volcanic activity followed by postrift thermal subsidence, with the deposition of the Rotliegend clastics and Zechstein evaporites. The deposition of primarily clastic and carbonate sediments occurred more or less continuously throughout the Mesozoic and Cenozoic in most parts of the CEBS. E-W directed extension and differential subsidence between the basement highs and the different basins within the CEBS during the Mesozoic, led to the development of the N-S orientated Central, Horn and Glückstadt Grabens (Clausen and Pedersen, 1999; Scheck-Wenderoth and Lamarche, 2005). Generally for the entire CEBS, after the differentiated subsidence during the Mesozoic, Late Cretaceous – Early Cenozoic inversion associated with the Alpine Orogeny and renewed subsidence throughout the Cenozoic are observed (Ziegler, 1990).

The CEBS acts as the natural laboratory for the Special Priority Program (Schwerpunkts Program) number 1135 of the German Science Foundation (Deutschen Forschungsgemeinschaft) that deals with the dynamics of sedimentary systems/basins under varying stress regimes. The NeoBaltic project is a part of this Priority Program with the main motivation to analyze the structural and sequence stratigraphic evolution of the post-Zechstein successions in the northernmost part of the Northeast German Basin, with a special emphasis on neotectonic activity and its relation to salt dynamics and the present-day stress field (Hübscher et al., 2004). The project is cooperation between the universities of Aarhus in Denmark (Department of Earth Sciences) and Hamburg in Germany (Institute of Geophysics). The NeoBaltic project has been carried out as a three-stage project as it includes the acquisition, processing and interpretation of three types of marine geophysical data.

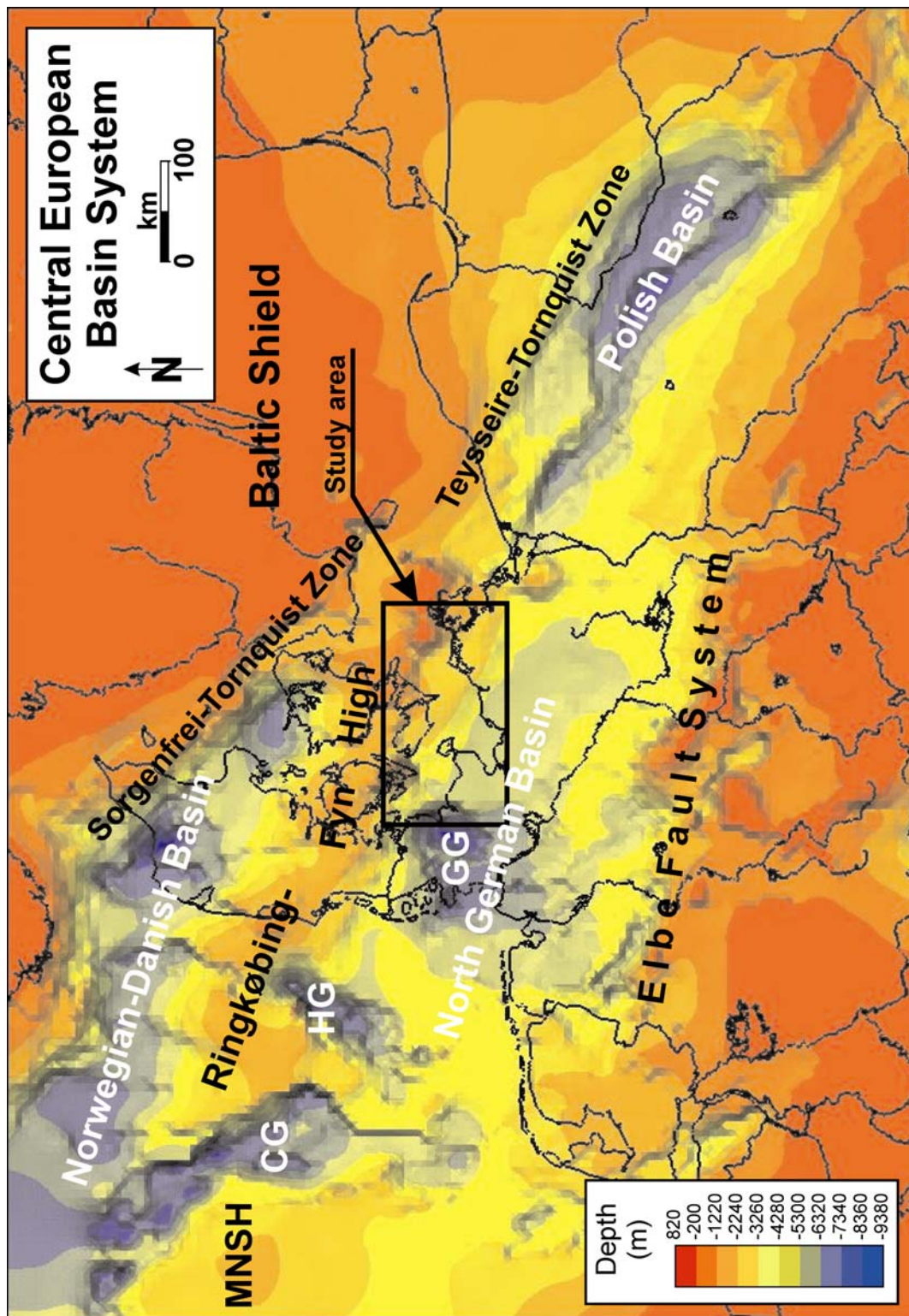


**Fig. 1.1** Structural framework of the Central European Basin System revealed from the depth to the Base Zechstein surface (modified from Scheck-Wenderoth and Lamarche, 2005). The NeoBaltic working area is marked by the black square. MNSH: Mid North Sea High, CG: Central Graben, HG: Horn Graben, GG: Glückstadt Graben.

The data pool of this dissertation work contains 2D high resolution reflection seismic data acquired during three field campaigns in the years between 2002 and 2004, supplied with seismic data from the BaltSeis project, acquired by the Department of Earth Sciences, University of Aarhus between 1998 and 2000.

The main objectives of this dissertation work have been the geological interpretation of the seismic data and the reconstruction and modeling of the Mesozoic and Cenozoic structural framework of the northeastern corner of the Northeast German Basin. Another objective was the determination of the neotectonic movement in the region. As the project comprises several phases of data acquisition and processing (one acquisition cruise per year) the overall study region has been divided into two sub-areas, the Bay of Kiel and the Bay of Mecklenburg, in two of the following chapters.

This dissertation is divided into following chapters:

1. A short introduction to the geological settings of the working area, objectives and structuring of this work.
2. Detailed description of the acquisition and processing of raw data from the working area. The focus in this chapter is on the seismic data since this is the focus of this dissertation.
3. An overall introduction to the deposition of evaporites and their special physical properties compared to other types of sediments. The reason for this chapter is that salt plays a key role for the post-depositional evolution of the different basins in the CEBS region.

The results of this study will be presented in the following three chapters. Each chapter represent a scientific article submitted for publication to an appropriate geo-scientific journal:

4. The Mesozoic – Cenozoic structural framework of the Bay of Kiel area, western Baltic Sea.

(Hansen, M.B., Lykke-Andersen, H., Dehghani, A., Gajewski, D., Hübscher, C., Olesen, M. and Reicherter, K. Published in the *International Journal of Earth Sciences*, vol. 94 no. 5-6, 1070-1082, 2005).

This publication presents a detailed mapping of five major Mesozoic and Cenozoic successions, as a result of the geological interpretation of a dense grid of multichannel high-resolution seismic sections from the Bay of Kiel sub-area. The structural evolution of the study area was interpreted from the

distribution of the sedimentary sequences and the section flattening of a key seismic line.

5. Structure and evolution of the northern part of the Northeast German Basin. (Hansen, M.B., Piñeiro Triñanes, S., Lykke-Andersen, H., Hübscher, C., Dehghani, A. and Gajewski, D. Submitted to *Marine and Petroleum Geology* 01/2006).

This paper presents the results the Mesozoic – Cenozoic structural and deposition reconstruction in the Bay of Mecklenburg sub-area. This is done from the geological interpretation of seismic data and section flattening.

6. Basin evolution of the northern part of the North German Basin – insights from a 3D structural model.

(Hansen, M.B., Scheck-Wenderoth, M., Hübscher, C., Lykke-Andersen, H., Dehghani, A. and Gajewski, D. Submitted to *Tectonophysics* 01/2006).

The description and backstripping of a 3D structural model based on the geological mapping of stratigraphic successions from the two sub-areas (Chapter 4 and 5) are presented in this publication. The results are furthermore compared to other 3D models from adjacent areas within the CEBS. Finally, a forward modelling was completed in order to predict the outcome of the neotectonic movement in the study region.

7. A final summary and conclusions chapter will recapitulate the results of the main chapters and compare them with similar studies from the adjacent areas. Additionally, it will be discussed whether some of the main objectives of the entire research project have been fulfilled.

## **2. Data Acquisition and Processing**

The results of this study are based on the interpretation of marine multichannel 2D high-resolution seismics. The seismic data for the NeoBaltic project were acquired during three research cruises onboard R/V Heincke in 2002 (HE172) & 2004 (HE217) and R/V Alkor in 2003 (AL185). The seismic source has varied during the different cruises, whereas the streamer configuration and recording system were the same. Additionally, potential field (gravimetric and magnetic) data were acquired along the ship track. These data were not incorporated into this work. Finally, the data pool was supplied with seismic data from the BaltSeis project, collected on three campaigns onboard the R/V Dana in the years between 1998 and 2000.

### **2.1 Study Area**

The overall study area for this project is the western Baltic Sea; including the Bays of Kiel and Mecklenburg and to a minor extend the Danish Belt Sea. The seismic data from the BaltSeis project was mainly acquired in the Danish territorial waters, while the first NeoBaltic campaign only acquired data in German Waters. The 2003 Alkor and the 2004 Heincke cruises had research permits to both Danish and German waters, which made it possible to collect data across the territorial boundary. In general, data from the NeoBaltic campaigns were systematically acquired from the Bay of Kiel and eastward, resulting in a relatively dense grid of 2D high-resolution seismic lines with a total length of more than 8000 km (Fig. 2.1). Potential field data were measured only on the NeoBaltic cruises.

As the author of this dissertation only used the seismic data, the potential field data will only be described briefly in the following.

## 2.2 Gravimetric Data

The gravity data from the NeoBaltic project was measured using a sea-gravimeter type KSS 30/31. This system can be installed and used on any research vessel with a sufficient navigation system. The measured gravity values are processed using powerful computer facilities in order to produce gravity anomaly maps. The measurements were done along the entire ship track (port to port) and correlated with a land-based reference station (typically adjacent to the ship on the pier).

## 2.3 Magnetic Data

The magnetic measurements were carried out with a sea-magnetometer type Geometrics™ G813. The measuring tool was, like the seismic equipment, deployed into the water and towed approximately 70 meters behind the ship. Magnetic measurements were carried out continuously along the different seismic profiles and during the transit between two lines.

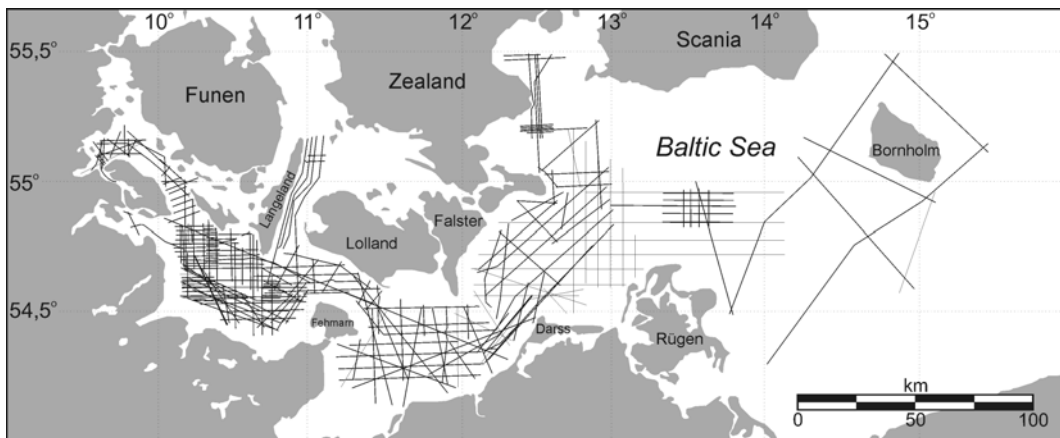


**Fig. 2.1** Survey map showing the position of each seismic line available in the data pool of this study.

## 2.4 Multichannel Seismic data

The seismic measurements were completed with different setups on the different cruises. The different acquisition parameters are listed in Table 2.1.

<b>Cruise</b>	<b>HE172</b>	<b>AL185</b>	<b>HE217</b>
<b>Source</b>	4 Sleeve guns	1 GI-Gun	4 Sleeve guns
<b>Volume</b>	70 cu. inch	45/105 cu. inch	70 cu. inch
<b>Shot Interval</b>	12.5 m	12.5 m	12.5 m
<b>No. of Channels</b>	96	96	96
<b>Active Length</b>	587.5 m	587.5 m	587.5 m
<b>Sample Rate</b>	1 ms	1 ms	1 ms
<b>Channel Interval</b>	6.25 m	6.25 m	6.25 m
<b>CMP Interval</b>	3.125 m	3.125 m	3.125 m
<b>Average CMP Fold</b>	24	24	24

**Table 2.1** Seismic acquisition parameters for the three NeoBaltic cruises.

The seismic acquisition system is designed for intermediate sediment penetration (1.5-2 sec.) with a vertical resolution of 5-10 m. All components are easily transportable and installation on any medium-sized ships, like R/V Heincke and R/V Alkor, is fairly easy. The entire seismic system is depicted in the schematic drawing (Fig. 2.2).

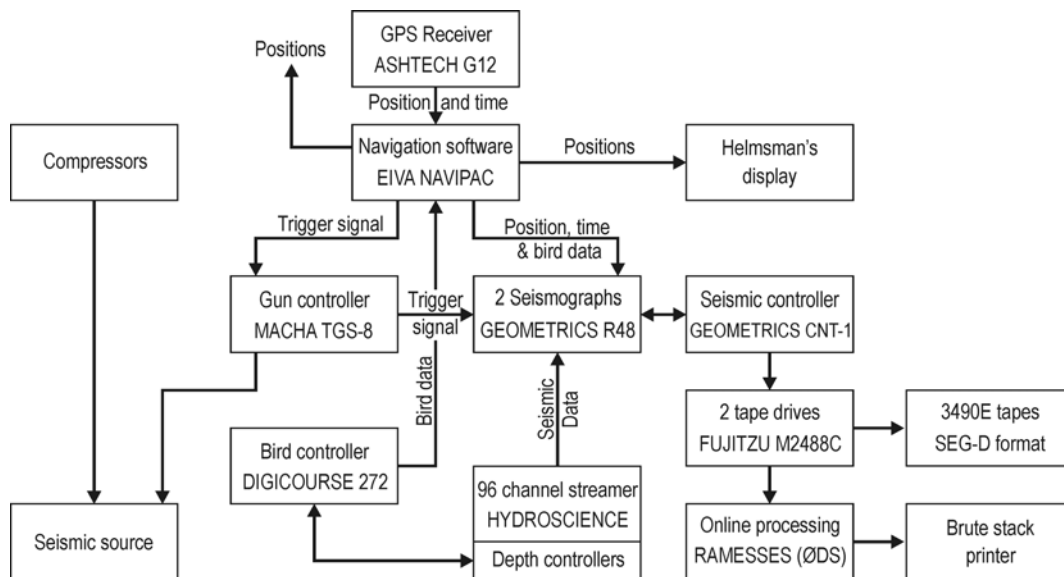


**Fig. 2.2** Schematic drawing of the seismic acquisition system.

## 2.4.1 Seismic Sources

### Sleeve-gun

The most widely used seismic source on the NeoBaltic campaigns has been the 40 inch<sup>3</sup> SG-1 Sleeve-gun (Input/Output). Four volume-reduced guns (2 x 10 inch<sup>3</sup> and 2 x 25 inch<sup>3</sup>) were operated in a cluster with an individual spacing of 50 cm. The shot intervals were five seconds.

### GI-gun

On the 2003 survey a single 45 inch<sup>3</sup> GI-gun (Generator/Injector), with an injection volume of 105 inch<sup>3</sup>, was used as the seismic source. The GI-gun is comprised of a generator to create the acoustic pulse and an injector to reduce or suppress the bubble. The GI-gun was developed to reduce or suppress the bubble oscillations of a traditional airgun. This is made possible by injecting air into the bubble from the release of air from the airgun into the water column. When the bubble reaches its maximum volume the right amount of additional air is injected into it, controlling the collapse of the bubble and its associated noise. The shot intervals with this source were five seconds.

### G-gun

In order to study the crustal structure underneath the Zechstein evaporites a single line was shot with a cluster of two 6 liter G-guns during the 2003 Alkor cruise.

The G-gun signal is generated by a sudden expansion of high-pressure air into the water column. The shot intervals were 40 seconds.

### Gun Controller

A Macha TGS-8 gun controller triggered the different seismic sources. Because the guns have individual delays (relative to a given trigger provided by the navigation system) depending on the individual solenoid functions, the firing of the guns was synchronized by the gun controller.

## 2.4.2 Seismic Recording System

### Streamer

The streamer used on the acquisition cruises is an analogue streamer (HydroScience) with 96 active hydrophone groups, each consisting of seven Benthos RDA hydrophones. The individual hydrophone spacing is 0.54 m, while the group-center separation is 6.25 m. The streamer is composed of six active sections, each containing 16 hydrophone groups. Thus, the total active length is 593.75 meters. In the front of the streamer are a 50-meter stretch section and a 50-meter tow cable located. Coils for the communication with the active depth controllers (Digicourse DigiBird 5010) are located in the rear ends of each active section and in front part of the stretch section. The streamer winch is housed in and operated from a modified 10-foot container.

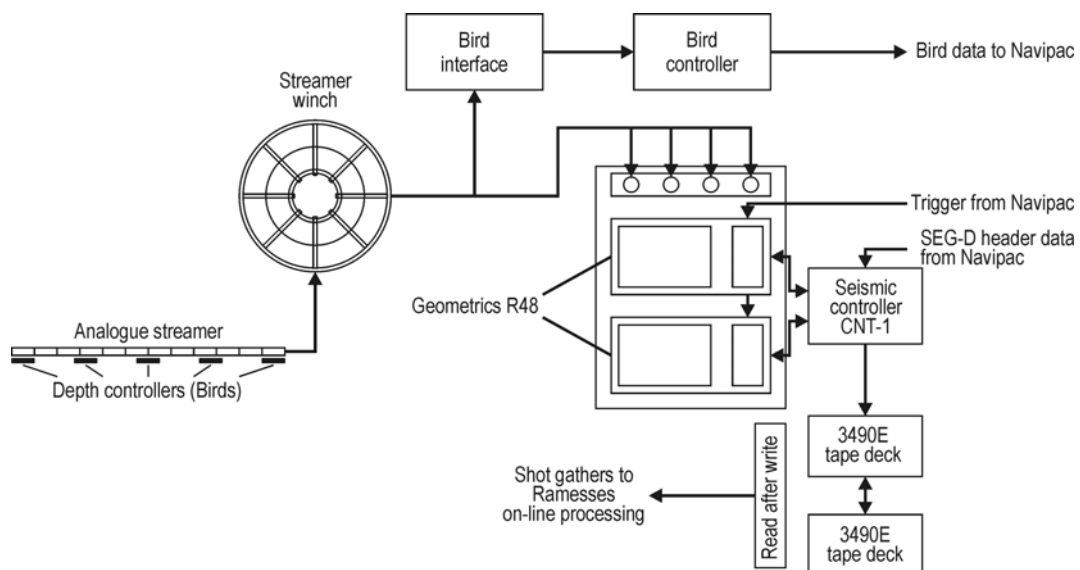


Fig. 2.3 Diagram of the seismic data flow.

### **Depth controllers**

Four to five active depth controllers (Digicourse DigiBird 5010), each with a maximum lift capacity of 15 kg at a ship velocity of 5 knots, were used on the NeoBaltic cruises. The DigiBirds were distributed with more or less equal distance along the streamer.

### **Seismographs**

The analogue signals from the streamer were received by two 48-channel seismographs (Geometrics R48), each with four cards containing 12 channels (Fig. 2.3). The digitalisation of the analogue signals was performed in 18-bit Sigma-Delta 4 bit IFP A/D converters. The two seismographs were controlled by the Geometrics software (CNT-1) installed on a Windows™ PC via a local 100 Mbit network. All the acquisition parameters (line name, tape numbers, recording length, sample rate, filter etc.) were set on the controller. For each line the controller generated a log file containing the pertinent data (file number, data, time, coordinates and error messages). The log files were saved on the PC hard disk. Furthermore, the controller provided a variety of facilities for the quality control of the data: Display of shotgathers, display of noise levels and frequency spectra for all channels, display of near trace plots and brute stacks.

Two 3490E tape decks (Fujitsu M2488C) were connected to the controller via a Fast Wide SCSI interface for the recording of the raw seismic data in a SEG-D 8048 Rev 0 demultiplexed format.

## **2.4.3 Navigation**

### **GPS Receiver**

The positions in UTM coordinates were obtained by a 12-channel GPS receiver (Ashtech G12). As there were no differential reference stations within the survey area on any of the three campaigns, the G12 was run in a non-differential mode. The positions were delivered to the navigation PC with the NaviPac Software in NMEA 183 format (GGA string) every second.

### **NaviPac**

NaviPac is a navigation and datalogging program that runs on a NT 4.0 computer. To provide sufficient input/output opportunities, the PC is extended with a “digiboard” with eight extra serial ports. The Ashtech G12 GPS receiver provided the navigation input to the NaviPac. The other input data was the depth data from the DigiBirds on the streamer. Outputs were the trigger to the gun controller

(TGS-8) and position and time information to the CNT-1 controller for transfer to the SEG-D headers in the seismic data.

The different runlines in the surveys were displayed on the Helmsman's display on the NaviPac computer. The beginning and end of the seismic recording were controlled from the Helmsman's display.

### Online Processing

On the 2003 Alkor (AL185) and 2004 Heincke (HE217) cruises a comprehensive online processing to brute stack level were carried out as a supplement to the quality control (QC) performed by the CNT-1 controller. This was done on the autonomous processing system Ramesses (Ødegaard & Danneskiold Samsøe). Ramesses was developed in the early eighties as a flexible QC system for conventional seismic data, but on the two late NeoBaltic cruises only the brute stack facility part of the system were used.

The essential part of the Ramesses system is the fast seismic processor based on an IBM VAX computer (Fig. 2.4). The processor receives data from a read-after-write interface on the 3490 tape drives. The processing sequence and plot specifications were set up on a PC interfaced to the seismic processor. The brute stack was handled by the host computer and printed on a jet ink matrix printer with an endless paper supply. The system can handle 1500 sample traces at the time. Thus, with a sample rate of 1 ms the upper 1.5 sec. TWT were target for the online processing on the NeoBaltic cruises.

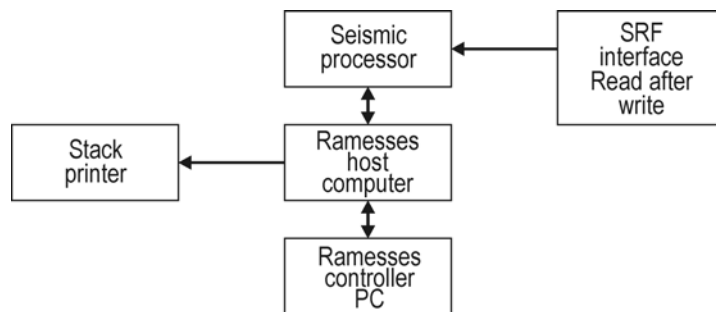


**Fig. 2.4** Schematic drawing of the Ramesses QC system (online processing system).

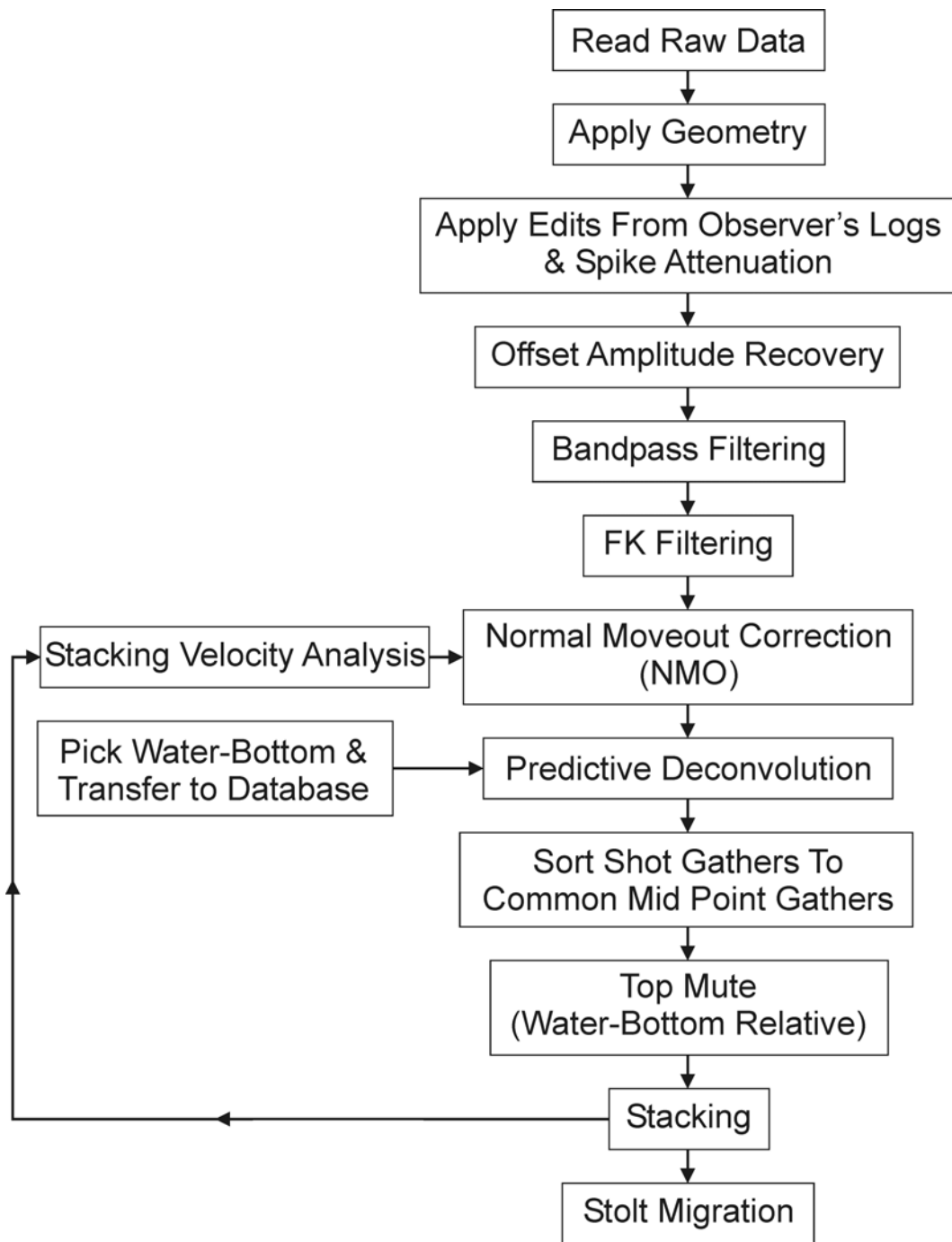


**Fig. 2.5** The main steps in the processing sequence.

### **2.4.3. Data Processing**

The raw seismic data was processed using Landmark's ProMAX™ 2D version 7.0 software on a UNIX (SunOS) workstation at SeisLab Aarhus. ProMAX™, in its different version, is one of the most widely used seismic data processing softwares in the industry. This software allows the user to build up flows of pre-programmed seismic processes, only requiring the manual input of the chosen parameters for each process. This makes the entire process less time-consuming, as the processing flows of the first line can be reused for the remaining lines in the survey. The software furthermore allows interactive picking of parameters such as FK polygons, mutes and velocities. The results (traces, gathers or final stacks) can be displayed on screen, sent to a plotter and saved to disk. Finalised stacked data are saved in SEG-Y format. The main steps in the processing sequence are shown in Figure 2.5. The most important flows will be described below (The convention of *italics* is used for expressing ProMAX™ process names).

#### **Reading raw Field Data**

The raw field data were recorded as SEG-D 8048 format in a demultiplexed format. This means that the data is ordered by traces onto 3480 tape cartridges. Each line was read into ProMAX™ using the *SEG-D Input* process.

#### **Geometry Processing**

Using the process *2D Marine Geometry Spreadsheet*, the geometry for each line was manually applied using the information from the Observer's Logs. The geometry was then applied to the raw shots using *Inline Geom. Header Load*.

#### **Editing and Removing Noise Spikes**

In this flow, bad shots listed in the Observer's Logs were viewed on screen using *Trace Display with Automatic Gain Control* applied over a 400 ms window. Truly bad shots (e.g. misfires) were removed from the dataset. Any consistently bad channels were zeroed using *Trace Kill/Reverse*. To remove any random noise spikes in the remaining data, the *Spike to Median Ratio Editor* process was used.

#### **Picking of Water-bottom Reflection**

The water-bottom reflection was picked interactively in this flow and saved to disc. This was done to enable desired subsequent processes to be water-bottom relative. The flow *Database/Horizon Transfer* was then used to transfer the horizon to the database.

### **Bandpass Filtering**

Test stack panels were created to test various high and low cut filters. A final 10-55-250-350 Hz Ormsby Filter, zero-phase, was chosen.

### **F-K Filtering**

Several representative shots were selected and read in using *Disk Data Input*. *Offset Amplitude Recovery* and the chosen *Bandpass Filter* were applied, and the shots were gain-correct using *Automatic Gain Control* over a 400 ms window. The process macro *F-K Analysis* was then used to pick an “accept” polygon in the F-K space on one shot to remove coherent linear noise (Fig. 2.6). The effect of the picked polygon was then checked on other representative shots.

### **Velocity Analysis and Normal Moveout Correction**

In the first part of the velocity analysis, the standalone process *Supergather Formation* was used to find every 100<sup>th</sup> common mid-point (CMP), reading in the 7 CMPs around this point for later combination into supergathers by the *Velocity Analysis* process. A water-bottom relative top-mute was applied to remove the direct arrivals and refractions. *Automatic Gain Control* was applied and *Velocity Analysis Precompute* was used to prepare the data for input into the *Velocity Analysis* process. This involved calculating the stacking velocities, stacking the CMPs to create supergathers, and creating velocity spectra using the constant velocity method. The second part of this flow involved the input of the supergathers into the *Velocity Analysis* process, which is an interactive velocity-picking tool (Fig. 2.7). Velocities were picked, saved and the velocity model was then applied to the shot gathers using the *Normal Moveout Correction* process.

### **Predictive Deconvolution**

For the reduction of reverberations and multiple energy a predictive deconvolution increased the quality of the CMP gathers. Because deconvolution works on a trace-by-trace basis and if top muting occurred before deconvolution, multiples were not effectively attenuated because the water-bottom reflector had been removed from certain traces. Top muting was required after deconvolution to remove any remaining multiples on the far offsets.

### **Sorting From Shot Domain to Common Mid-Point Domain**

*In-line Sort* was used to sort the shot-channel ordered data into common mid-point (CMP) offset order in preparation.

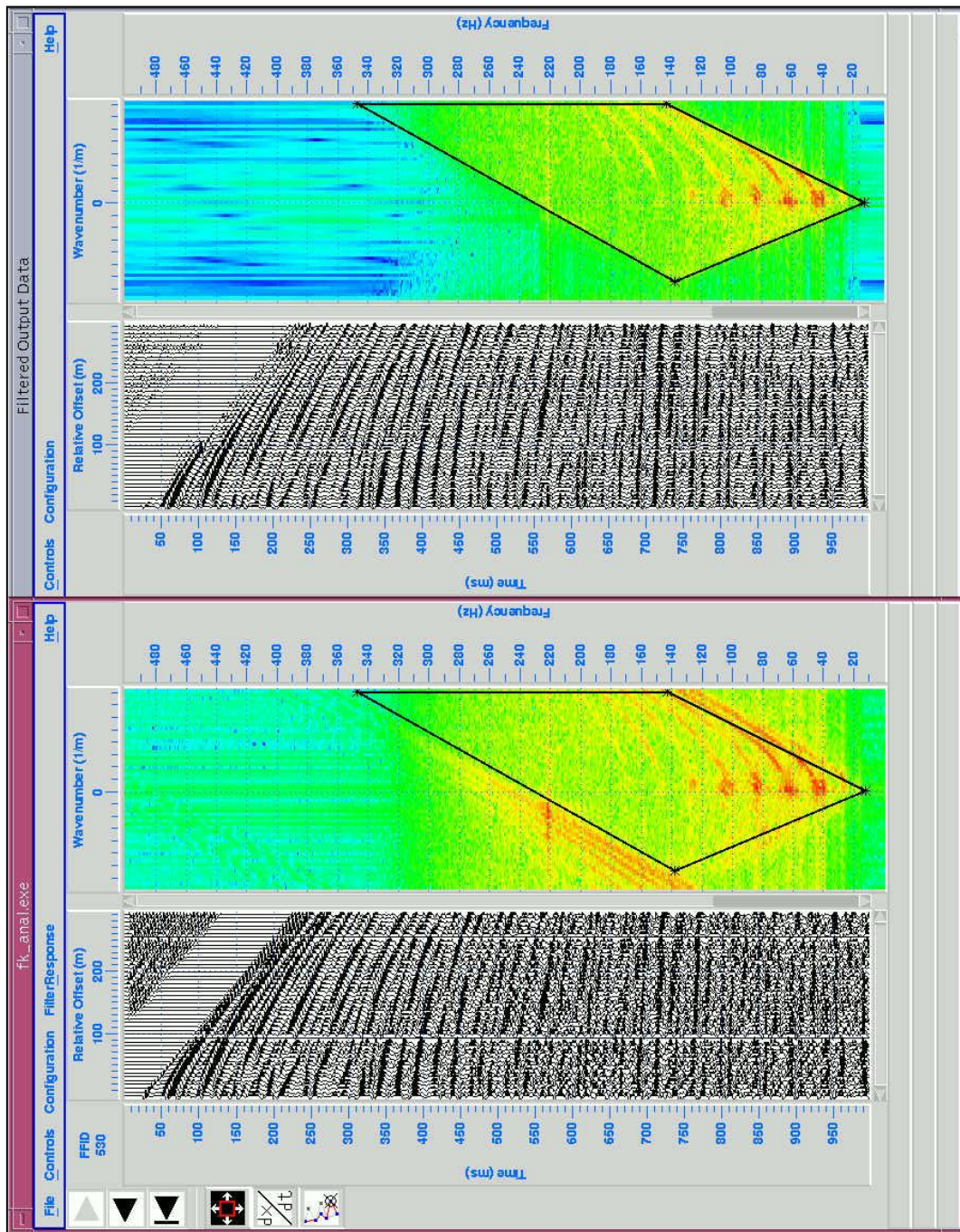


**Fig. 2.6** Screen-shot example from ProMAX™ showing an example of the *F-K Analysis* display used to pick an “accept” polygon. The first window (lower one) is the design window, and the second (upper one) is the filtered output. Note the removal of the majority of linear diagonal noise. The refractions and direct arrival have also been removed. Two killed channels are present in the design window, but the action of the filter introduces realistic data into them (Courtesy of Kathryn Brookes).

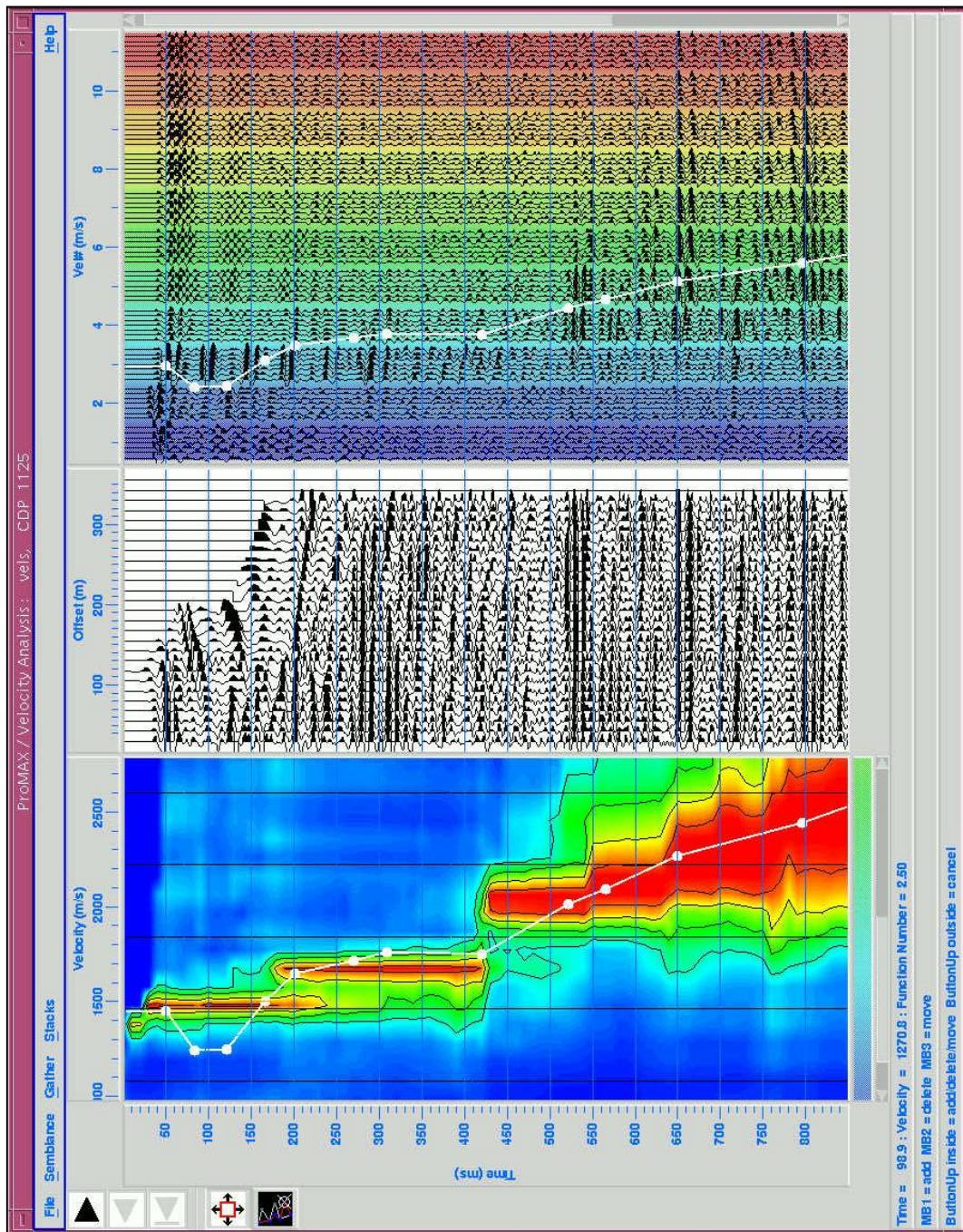


**Fig. 2.7** Screen-shot example from ProMAX™ showing an example of the *Velocity Analysis* display used for interactive velocity picking. Shown, from figure bottom to top (left to right), are the stacking velocity spectrum, the “supergather” with NMO correction applied, and the constant velocity stack panels. Note that the “bullseyes” on the velocity spectrum plot do not necessarily correspond to the best picked velocities - the use of all three panels is required to ensure that real reflections are “flattened” to create a good stack, not multiples (Courtesy of Kathryn Brookes).

**Top Mute and Stacking**

After deconvolution before stack was applied, the shots were viewed using *Trace Display*. A top mute removing all signals above the sea floor was then applied. The CMPs were stacked using *CDP/Ensemble Stack* to generate the zero offset section. This stack was then saved as SEG-Y format.

**Migration**

*Memory F-K Stolt Migration* was used to migrate the seismic stacked data using an interval velocity function derived from the stacking velocities. This process moves dipping events to their true sub-surface positions, and collapses diffractions that result from point reflections (e.g. fault edges). The final stacked and migrated sections were then saved in SEG-Y format ready for digital interpretation.



### **3. The Zechstein Evaporites of the Central European Basin System**

This chapter gives a brief overview of the Upper Permian Zechstein evaporites of the Central European Basin System (CEBS), both in terms of the depositional character and the physical properties of the sediments. The reason for this is because salt plays an important role in the depositional history of the basins. Furthermore, evaporites play a key role, both passively and actively, for the oil and gas exploration within the CEBS. Passively, because of its sealing properties and actively, due to trap developments as result of halokinesis. Finally, it is believed that neotectonics in some areas are occurring because of ongoing salt movements.

#### **3.1 Primary Evaporite Deposition**

The term *Primary Evaporites* applies to the evaporitic sediments precipitated via solar radiation from a brine pool or brine-filled larger basin under normal temperature. The terms *Secondary and Tertiary Evaporites* refer i.a. to salts precipitated under the influence of burial diagenesis or the partial dissolution and re-precipitation of an existing evaporite bed (Einsele, 2000). This sub-chapter will only focus on the deposition of primary evaporites, as the secondary or tertiary salts do not have any relevance for this study.

The literature distinguishes between several basic models of primary evaporite deposition. Some of these are:

- Closed seawater basin.
- Shallow salt lagoon (barred basin or seepage basin).
- Drawdown of water level in deep basin.
- Minor evaporite cycles controlled by sea-level changes.
- Coastal sabkhas.

Some models can also be a combination of the different salt basin types mentioned above. Common for all these types of depositional basins is that they all lie in arid to semi-arid zones and loses more water to evaporation than it receives by precipitation and inflow of water from different sources (Einsele, 2000). This makes evaporites important paleoclimatic indicators, as arid and semi-

arid zones are normally located in low-latitude regions opposed to wet tropical equatorial or temperate and cold high-latitude areas.

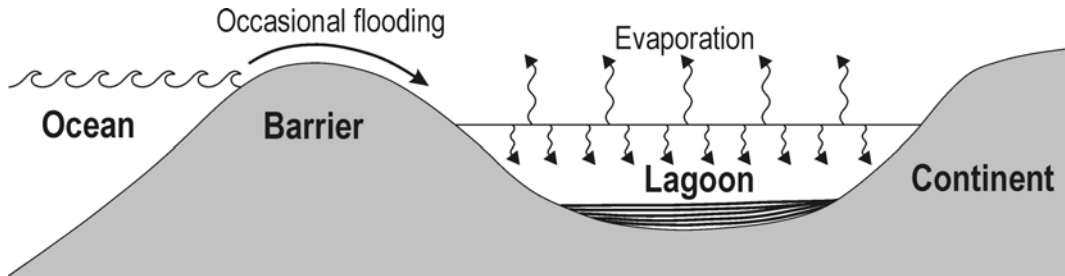


**Fig. 3.1** Shallow salt lagoon model (modified from Warren, 1999; Einsele, 2000). The hot and dry climate is the reason why more water is lost to evaporation than the basin receives from the inflow of various sources. Occasional flooding renews the salt content within the lagoonal water column. The tectonic subsidence within the lagoonal basin is enhanced by the isostatic effect of the rapidly accumulating salt deposits allowing great evaporitic successions to be deposited.

This study will focus on the “shallow salt lagoon” model (Fig. 3.1), as this is the one that fits the Zechstein Basin of central and northern Europe. For other models we refer to the chapter on marine evaporites in Einsele (2000).

This type of basin is disconnected from the open sea by a barrier. Because of the hot and dry climate the lagoonal water experience an intensive evaporation and therefore lowering of the surface level. With the ongoing evaporation, the salinity increases in the water column, which finally gets oversaturated. The first minerals to precipitate are the carbonates followed by the sulfates. Precipitation of halite starts at 10 to 12 times the salinity of normal seawater and if an entire evaporitic cycles is completed the final minerals to precipitation are potassium and magnesium salts (Warren, 1999).

Occasional flooding from the open sea into the salt lagoon renews the salt content in the lagoonal waters and enables a new evaporitic cycle to begin. Because of the rapidly accumulating salt deposits on top of the thinned crust, the normal slow tectonic subsidence is enhanced by the isostatic effect, which enables the deposition of a thick evaporitic succession, like e.g. the one from the Zechstein Basins (Einsele, 2000).

### 3.2 Composition and Physical Properties of Rock Salt

Marine evaporites are chemically precipitated sediments from saturated seawater. The exact mineral composition differs from basin to basin, due to various depositional environments. Only a limited number of cases exist in which the sequence and amount of marine rock salts can be explained just by evaporation of a certain volume of seawater (Einsele, 2000). The most common evaporite minerals are Halite ( $NaCl$ ), Anhydrite ( $CaSO_4$ ), Calcite ( $CaCO_3$ ), Gypsum ( $CaSO_4 \cdot 2H_2O$ ) and to some extent Potash Salt ( $KCl$ ) and Magnesium Salt ( $MgCl_2$ ). Normal seawater has an average density of  $1.025 \text{ g/cm}^3$  and contains about 35 g per litre dissolved constituents (Warren, 1999). With continued evaporation the seawater becomes oversaturated and the different minerals will precipitate. When the right environmental conditions are present, the deposited salt succession can reach thicknesses on a kilometer scale. Almost 80% of the precipitated evaporites consist of Halite (Einsele, 2000).

The physical properties of evaporites differ from other sediments. Salt has almost no porosity and is therefore incompressible under increasing burial depth. Furthermore, the average density for salt ( $\rho_{salt} = 2.2 \text{ g/cm}^3$ ) is lower than other sediments. Thus, a positive buoyancy effect will occur when the density of the overburden exceeds the density of the salt during burial (Tucker, 1991).

Rock salt behaves like a viscoelastic fluid on a geological timescale. Because of its viscoelastic nature a hydraulic (pressure) gradient exists within the salt body. A hydraulic gradient is defined by a difference in hydraulic head between two points within the salt layer. Halokinesis occurs only if the differential pressure of stress exceeds this yield point within the evaporites. Salt flow normally occurs in the direction of the maximum hydraulic gradient, i.e. from the area of the highest hydraulic head to that of the lowermost one (Fig. 3.2). The size, shape and type of salt structures are highly dependent on the position within the basin, the original thickness of the evaporites, the history of subsidence and sediment accumulation and the regional stress regime (Einsele, 2000). Finally, the viscoelastic properties are responsible for, that the salt body acts as a decoupling layer between overburden and the underlying sediments and basement (Warren, 1999).

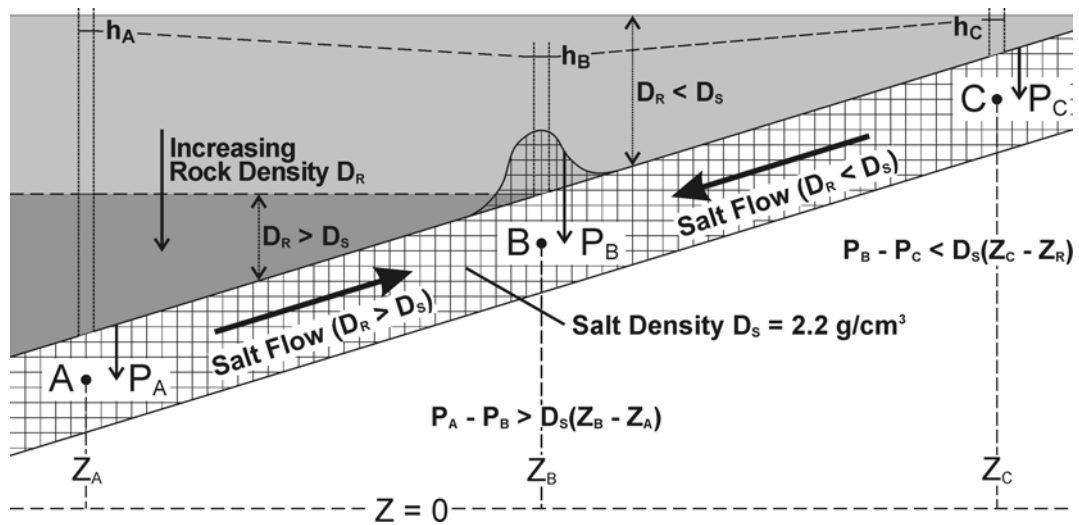


**Fig. 3.2** Flow of evaporites in the subsurface in relation to hydraulic gradient ( $h_x$ ) within the salt layer. Downhill and uphill salt flow due to the lower or higher density  $D_R$  of the overlying sedimentary body compared to the density of the evaporitic layer  $D_s$ . In this theoretical model a salt structure will be created at point B, where  $D_R = D_s$ .  $P_X$ : Pressure head at point X.  $Z_X$ : Elevation (depth) for point X (modified from Einsele, 2000).

### 3.3 The Late Permian Zechstein Basins

The Northern and Southern Permian Basin, which are more or less identical to the Central European Basin System (Fig. 1.1), experienced up to eight large depositional cycles, after seawater drownings from the northern Boreal Ocean (Taylor, 1998). Their total thickness varies considerably from some tens of meters in the marginal areas and up to 3500 meters in troughs and grabens in the central parts of the basin system. The thicknesses of the salt deposits of a single cycle often reach several hundred meters, but also vary considerably from marginal to the central parts. Halite was precipitated in the central parts of the two basins when the margins were exposed and karstified. The basins may have been 100-300 m deep during the transgressions from the north (from Einsele, 2000).

## **4. The Mesozoic – Cenozoic structural framework of the Bay of Kiel area, western Baltic Sea**

by Martin Bak Hansen, Holger Lykke-Andersen, Ali Dehghani, Dirk Gajewski, Christian Hübscher, Morten Olesen and Klaus Reicherter.

Published in *International Journal of Earth Sciences*, vol. 94, no. 5-6, 1070 – 1082, 2005

### **4.1 Abstract**

A dense grid of multichannel high-resolution seismic sections from the Bay of Kiel in the western Baltic Sea has been interpreted in order to reveal the Mesozoic and Cenozoic geological evolution of the northern part of the North German Basin. The overall geological evolution of the study area can be separated into four distinct periods. During the Triassic and the Early Jurassic, E-W extension and the deposition of clastic sediments initiated the movement of the underlying Zechstein evaporites. The deposition ceased during the Middle Jurassic, when the entire area was uplifted as a result of the Mid North Sea Doming. The uplift resulted in a pronounced erosion of Upper Triassic and Lower Jurassic strata. This event is marked by a clear angular unconformity on all the seismic sections. The region remained an area of non-deposition until the end of the Early Cretaceous, when the sedimentation resumed in the area. Throughout the Late Cretaceous the sedimentation took place under tectonic quiescence. Reactivated salt movement is observed at the Cretaceous Cenozoic transition as a result of the change from an extensional to compressional regional stress field. The vertical salt movement influenced the Cenozoic sedimentation and resulted in thin-skinned faulting.

*Key words: Seismic interpretation, North German Basin, basin evolution, Mesozoic, Cenozoic*

## 4.2 Introduction

Over the years, several seismic studies have been carried out in the region around the western Baltic Sea for example the EUGENO-S (EUGENO-S working group, 1998), BABEL (BABEL working group, 1991; 1993), DEKORP-BASIN (e.g. Meissner and Krawczyk, 1999; Krawczyk et al., 1999), and POLONAISE '97 (e.g. Guterch et al., 1999; Grad et al., 1999) projects. These projects were carried out to obtain a better understanding of the deep-rooted tectonic structure of the region. Poprawa et al. (1999) did a study on the tectonic evolution of the Baltic Basin based on a subsidence analysis from boreholes. Detailed studies of the sedimentary cover were carried out in the adjacent Northeast German Basin (Scheck and Bayer, 1999; Bayer et al., 1999; Kossow et al., 2000; Kossow and Krawczyk, 2002; Scheck et al., 2003a; 2003b) and in Northwest Germany and the German North Sea Sector (e.g. Baldschuhn et al., 2001), but until now no or very little systematic and localised research has been carried out to investigate the post-Permian structural framework of the south-western Baltic Sea.

In order to investigate the post-Palaeozoic structural and depositional evolution of the western Baltic Sea, which corresponds to the northern part of the North German Basin and the transition towards the Baltic Shield (Fig. 4.1), the Universities of Aarhus (Denmark) and Hamburg (Germany) have joined forces completing seven marine geophysical surveys in the area between 1998 and 2004 in the frame of the Baltseis and the NeoBaltic (Hübscher et al., 2004) projects. During these research cruises a dense grid of high-resolution seismic data was acquired together with potential field data (gravity and magnetic) along the ship track. This paper presents the results of the seismic interpretation of the Bay of Kiel sub-area of this regional study. For this purpose a dense grid of 96 seismic sections and the information from four explorational wells (Kegnæs-1, Søllested-1, Rødby-1 and Rødby-2) were used (Fig. 4.2).

## 4.3 Geological framework

The North German Basin (NGB) (Fig. 4.1), which is a subbasin of the Southern Permian Basin (Ziegler, 1990; Scheck and Bayer, 1999), belongs to a series of related Carboniferous-Permian intracontinental basins extending from the southern North Sea to Northern Poland (Kossow et al., 2000), referred to as the Central European Basin System (CEBS). The Ringkøbing-Fyn High (RFH) is a series of east-west striking basement highs running across the North Sea and the Danish mainland (Clausen and Pedersen, 1999) that bounds the NGB to the north.

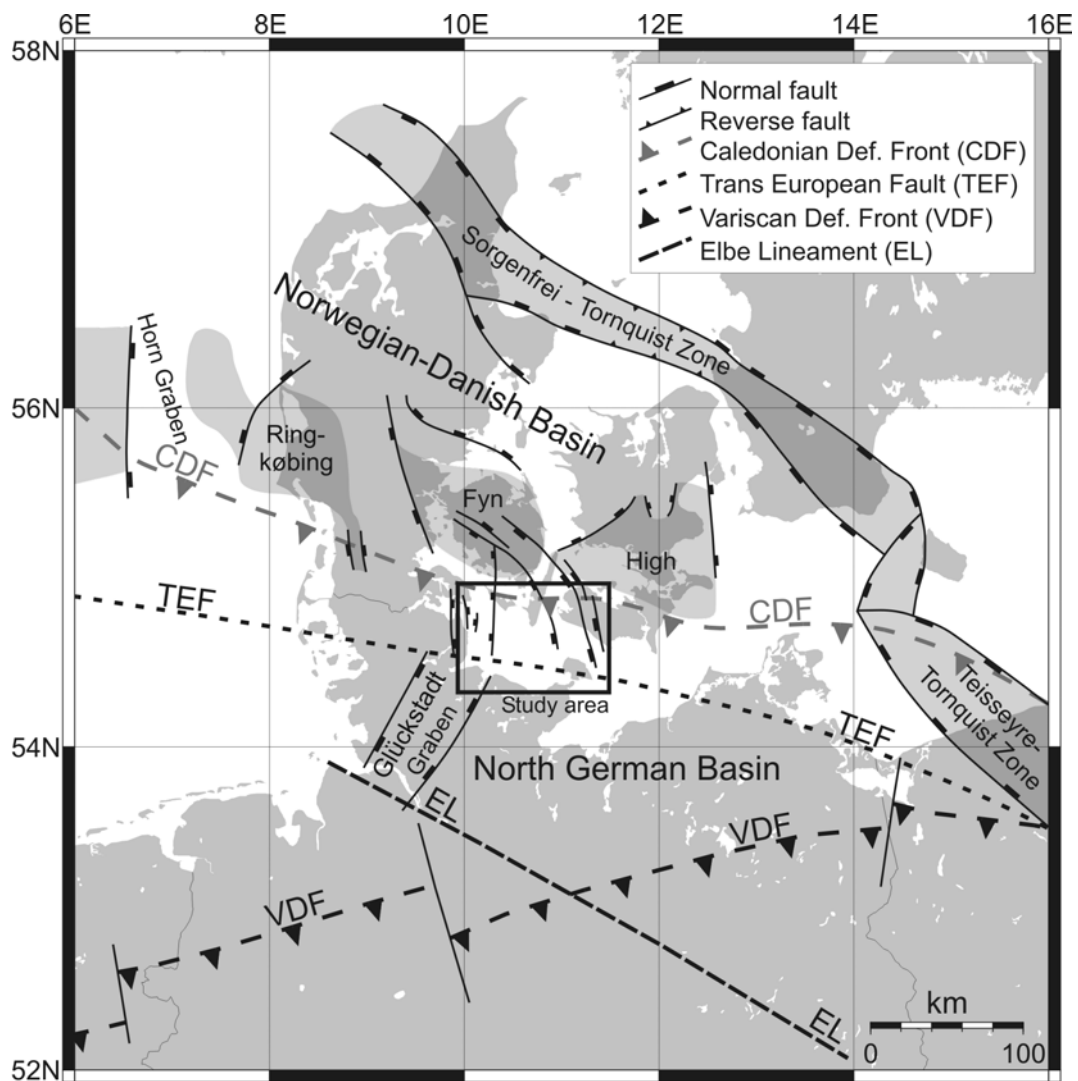


**Fig. 4.1** Location of the study area and the main structural elements of the region (after Krauss, 1994; Vejrbæk, 1997; Bayer et al., 1999; Clausen and Pedersen, 1999)

The southern flank of the RFH is more or less identical to the path of the Caledonian Deformation Front (CDF). To the south, the NGB terminates at the Variscan Deformation Front (VDF) and to the east at the Teisseyre-Tornquist Zone (TTZ). Furthermore, two approximately E-W striking structural lineaments cross the NGB: The so-called Trans European Fault (TEF) and the Elbe Lineament (EL) further to the south.

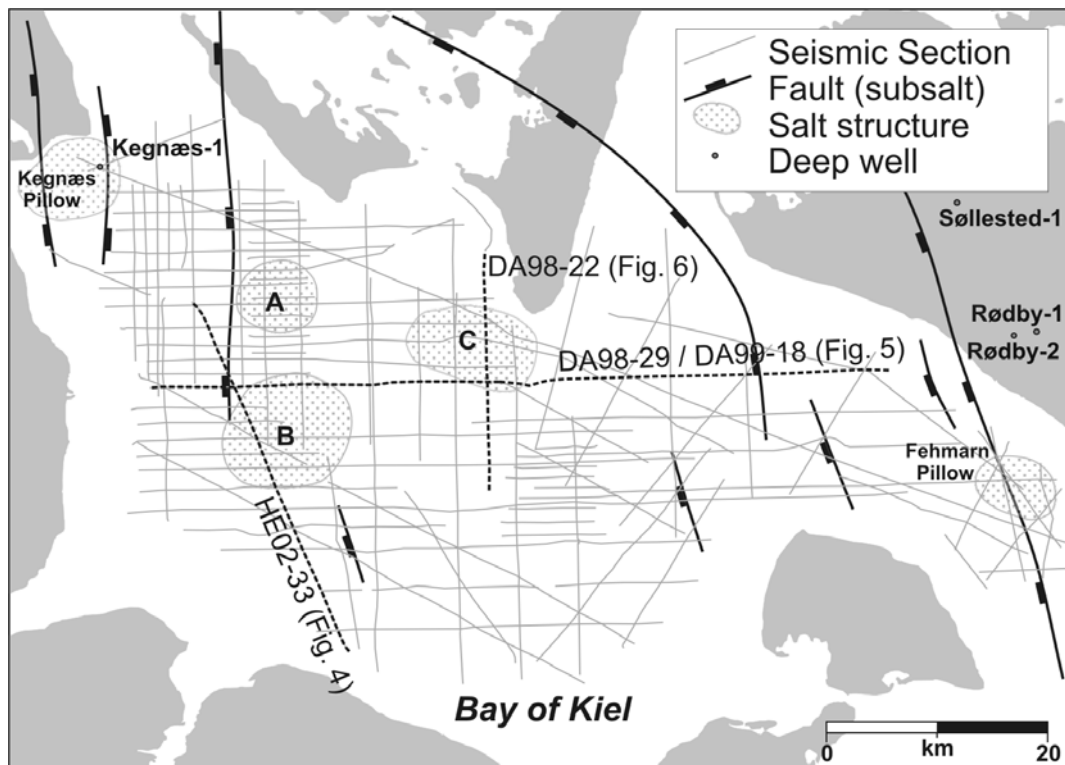


**Fig. 4.2** Map of the study area, showing the positions of the seismic sections and the deep wells used in this work. The positions of the salt structures are based on Vejgåk (1997), Clausen and Pedersen (1999) and this study. The positions of the sub-salt faults are from Vejgåk (1997).

The initial main phase of thermal subsidence in the NGB began in Early Permian and continued until the Middle Triassic (van Wees et al., 2000). The lowermost deposits consist of Carboniferous-Permian volcanics and aeolian, fluvial and shallow-lake sediments overlain by Upper Permian (Zechstein) evaporites (Scheck and Bayer, 1999). The Zechstein evaporite sequence developed as a result of a series of marine transgressions into the intracontinental basin from the north after a period of terrestrial condition (Ziegler, 1990; Kossow et al., 2000). The Triassic succession is characterised by a Lower Triassic red-bed clastic sequence (Buntsandstein), deposited rapidly under terrestrial conditions and overlain by marine carbonates (Muschelkalk) (Kossow and Krawczyk, 2002). A sea level drop during the Late Triassic (Keuper) led to renewed terrestrial sedimentation (Nöldeke and Schwab, 1976). The Triassic succession was overlain by a Lower Jurassic sequence, deposited under shallow-marine conditions (Gearhart Geo Consultants, 1985). The subsidence pattern of the NGB was interrupted by a period of uplift from the Middle Jurassic to Early Cretaceous (Ziegler, 1990;

Underhill, 1998). As a result of the uplift, parts of the Lower Jurassic and Upper Triassic sedimentary sequences were eroded (Kossow et al., 2000). Sedimentation resumed towards the end of the Early Cretaceous (Albian) with the deposition of a terrestrial clastic sequence followed by Upper Cretaceous marine marls and carbonates, indicating a period of tectonic quiescence and rising sea level (Kossow and Krawczyk, 2002). Towards the end of the Late Cretaceous and during the Palaeogene the NGB was inverted as a result of several inversion pulses related to the Alpine Orogeny (Ziegler, 1990; Krauss, 1994). The Cenozoic succession shows a facies pattern of terrestrial and shallow-marine clastic sediments deposited under strong influence of halokinesis (Kossow et al., 2000).

## **4.4 Database**

### **4.4.1 High-resolution multichannel seismic data**

During 1998-2000, the University of Aarhus (AU) onboard R/V Dana acquired parts of the high-resolution multichannel seismic sections used in this study as part of the BaltSeis project (survey names: DA98, DA99, DA00). The seismic equipment for these three surveys consisted of a 70 cubic inch, 100 bar sleeve gun cluster fired every 12.5m, and a 48-channel streamer (300m long) with a hydrophone group separation of 6.25m. This configuration gives a common mid point distance of 3.125m. Source and receivers were towed 3m below the sea surface.

The data acquisition was continued by the University of Hamburg in cooperation with AU between 2001 and 2003 onboard R/V *Alkor* (AL 185, AL 225) and R/V *Heincke* (HE 172) (survey names: AL01, HE02, AL03) as a part of the NeoBaltic project. During the HE 172 cruise, the same source configuration was used, but this time a 96-channel streamer (600m long) with the same hydrophone group separation was used.

On the 2003 AL 225 cruise, a single 105 cubic inch, 140 bar, G-gun, fired every 12.5m, was used, along with the 96-channel streamer. The data were recorded digitally on all five cruises and sampled every 1ms, with a recording length between 2-3 seconds. The penetration is in the order of 1.5-2s two-way travel time (TWT) for all the profiles. The vertical resolution of the seismic data is between 8-10m whereas the horizontal resolution is in the order of 20-25m.

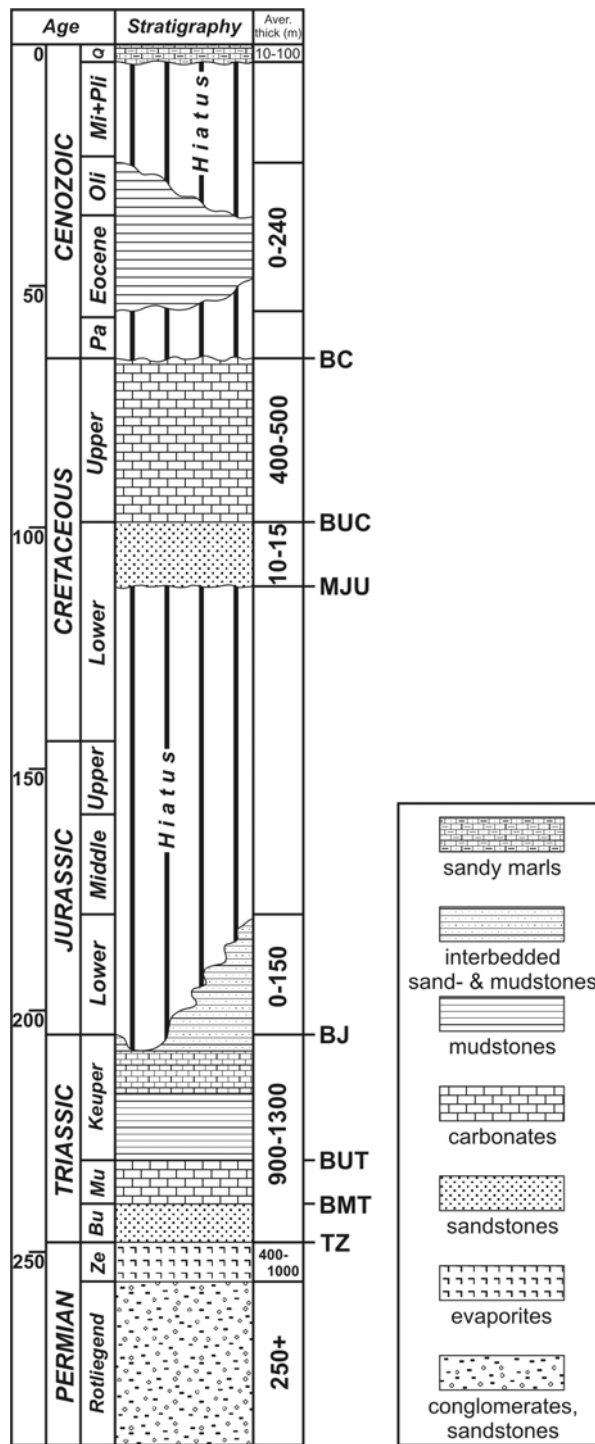


**Fig. 4.3** Stratigraphic table showing the dominant lithologies, average thicknesses and the ages of the major horizons interpreted in the northern part of the North German Basin. The thickness data are from Nielsen and Japsen (1991). TZ: Top Zechstein, BMT: Base Middle Triassic, BUT: Base Upper Triassic, BJ: Base Jurassic, MJU: Mid Jurassic Unconformity, BUC: Base Upper Cretaceous, BC: Base Cenozoic.

#### **4.4.2 Well data**

The stratigraphic report of the offshore Kegnæs-1 exploration well (Gearhart Geo Consultants, 1985) and stratigraphic information from the three onshore exploration wells, Søllested-1, Rødby-1 and Rødby-2 (Fig. 4.2) (Nielsen and Japsen, 1991), were used for correlating the different interpreted horizons on the seismic profiles.

### **4.5 Stratigraphic interpretation**

Using the data from the offshore exploration well Kegnæs-1 (Gearhart Geo Consultants, 1985), situated in the northwestern corner of the survey area (Fig. 4.2), it was possible to date six major horizons traced across the entire survey. These are: Base Middle Triassic (BMT), Base Upper Triassic (BUT), Base Jurassic (BJ), Mid Jurassic Unconformity (MJU), Base Upper Cretaceous (BUC) and Base Cenozoic (BC). It was only possible to trace the Top Zechstein (TZ) horizon on a few sections. In addition, some internal reflectors within the Upper Triassic, Upper Cretaceous and the Cenozoic successions were used for the structural and depositional interpretation. A stratigraphic table is presented in Figure 4.3.

#### **4.5.1 Sedimentary sequences (Fig. 4.3)**

##### **Lower Triassic (Buntsandstein)**

This sequence, bounded by the TZ and BMT horizons, consists of fluvial to lacustrine sediments and playa-lake deposits (Scheck and Bayer, 1999). Due to the limited penetration on the seismic sections, the TZ reflection in this succession is only well defined on a few profiles.

##### **Middle Triassic (Muschelkalk)**

This sequence comprises carbonates deposited during transgressive to shallow marine conditions (Gearhart Geo Consultants, 1985), bounded by the BMT and BUT reflectors. This is the oldest sedimentary sequence that is traceable around the entire survey area.

### **Upper Triassic (Keuper)**

This sequence is a succession of limnic-fluvial and playa-type sediments (Scheck and Bayer, 1999). The base of this sequence is defined by the BUT horizon. In the central parts of the study area, the Upper Triassic sequence truncates at the MJU horizon, while in the marginal areas the BJ reflector is its upper boundary. In addition, two internal reflectors were also traced within this succession.

### **Jurassic**

Three successions of Jurassic sediments were interpreted in different places within the survey area, but unfortunately none of them are located in areas with deep well control. The BJ reflector bounds the base of the sequence and upward it is truncated by the MJU horizon, in accordance with an Early Jurassic age. According to Kossow et al. (2000), the Lower Jurassic sequence in the North German Basin consists of interbedded marine mud and sandstones.

### **Lower Cretaceous**

This is a thin succession of homogenous thickness, traceable over the entire study area. The MJU and BUC reflectors bound the sequence. The base marks a major transgression of Albian age from non-deposition to shallow marine conditions (Gearhart Geo Consultants, 1985; Kossow et al., 2000). The sequence consists of calcareous sediments, primarily red marls.

### **Upper Cretaceous**

This sequence is bound by the BUC and BC reflectors and consists of chalk sediments deposited during shallow marine becoming open marine conditions. The sequence is successfully mapped over the entire study area. The upper boundary marks an unconformity (Gearhart Geo Consultants, 1985; Kossow et al., 2000). Two internal reflectors within this succession were also traced throughout the survey area.

### **Cenozoic**

This sequence, which is basally bound by the BC horizon and is present at the seafloor, consists of brackish marine clay-silt sediments (Scheck and Bayer, 1999) of Tertiary age, deposited under strong influence of salt movement (Kossow et al.,

2000). The succession consists of Quaternary glacial deposits at the top. Three internal horizons within the sequence were also traced.

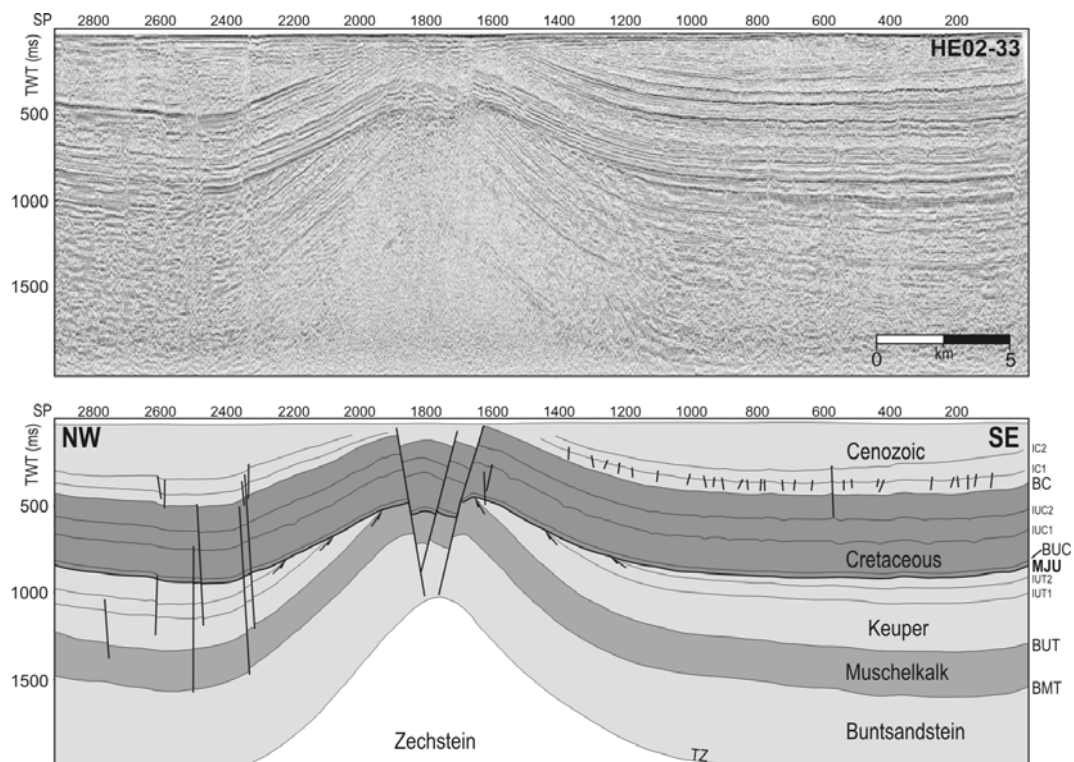


**Fig. 4.4** Time-migrated seismic section HE02-33 (see Fig. 4.2 for location) and interpreted section crossing Salt Pillow B in the southwestern corner of the Bay of Kiel. The section shows that the fault system above the salt structure developed thin-skinned as a result of halokinesis. TZ: Top Zechstein, BMT: Base Middle Triassic, BUT: Base Upper Triassic, IUT1 & 2: Internal Upper Triassic 1 & 2, MJU: Mid Jurassic Unconformity, BUC: Base Upper Cretaceous, IUC 1 & 2: Internal Upper Cretaceous 1 & 2, BC: Base Cenozoic, IC 1 & 2: Internal Cenozoic 1 & 2.

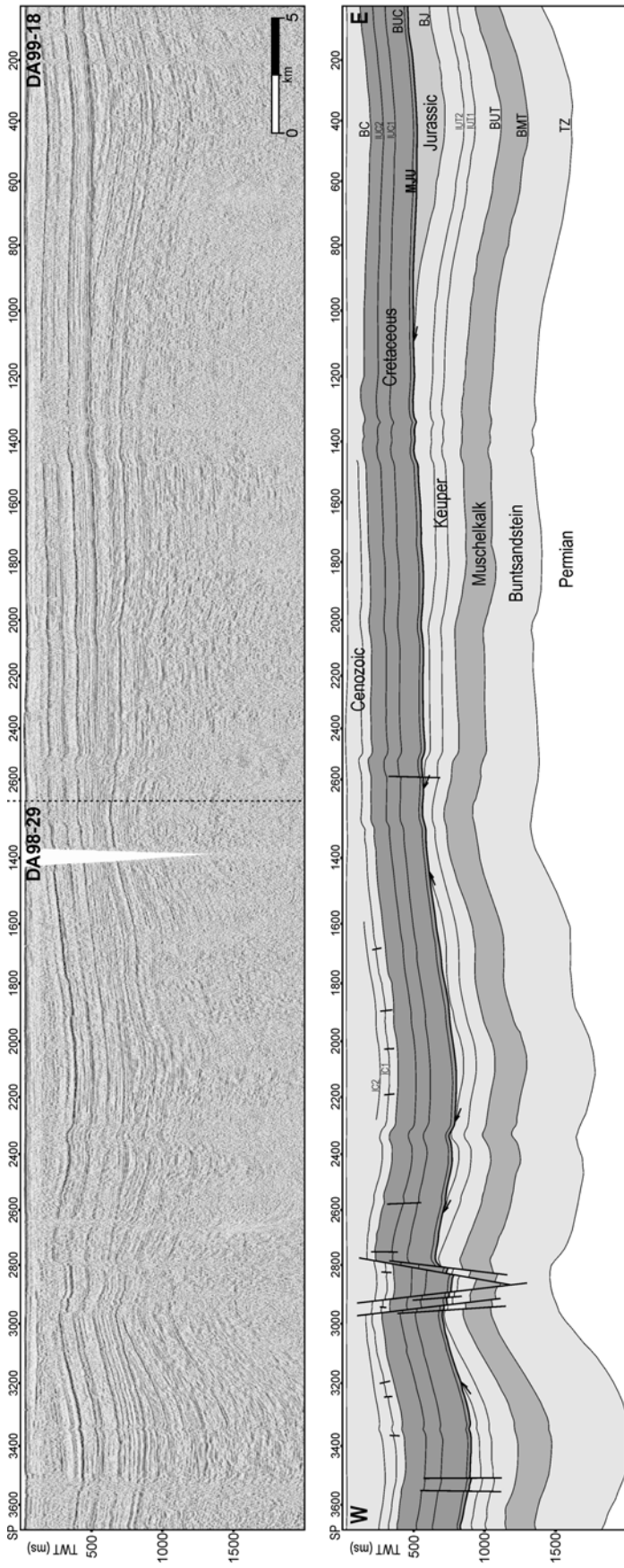


**Fig. 4.5** Time-migrated seismic section (compilation of line DA98-29 and line DA99-18) and interpreted section (see Fig. 4.2 for location) of an E-W directed line across the Bay of Kiel. The general distribution reveals how the angular Mid Jurassic Unconformity separates the Triassic and the Jurassic successions from the Cretaceous and the Cenozoic successions. The entire Mesozoic and Cenozoic succession have been deposited under the influence of halokinesis. TZ: Top Zechstein, BMT: Base Middle Triassic, BUT: Base Upper Triassic, IUT1 & 2: Internal Upper Triassic 1 & 2, BJ: Base Jurassic, MJU: Mid Jurassic Unconformity, BUC: Base Upper Cretaceous, IUC 1 & 2: Internal Upper Cretaceous 1 & 2, BC: Base Cenozoic, IC 1 & 2: Internal Cenozoic 1 & 2.

## 4.5.2 Seismic stratigraphy

Figures 4.4, 4.5 and 4.6 show examples of interpreted seismic sections in the study area (for location see Fig. 4.2). All three profiles show that the Mesozoic and Cenozoic strata were deposited under the influence of salt movement. Furthermore it can be seen that an angular unconformity (MJU) at depths between 500 and 1000ms separates the Cretaceous and Cenozoic successions from older strata. In the central part of the Bay of Kiel it is Upper Triassic strata that truncates at the MJU horizon (Fig. 4.4 and 4.6), while a succession of Lower Jurassic sediments is preserved in the eastern part of the study area (Fig. 4.5).

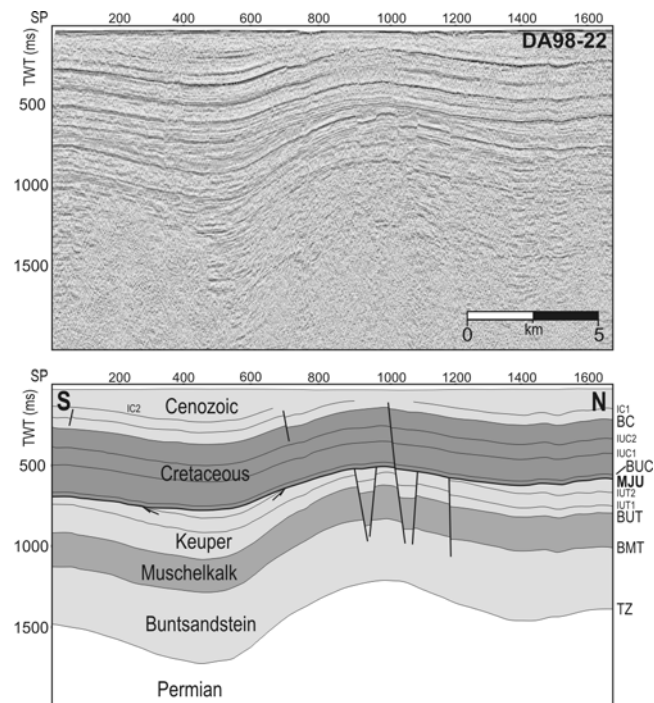


**Fig. 4.6** Time-migrated seismic section DA98-22 (see Fig. 4.2 for location) and interpreted section crossing Salt Pillow C in the northern part of the Bay of Kiel. The section reveals how most of the individual faults of the fault system on top of the salt structure terminate at the Mid Jurassic Unconformity. TZ: Top Zechstein, BMT: Base Middle Triassic, BUT: Base Upper Triassic, IUT1 & 2: Internal Upper Triassic 1 & 2, BJ: Base Jurassic, MJU: Mid Jurassic Unconformity, BUC: Base Upper Cretaceous, IUC 1 & 2: Internal Upper Cretaceous 1 & 2, BC: Base Cenozoic, IC 1 & 2: Internal Cenozoic 1 & 2.

## **4.6 Geological evolution**

### **4.6.1 Methods**

The interpretation of the depositional and structural evolution of the Bay of Kiel is based on the created time-structure maps (Fig. 4.7 and 4.8), time-isochore maps (Fig. 4.9 – 4.13) and the restored sections of seismic profile HE02-33 (Fig. 4.14). The time-structure maps show the present day vertical depth in two way travel time (TWT) to the specific surfaces. These were used to map out the position of important salt structures and to identify the trends of different fault systems. The time-isochore maps show the present day vertical thickness in TWT of given sedimentary sequences bounded by two specific surfaces. These maps were used to determine periods of active faulting, salt movement and the trends of local palaeo-depocenters. Generally, for both types of map, only the fault trends that can be traced from line to line across the survey have been included.

The restoring method used in Figure 4.14 is a simple 2D model backstripping, with the assumption that all sedimentary layers are deposited horizontally. In this model, neither volumetric proportions, nor compaction, have been taken into consideration.

Because of the limited penetration of the seismic data, it has not been possible to map the Top Rotliegend surface underneath the Zechstein evaporites, and the Top Zechstein surface has only been traceable on few of the seismic sections. Thus, it is not been possible to give any volumetric estimate of the degree of salt movement in the study area. Because of the limited mapping of the Top Zechstein horizon on the HE02-33 line, the backstripping is made with the assumption that the Lower Triassic sequence (Buntsandstein) is deposited with an almost homogenous thickness across the seismic section.

### **4.6.2 Present day structures**

The BMT surface (Fig. 4.7) displays a gentle dip towards the south and southwest towards the centre of NGB from basin margin in the north. The general dip of the surface is disturbed by several anomalies, interpreted to be the result of halokinesis. In the western part three anomalies are seen where the surface is elevated to between 500-900ms TWT.

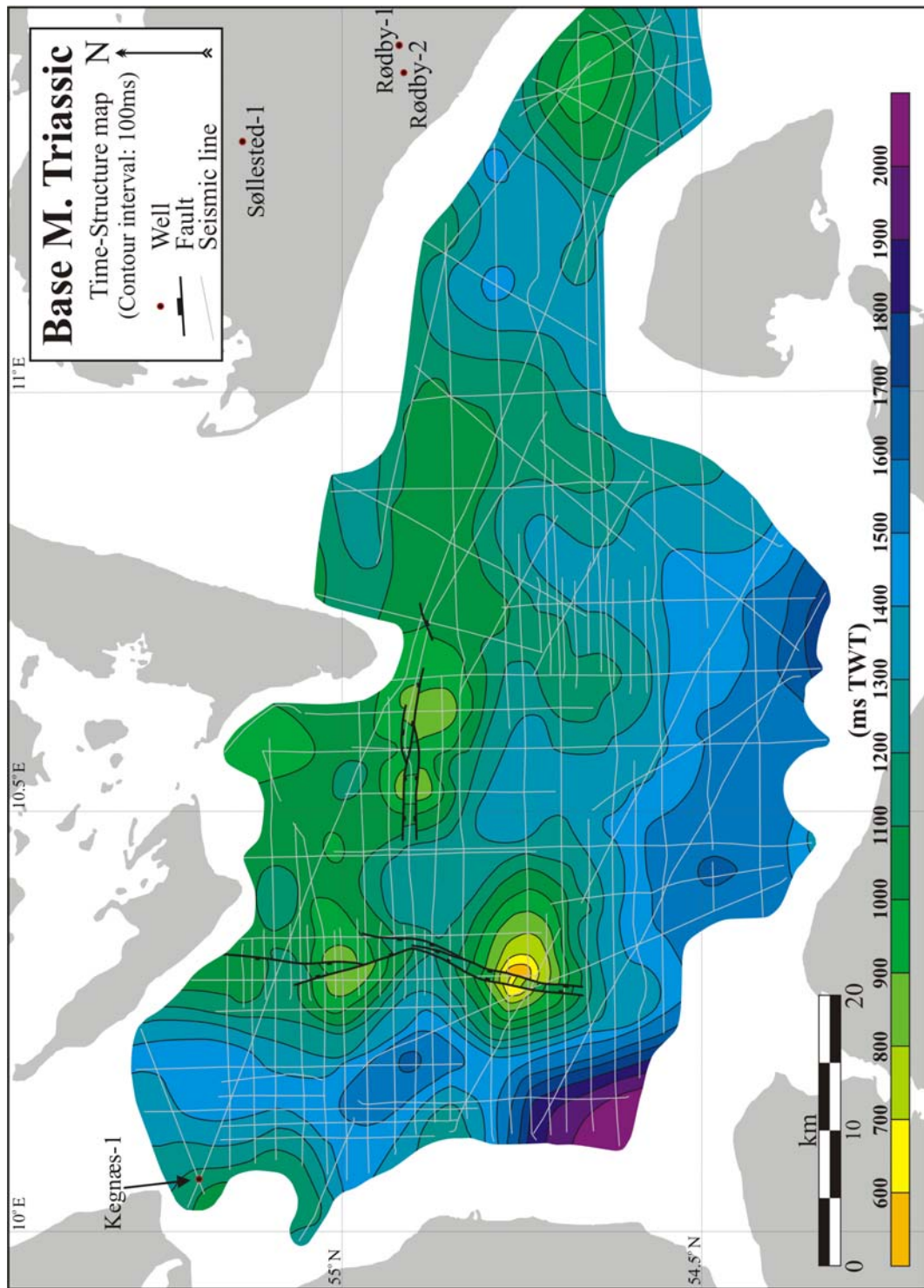


**Fig. 4.7** Time-structure map of the Base Middle Triassic (Base Muschelkalk) surface in ms TWT. Contour interval is 100 ms. Wells referred to in the text are also shown. The orange colour shows the shallowest part of the surface on top of Salt Pillow B whereas the purple colour shows the deepest part in the southwestern corner.

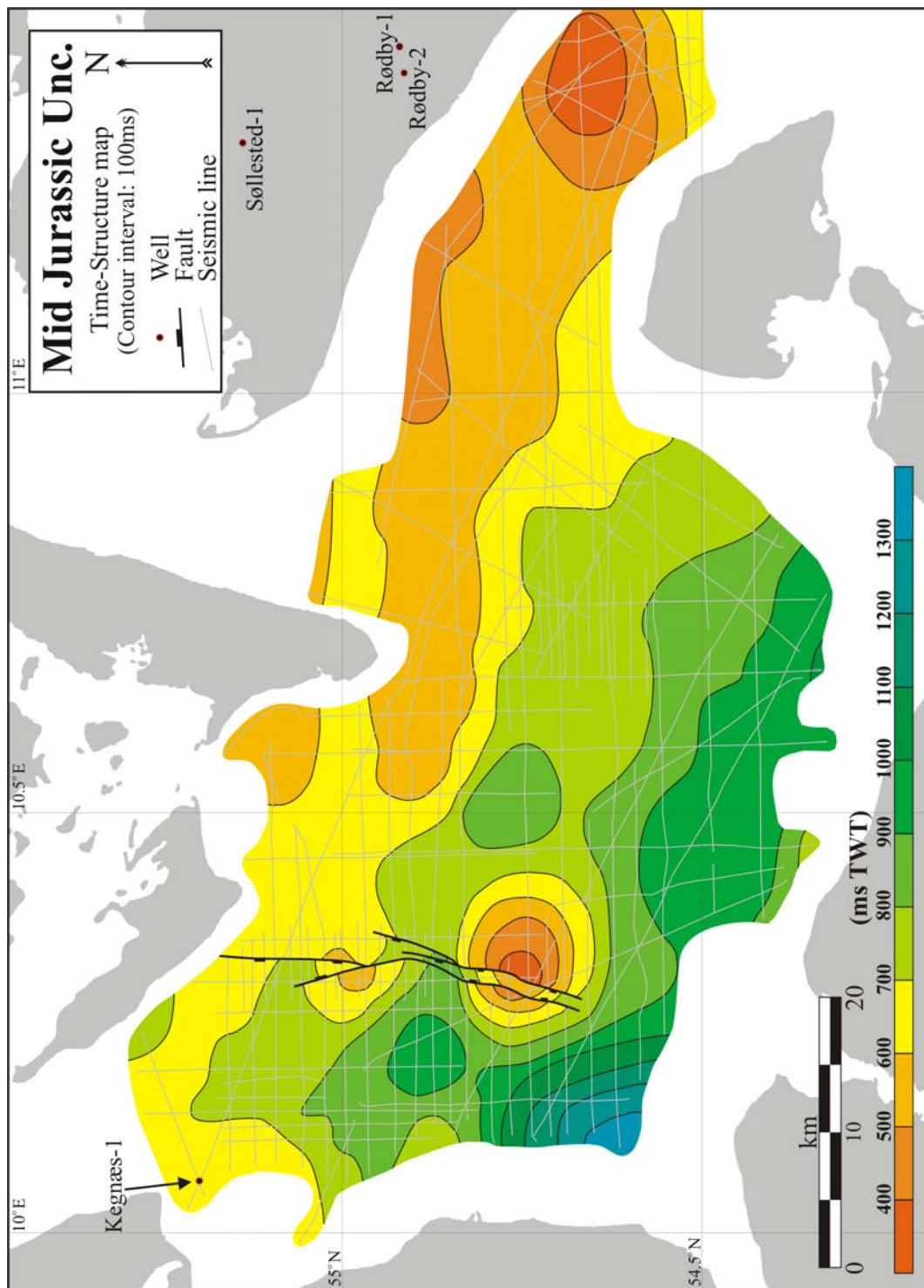


**Fig. 4.8** Time-structure map of the Mid Jurassic Unconformity surface in ms TWT. Contour interval is 100 ms. Wells referred to in the text are also shown. The dark orange colour shows the shallowest parts of the surface on top of Salt Pillow B and the Fehmarn Pillow whereas the blue colour shows the deepest part in the southwestern corner.

These three updomed areas will subsequently be referred to as Salt Pillow A, B and C (Fig. 4.2). Besides these, two other salt structures will also be referred in the interpretation below, the Kegnæs Pillow (Clausen and Pedersen, 1999) and the Fehmarn Pillow (Nielsen, 1998). The positions of these salt structures are shown on Figure 4.2 along with the sub-salt fault trends (Vejbæk, 1997).

Two different fault systems cut the BMT surface: one striking N-S crossing Salt pillows A and B, and one striking E-W on top of Salt pillow C. A maximum displacement of more than 200ms TWT on the N-S striking fault system is seen on top of Salt Pillow B. The maximum displacement of the E-W striking fault system is seen to be a little more than 100ms TWT.

As with the BMT surface, the MJU surface (Fig. 4.8) also shows a general dip from the north-northwest towards the south-southeast. The surface dip is disturbed by a few anomalies in the western part of the study area. Again these are interpreted to be a result of salt withdrawal from the deeper areas, into Salt Pillows A and B. Another clear anomaly is seen in the eastern part of the region around the Fehmarn Salt Pillow. The shallowest parts of the MJU surface (less than 400ms TWT) is found on top Salt Pillow B and the Fehmarn Salt Pillow, while the deepest part (more than 1300ms TWT) is found in the southeastern corner towards the centre of the basin.

The MJU surface is cut by the same N-S trending fault system as the BMT surface (Fig. 4.4, 4.5 and 4.7). The maximum displacement is more than 100ms TWT on top of Salt Pillow B. The E-W striking fault system on the BMT surface is seen to terminate underneath this surface (Fig. 4.6), showing that the active faulting within this system ceased before the Albian Transgression. On Figure 4.6 it is seen that one fault in the E-W striking system cuts the MJU surface with a minor displacement, but this has only been detected on this particular seismic section and is therefore not considered as a general fault trend in the post MJU sediments.

### **4.6.3 Early Triassic (Buntsandstein)**

Because of the limited resolution of the Top Zechstein reflector it is difficult to conclude on the general distribution of the Buntsandstein sequence in the Bay of Kiel. Figure 4.5 shows a thickening of the succession in at westwards direction, without any thinning anomaly on the northern flank of Salt Pillow B. The same trend is seen across Salt Pillow C (Fig. 4.6). Based on these observations, it is supposed that the Lower Triassic terrestrial red beds were deposited in the Bay of Kiel during a period of relative tectonic quiescence. The westward thickening is a

result of greater subsidence towards the centre of the NGB southwest of the study area.

#### **4.6.4 Middle Triassic (Muschelkalk)**

The time-isochore map of the Middle Triassic (Fig. 4.9) shows an overall thickness of between 100-300ms TWT, with an average of between 200 and 250ms. The higher degree of subsidence away from the basin margin is seen as a general thickening trend towards the centre of the basin in the southwards direction. The three thickness anomalies observed over the Kegnæs Pillow and Salt Pillow A and B provide a clear indication that the initial vertical salt movement into these structures began during the Middle Triassic. This is supported by the slight thinning of the Middle Triassic succession over Salt Pillow B in the BUT restored section (Fig. 4.14a).

It should be mentioned that the thin succession on top of Salt Pillow B is the result of later erosion, (see Fig. 4.14d), and not due to a more accelerated halokinesis in this particular structure.

The randomly distributed four areas of thicker Middle Triassic successions around Salt Pillow A and B than on top of the structures, gives no specific indication of the direction of the salt movement. It is supposed that the Muschelkalk sequence was deposited under constant subsidence and under the influence of salt movement initiation in the western part of the Bay of Kiel.

#### **4.6.5 Late Triassic (Keuper)**

Due to the erosion of the Upper Triassic sequence (Fig. 4.10) in the western part of the study area it has not been possible to describe an overall distribution pattern for this succession. In the areas without erosion, thicknesses of more than 300ms TWT are seen, with an exception on top of the Fehmarn Pillow. Within the area of erosion, the thickness varies from zero on top of Salt Pillow B to more than 450ms TWT in the southern part of the Bay of Kiel. The thinnest successions are found on top of Salt Pillows A, B and C and the thickest successions in the local depocentres between the salt structures.

The more abrupt thickness variation of the succession around the E-W striking fault system on top of Salt Pillow C shows that this system developed during the Late Triassic.

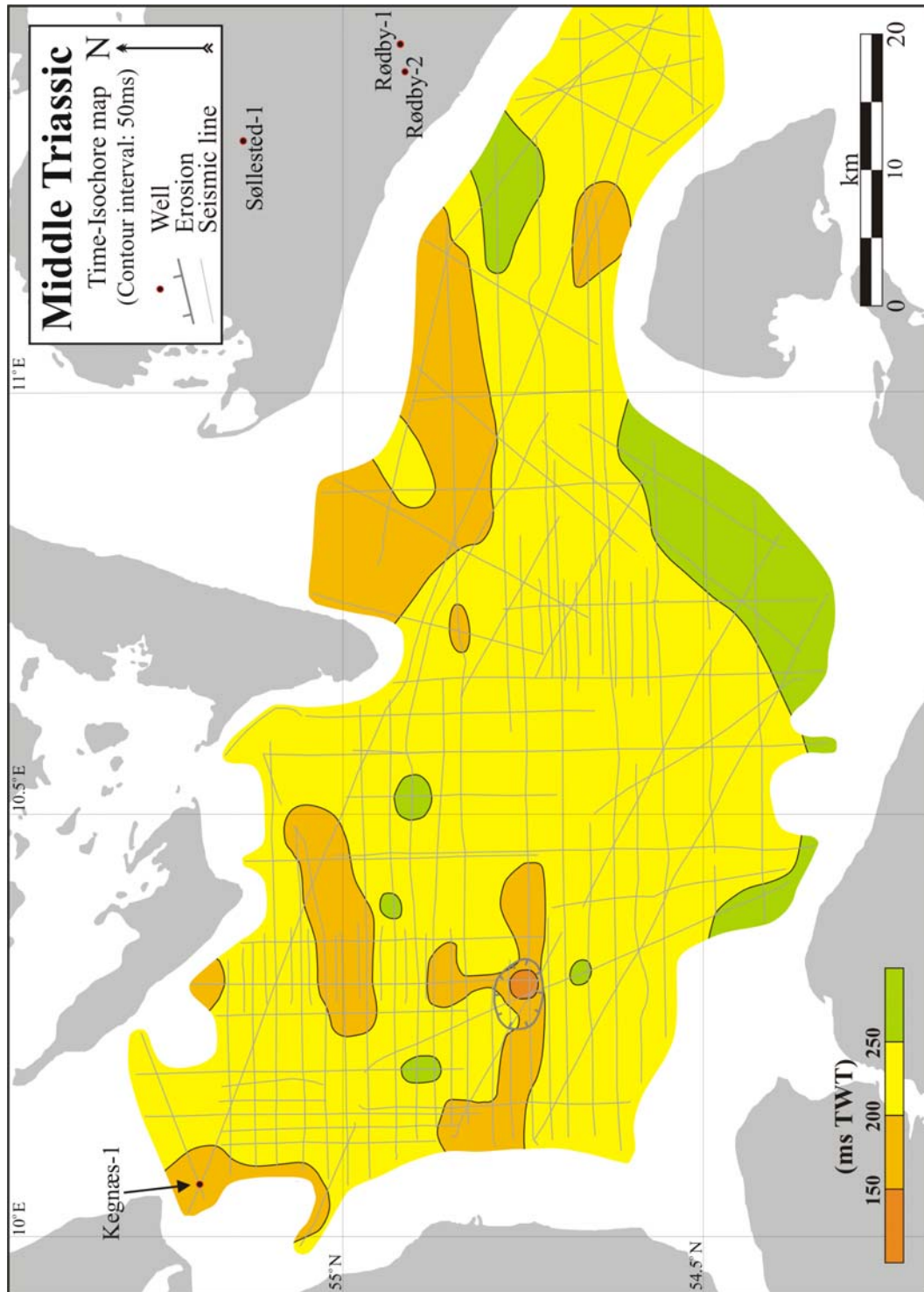


**Fig. 4.9** Time-isochores map of the Middle Triassic (Muschelkalk) succession in ms TWT. Contour interval is 50 ms. Wells referred to in the text are also shown. The orange colour shows the thinnest part of the succession on top of Salt Pillow B whereas the light green colour shows the thickest parts. The thick grey line around Salt Pillow B marks the area where the succession has been exposed to later erosion.

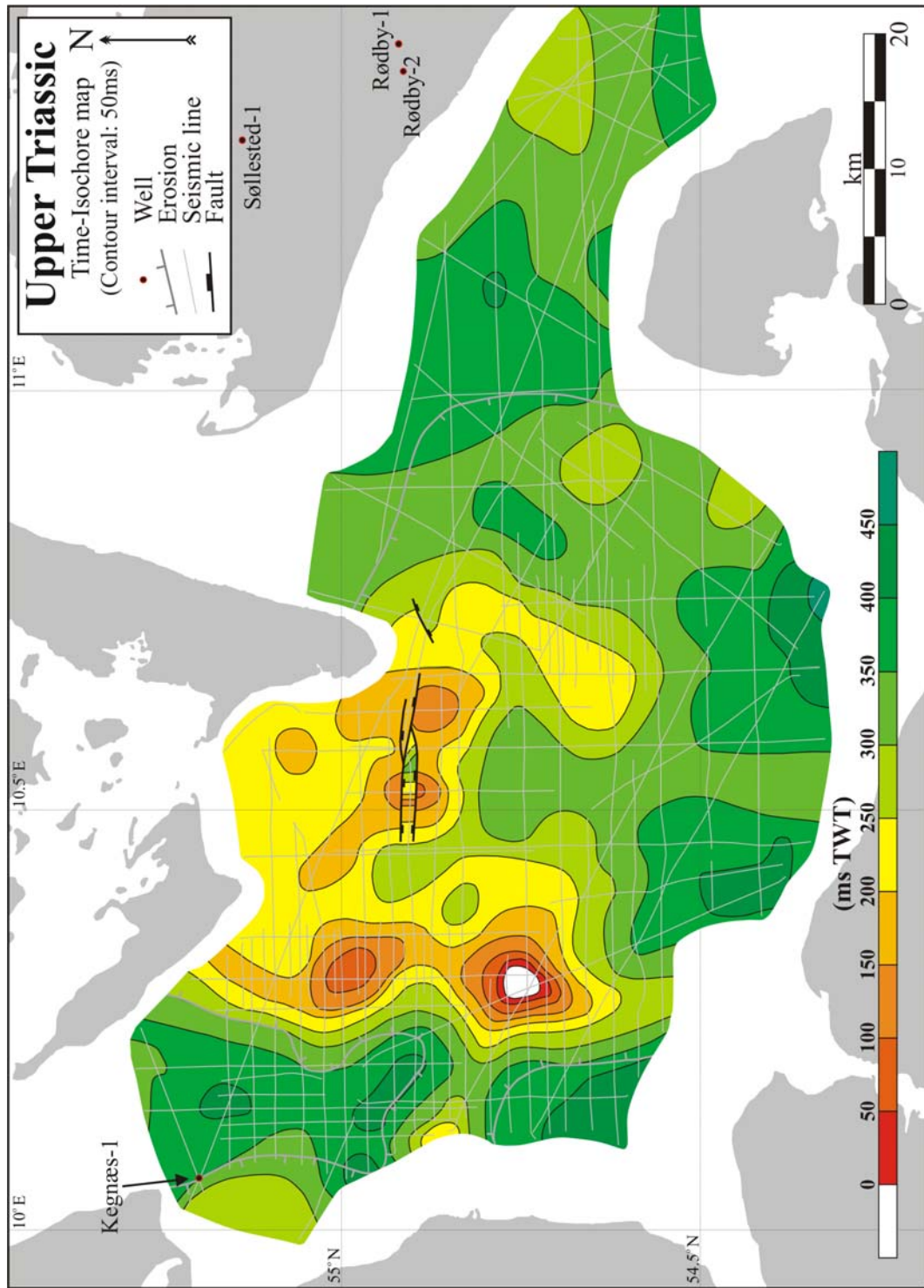


**Fig. 4.10** Time-isochore map of the Upper Triassic (Keuper) succession in ms TWT. Contour interval is 50 ms. Wells referred to in the text are also shown. The red-orange colours show the thinnest parts of the succession on top of Salt Pillow A, B and C whereas the dark green colour shows the thickest parts in the rim synclines between the salt structures. The thick grey line marks the area where the succession has been exposed to later erosion.

Even though the Upper Triassic succession was later subject to erosion (Fig. 4.4, 4.5 and 4.6), the general present day thickness variation throughout the study area shows that the sequence was deposited under the influence of vertical salt movement from the areas with a thick succession into the salt structures. This interpretation is supported by the clear thinning of the succession bound by the internal Upper Triassic horizons on top of Salt Pillow B (Fig. 4.14).

By comparing the position of the depocentres with the position of the salt structures it can be seen that the evaporites presumably moved in a preferred east-west direction into the structures an indication for an east-west main stress direction. This is supported by the direction of the east-west striking fault system over Salt Pillow C. This fault system developed as a result of localised north-south directed thin-skin extension over the structure, resulting from the upward salt movement.

#### **4.6.6 Early Jurassic**

According to Nielsen and Japsen (1991), the Jurassic sediments recovered from the four deep wells in the study area are all of Early Jurassic age and the upper boundary succession is characterised by an erosional surface of presumably Middle Jurassic age. Figure 4.11 therefore only shows the present day thickness variation of the Lower Jurassic sequence in the Bay of Kiel.

Lower Jurassic sediments are preserved in two areas in the western part of the region, and in the entire eastern part. On Figure 4.11 it is seen that the two Early Jurassic packages in the western part of the study area are located in rim synclines between salt structures. This shows that the centre of the uplifted area is located to the west of the study area, due to the higher degree of erosion in this direction. The preservation of Lower Jurassic sediments in the rim synclines between the salt structures also suggests that this succession was deposited under the influence of halokinesis. This is deduced using the assumption that the erosion occurred more or less horizontally (Fig. 4.14b).

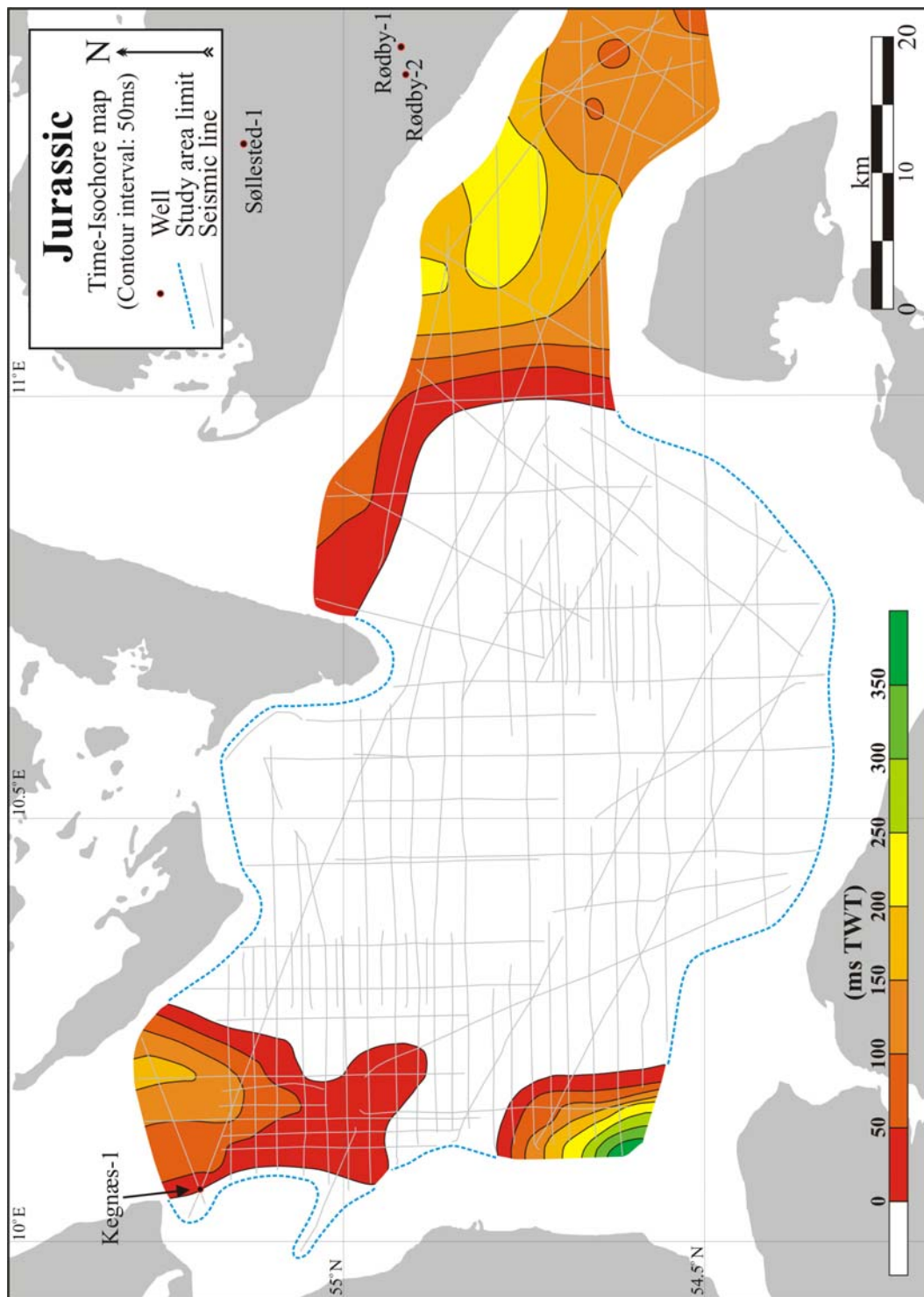


**Fig. 4.11** Time-isochore map of the Jurassic succession in ms TWT. Contour interval is 50 ms. Wells referred to in the text are also shown. The map shows that Jurassic sediments are preserved in the eastern part of the study area and in two pockets in the western part.

#### **4.6.7 Middle Jurassic – Early Cretaceous**

Due to the absence of Middle and Upper Jurassic and Lower Cretaceous sediments, it can only be concluded that the study region was an area of non-deposition during these time intervals. It cannot be determined whether the upward salt movement, detected during the Late Triassic and Early Jurassic, continued throughout the Middle and Late Jurassic or if it ceased at the onset of the erosional event. The reason for this is that the MJU flattened section (Fig. 4.14b) reflects the basin geometry at the end of the period of non-deposition.

#### **4.6.8 Cretaceous**

The Cretaceous succession (Fig. 4.12) generally thickens towards the centre of the NGB in the south to southwest, which again is interpreted as the result of greater subsidence in the central part of the NGB. Minor variations are observed on top of the Fehmarn Pillow and Salt Pillow A, whilst more pronounced thickness variations are seen on the top of Salt Pillow B and in the areas to the south and to the west of the structure. These variations are the result of halokinesis.

On all the interpreted seismic sections (Fig. 4.4, 4.5 and 4.6) it is seen that the thin Lower Cretaceous succession was deposited with a very uniform thickness throughout the Bay of Kiel. This observation is supported by the Base Cenozoic restored section of the HE02-33 line (Fig. 4.14c). This shows that the sedimentation resumed in the Bay of Kiel during a period of tectonic quiescence.

Figure 4.14c also shows that the thinning over Salt Pillow B only can be recognised in the upper succession, bound by the IUC1 and the BC horizons, of the Upper Cretaceous sequence. Thus, it can be concluded that the tectonic quiescence detected at the time of resumed sedimentation continued towards the end of the Late Cretaceous where several salt structures were reactivated in the study area.

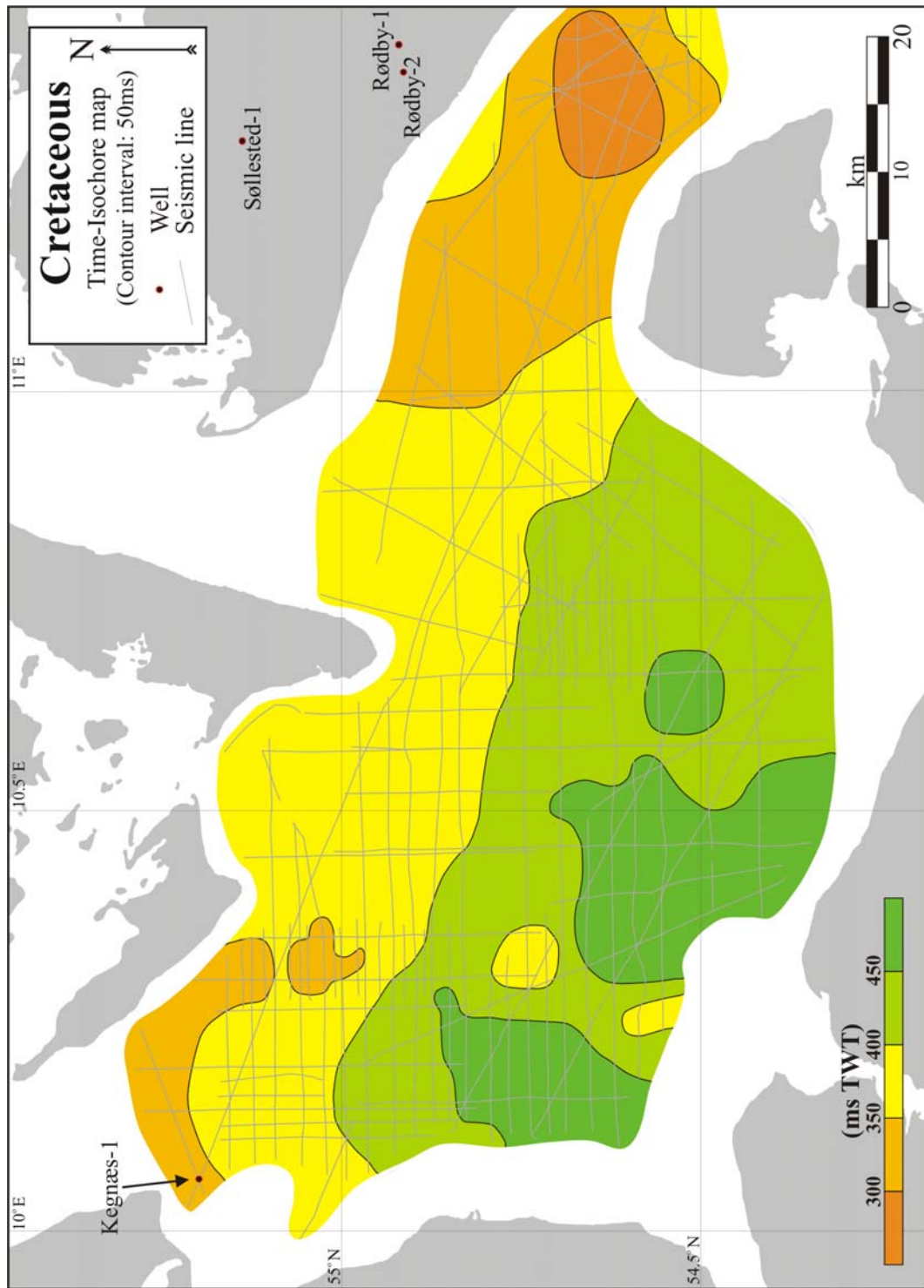


**Fig. 4.12** Time-isochore map of the Cretaceous succession in ms TWT. Contour interval is 50 ms. Wells referred to in the text are also shown. The orange colour shows the thinnest part of the succession on top of the Fehmarn Pillow whereas the green colour shows the thickest parts in the southwestern corner.

#### 4.6.9 Cenozoic

Like the previously described successions, the distribution of the Cenozoic sediments also shows an overall thickening trend towards the centre of the basin in the south to southwest (Fig 4.13). Two pronounced thickness anomalies are seen on top of the Fehmarn Pillow and on top of Salt Pillow B. On the very top of both structures, the Cenozoic succession is actually absent. Furthermore a minor anomaly is seen on top of Salt Pillow A. In addition to the southwestern corner, the thickest successions are found in the rim synclines between the Kegnæs Pillow, Salt Pillow A and Salt Pillow B and southeast of Salt Pillow B. More abrupt thickness variations are detected around the N-S striking fault system crossing Salt Pillow A and B, showing that active faulting took place within this system during the Cenozoic. The thickness anomalies show that the reactivated vertical salt movement observed towards the end of the Late Cretaceous in the structures must have continued throughout the Cenozoic Era (Fig. 4.4, 4.5, 4.6, 4.13 and 4.14d).

On the isochore map of the Cenozoic sequence (Fig. 4.13), it can be seen that the depocentres in the rim synclines between the salt structures reflect a WNW-ESE striking trend. This indicates that the main stress direction at this time was SSW-NNE. The strike direction of the fault system above Salt Pillow A and B (Fig. 4.7, 4.8 and 4.13) also supports this. This fault system developed as a thin-skinned extension on top of the structures as a result of the reactivated vertical salt movement in the region (Fig. 4.14d). Due to the poorly defined reflection pattern within the Cenozoic succession on the seismic profiles and the limited description of the Cenozoic sediments in the reports from the exploration wells in the area (Gearhart Geo Consultants, 1985; Nielsen and Japsen, 1991), it can not be determined whether the vertical salt movement ceased sometime during the Cenozoic Era or if it is still ongoing at the present day.

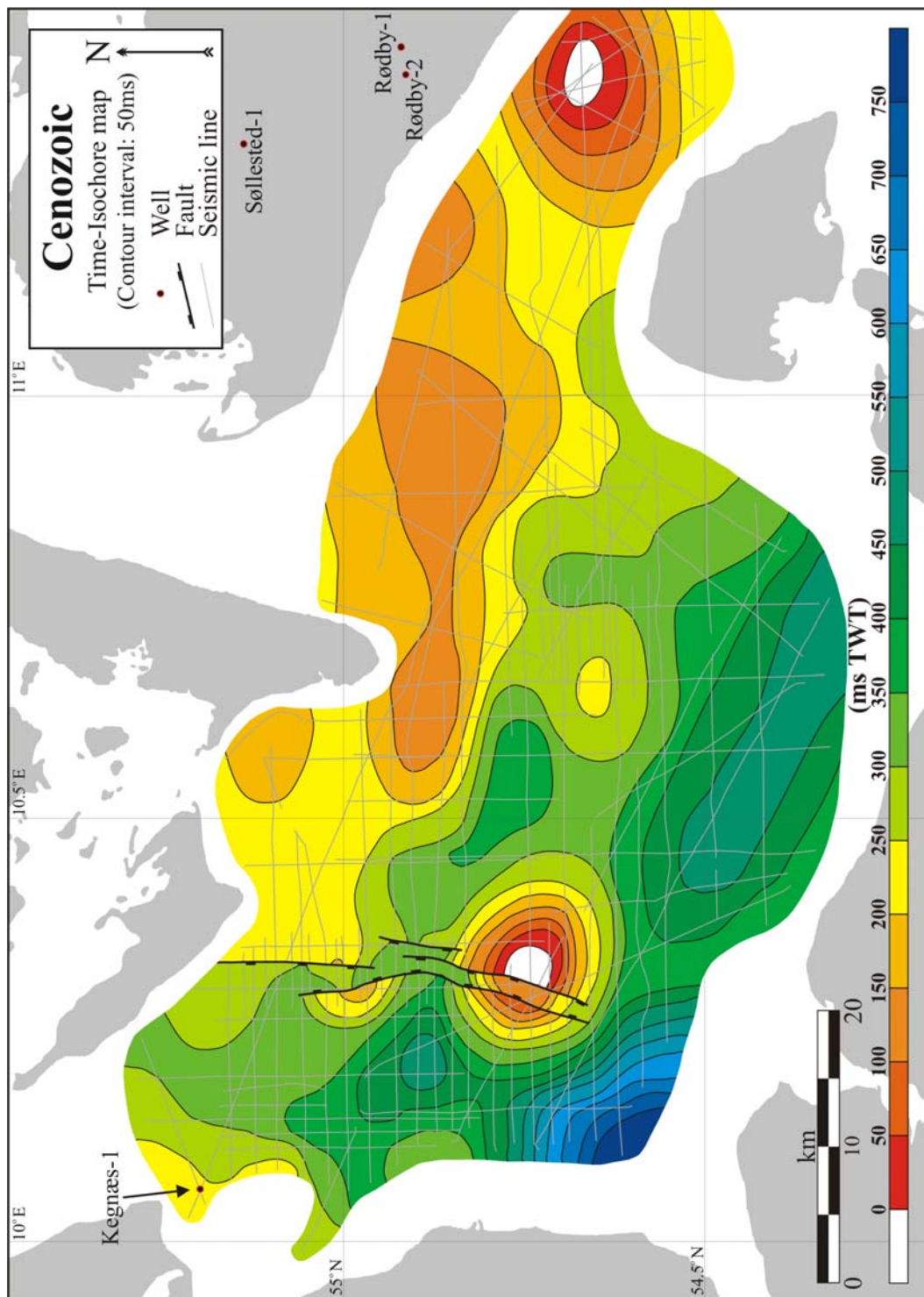


**Fig. 4.13** Time-isochore map of the Cenozoic succession in ms TWT. Contour interval is 50 ms. Wells referred to in the text are also shown. The red colour shows the thinnest parts of the succession on top of the Salt Pillow B and the Fehmarn Pillow and the white colour where the succession is absent. The purple colour shows the thickest part in the southwestern corner.

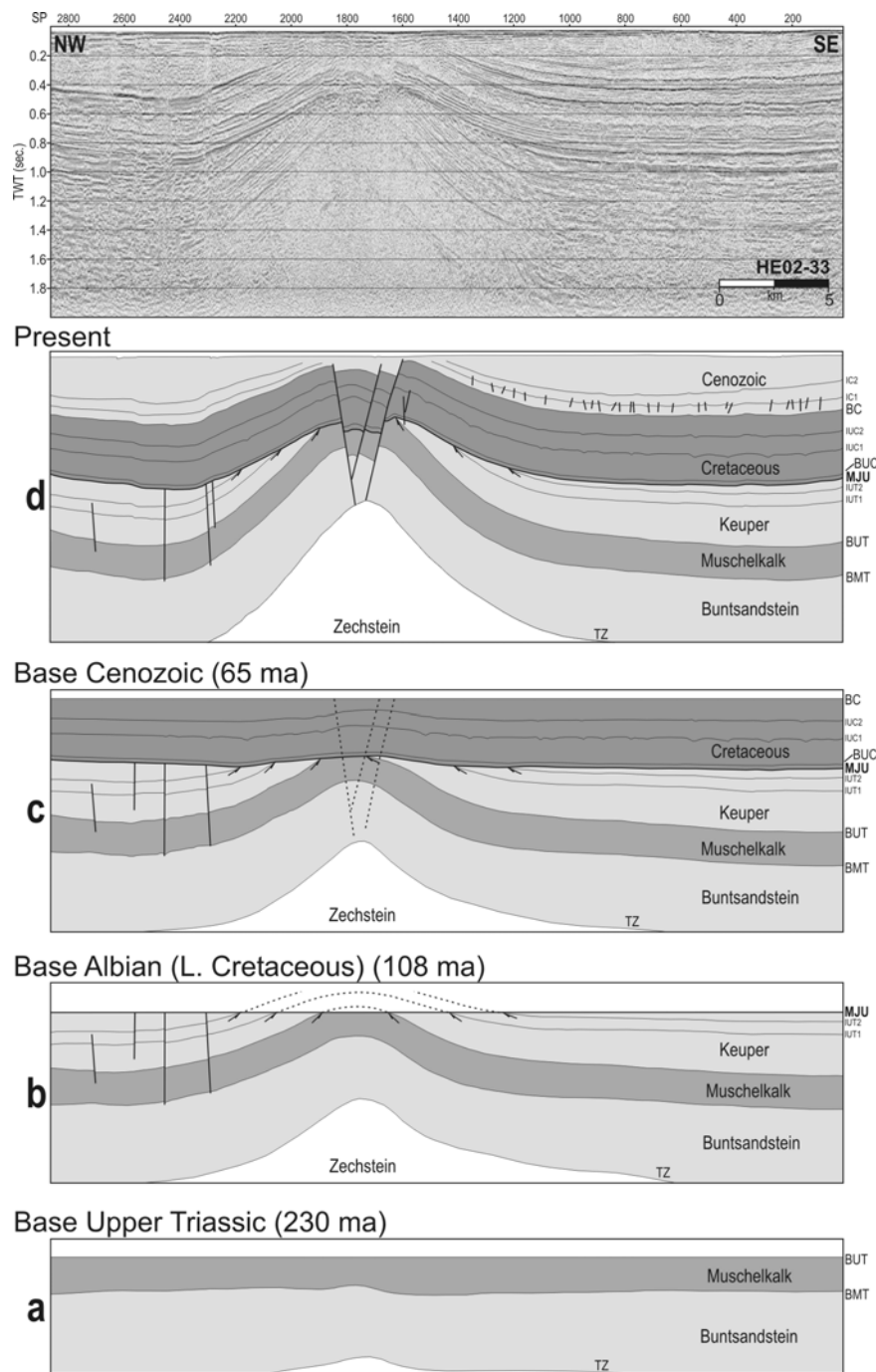


**Fig. 4.14** Structural reconstruction of the seismic line HE02-33 (Fig. 4.4) (see Fig. 4.2 for location). (a) – (d) shows the geometric reconstruction of the section. (b) Shows that the initial salt movement took place during the Late Triassic followed by pronounced erosion. (d) Shows that the salt movement was reactivated during the Cenozoic and caused the thin-skinned faulting above the salt structure. TZ: Top Zechstein, BMT: Base Middle Triassic, BUT: Base Upper Triassic, IUT1 & 2: Internal Upper Triassic 1 & 2, MJU: Mid Jurassic Unconformity, BUC: Base Upper Cretaceous, IUC 1 & 2: Internal Upper Cretaceous 1 & 2, BC: Base Cenozoic, IC 1 & 2: Internal Cenozoic 1 & 2.

## 4.7 Discussion and conclusions

The results of this seismic interpretation of the Bay of Kiel show that the post-Palaeozoic sedimentary deposition took place during two different periods of generally continuous subsidence in the northern part of the NGB. These periods were separated by a period of pronounced uplift and erosion from the Middle Jurassic and towards the end of the Early Cretaceous. The deposition during both periods of subsidence took place under the influence of halokinesis controlled by the regional stress field. The observed sedimentation during the Early and Middle Triassic without major tectonic activity is confirmed by the observations by others in the adjacent areas of the Bay of Kiel (e.g. Scheck and Bayer, 1999; Kossow and Krawczyk, 2002; Scheck et al., 2003a).

The initiation of vertical salt movement on the transition between the Middle and Late Triassic creating N-S trending depocentres and salt structures correlates with the onset of a regional E-W directed extension. This extension is indicated by accelerated subsidence and basement-affected normal faulting in the N-S trending Central Graben and Horn Graben in the North Sea area, the nearby Glückstadt Graben west of the study area, and the development of the Rheinsberg Trough to the southeast of the Bay of Kiel (Ziegler, 1990; Fisher and Mudge, 1998; Scheck et al., 2003b). The E-W directed regional extension during the Late Triassic and Early Jurassic agrees with the assumption that the E-W striking fault system on top of Salt Pillow C (Fig. 4.6, 4.7 and 4.10) developed thin-skinned as a result of vertical salt movement, and not as a basement controlled structure.

The Middle Jurassic to Early Cretaceous period of uplift and erosion removed parts of the Lower Jurassic and Upper Triassic successions within the study area, can be correlated with the development of the Central North Sea Dome due to plutonic activity (Ziegler, 1990, Underhill, 1998). The uplifted area, as a result of the plume, was centred upon what was to become the North Sea rift triple junction (Underhill, 1998). This explains the higher degree of erosion in the westwards direction in the Bay of Kiel towards the centre of the dome. Others have reported the adjacent Northeast German Basin to be an area of non-deposition during the Middle and Upper Jurassic and Lower Cretaceous (Kossow et al., 2000; Kossow and Krawczyk, 2002; Scheck et al., 2003b), which is also seen on the Ringkøbing-Fyn High to the north (Ziegler, 1990). This correlates well with the observations from this study area. The resumed sedimentation towards the end of the Early Cretaceous and the continued subsidence without major tectonic activity during the Late Cretaceous is confirmed by regional scale observations (e.g. Ziegler, 1990).

The reactivated vertical salt movements observed on the Cretaceous Cenozoic transition were initiated due to a change in the regional stress field from extensional to compressional due to the onset of the Alpine Orogenesis (Ziegler, 1990; Gemmer et al., 2003). This explains the WNW-ESE striking long axial trend of the depocentres between the salt structures during the deposition of the Cenozoic succession (Fig. 4.13). The direction can be compared with the direction of the folds observed in the Northeast German Basin by Scheck et al. (2003a). The NNE-SSW directed compressive stress field also confirms that the N-S striking fault system upon Salt Pillow A and B (Fig. 4.4, 4.5, 4.7, 4.8, 4.13 and 4.14d) developed thin-skinned as a result of halokinesis.

## **4.8 Acknowledgements**

The authors would like to thank Per Trinhammer for his technical assistance during the data acquisition, Egon Nørmark for the processing of the Baltseis surveys and his assistance during the processing of the NeoBaltic surveys, Ole Rønø Clausen for the fruitful discussions and Kathryn Brookes for her constructive comments. The Baltseis surveys were funded by the Danish Natural Science Research Council (grant no. 970176, 9802129 and 9901810). The NeoBaltic project is funded by the German Research Foundation (DFG) grant no. HU698/7-1 in the frame of the Special Research Project 1135. The authors would like to thank two anonymous reviewers for their help in improving the manuscript.



## **5. Structure and evolution of the northern part of the Northeast German Basin**

By Martin Bak Hansen, Sheila Piñeiro Triñanes, Holger Lykke-Andersen, Christian Hübscher, Ali Dehghani and Dirk Gajewski.  
Submitted to *Marine and Petroleum Geology*, 01/2006

### **5.1 Abstract**

A dense seismic grid from the Bay of Mecklenburg sub-area of the southwestern Baltic Sea has been investigated in detail in order to study the Mesozoic and Cenozoic structural and depositional evolution of the northern part of the Northeast German Basin (NEGB) and the transition onto the Baltic Shield. From the mapping five major sequences (Middle Triassic, Upper Triassic, Jurassic, Cretaceous and Cenozoic) and the horizon flattening of two key seismic lines crossing the study region, the geological evolution of the area was reconstructed and compared with geological processes on a regional scale. The present day structural framework of the northern part of the NEGB is the result of several deformation events. Following the deposition of the Zechstein evaporites the study area experienced subsidence due to a regional E-W directed extension during the Triassic-Early Jurassic. This extensional stress regime initiated the first period of salt movement accompanied by thin-skinned faulting and the brittle thick-skinned deformation in the areas outside the limit of the Zechstein evaporites. The entire region was uplifted due to the Mid North Sea Doming event in Middle Jurassic times, followed by a pronounced erosion of Upper Triassic and Lower Jurassic strata. Due to a reorganisation of the regional stress field at the Jurassic/Cretaceous transition, the northern part of the NEGB remained uplifted until the end of the Early Cretaceous when sedimentation resumed in the area. The sedimentation throughout the Late Cretaceous occurred during a period of rising sea level, tectonic quiescence and no halokinesis. A change in the regional stress field from extensional to compressional at the Cretaceous/Cenozoic transition caused the inversion of the Grimmen High and the reactivation the salt movement in the area. The deposition of the Cenozoic sequence in the southwestern corner of the Bay of Mecklenburg occurred under strong influence of this N(NNE) directed main stress field.

*Key words: Seismic interpretation, Northeast German Basin, Central European Basin System, Mesozoic and Cenozoic structural evolution*

## 5.2 Introduction

During the last three decades, several deep refraction and reflection seismic studies have been carried out in the southwestern Baltic Sea including the EUGENO-S (EUGENO-S working group, 1998), BABEL (BABEL working group, 1991, 1993), DEKORP-BASIN (e.g. Meissner & Krawczyk, 1999; Krawczyk et al., 1999), and POLONAISE '97 (e.g. Guterch et al., 1999; Grad et al., 1999) projects. All these projects were completed to obtain a better understanding of the deep-rooted structural framework of the region. Lassen et al. (2001) and Krawczyk et al. (2002) both found seismic evidence for Caledonian deformed sediments in the southwestern Baltic Sea, while Poprawa et al. (1999) did a subsidence analysis of the Baltic Basin based on borehole information. Detailed studies of the sedimentary cover were carried out in the central part of the Northeast German Basin (Scheck & Bayer, 1999; Bayer et al., 1999; Kossow et al., 2000; Kossow & Krawczyk, 2002; Scheck et al., 2003a; Scheck et al., 2003b) and in the adjacent Northwest Germany and German North Sea sector (e.g. Baldschuhn et al., 2001; Maystrenko et al., 2005a, 2005b). Studies of the paleo- and present-day stress field of the North German Basin have been described in several publications (e.g. Marotta et al., 2000; Marotta et al., 2001; Marotta et al., 2002; Marotta & Sabadini 2003; Kaiser et al., 2005). Despite the high research activity in the region, only very little systematic and localised research (e.g. Clausen & Pedersen, 1999; Hansen et al., 2005) has been carried out to investigate the Mesozoic-Cenozoic structural and depositional evolution of the southwestern Baltic Sea.

In order to investigate the post-Palaeozoic geological evolution of the northeastern part of the entire North German Basin and the transition (the Caledonian Deformation Front) onto the Baltic Shield (Fig. 5.1), the universities of Aarhus in Denmark and Hamburg in Germany have completed eight marine geophysical surveys in the southwestern Baltic Sea since 1998 in the frame of the Baltseis and the NeoBaltic (Hübscher et al., 2004) projects. During these research cruises, a dense grid of high-resolution multichannel seismic data was acquired, together with gravity and magnetic data. The post-Permian structural evolution of the Bay of Kiel sub-area of the southwestern Baltic Sea is presented in Hansen et al. (2005). The results of the seismic interpretation in the Bay of Mecklenburg sub-area are presented here. The interpretation was supported with stratigraphic information from surrounding explorational wells (Fig. 5.2).

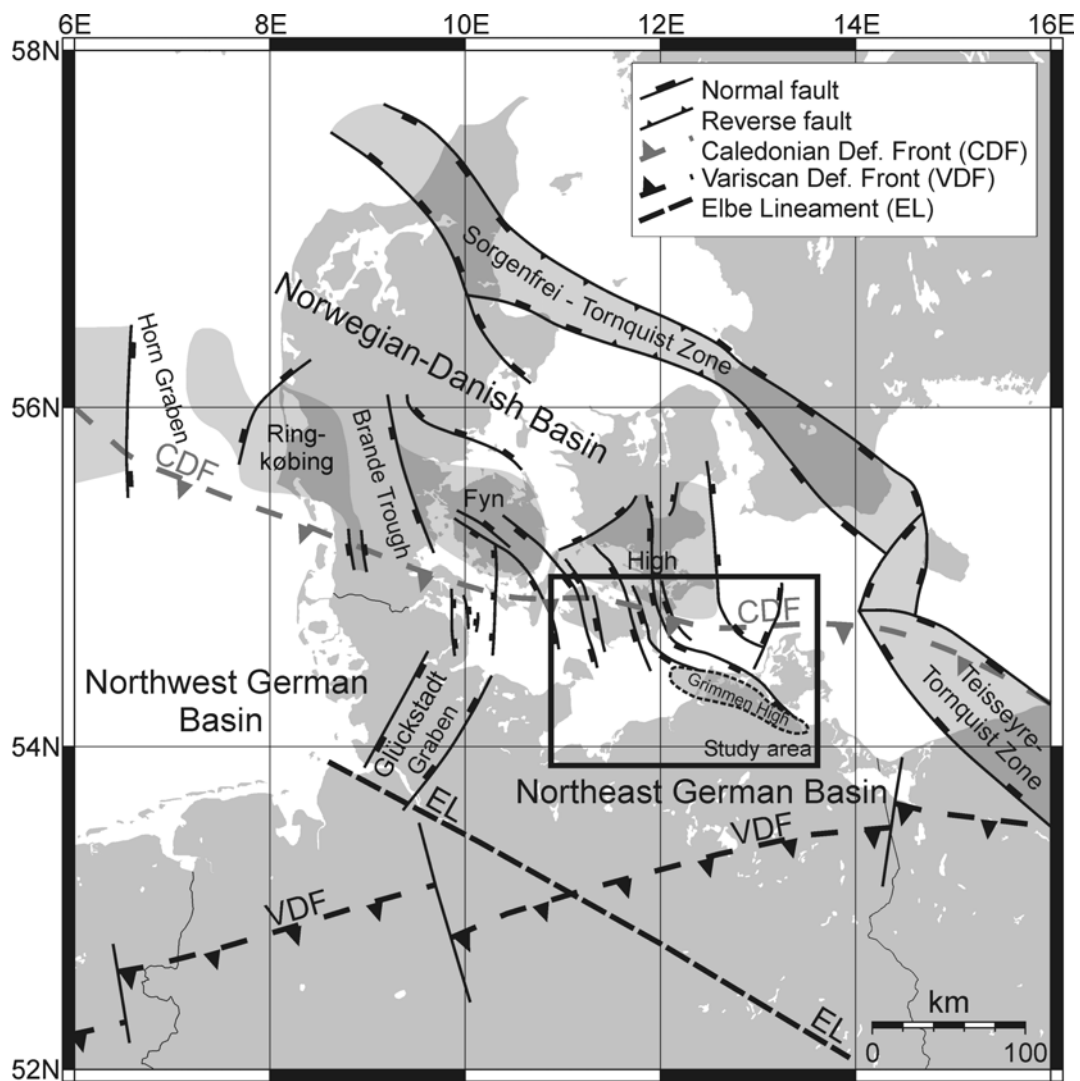


**Fig. 5.1** Location of the study area and the important structural elements of the region around the study area (compiled from Krauss, 1994; Vejrbæk, 1997; Bayer et al., 1999; Clausen and Pedersen, 1999; Kossow et al. 2000).

### 5.3 Geological settings

The Northeast German Basin (NEGB) (Fig. 5.1), a sub-basin of the Southern Permian Basin (Ziegler, 1990), belongs to a series of related Carboniferous-Permian intracontinental basins extending from the southern North Sea to northern Poland (Kossow & Krawczyk, 2002), referred to as the Central European Basin System (CEBS). To the north, the NEGB is bounded by the Ringkøbing-Fyn High (RFH), a series of WNW-ESE striking crystalline basement highs running from the North Sea across the Danish mainland separating the NEGB from the Norwegian-Danish Basin (Cartwright, 1990; Clausen & Pedersen 1999). The path of the Caledonian Deformation Front is more or less identical to the southern flank of the RFH in the area around the NEGB. The NEGB is bounded to the east by the Teisseyre-Tornquist Zone and to the west by the Glückstadt Graben. The Elbe Lineament marks the southern border of the basin (Bayer et al., 1999). Sediments ranging in age from Permian to present have a thickness of 10-12 km (Scheck et al., 1996; Benek et al., 1996).

The initial main phase of subsidence of the NEGB took place between Early Permian and Middle Triassic (van Wees et al. 2000; Kossow et al., 2000). The lowermost deposits consist of Carboniferous-Permian volcanics and aeolian, fluvial and shallow-lake sediments overlain by Upper Permian (Zechstein) evaporites (Scheck & Bayer, 1999). The succession of Zechstein evaporites was deposited as a result of several marine transgressions from the north into the basin after a period of terrestrial conditions (Ziegler, 1990; Taylor, 1998; Kossow et al., 2000). The following Triassic succession consists of a Lower Triassic red-bed clastic sequence (Buntsandstein) deposited under terrestrial conditions, overlain by marine carbonates of Middle Triassic age (Kossow & Krawczyk, 2002). An eustatic sea level drop at the Middle-Late Triassic transition led to renewed terrestrial sedimentation (Keuper) (Nöldeke & Schwab, 1976). The Triassic succession is overlain by a Lower Jurassic sequence, which was deposited under shallow-marine conditions (Underhill, 1998). After the long period of subsidence, the northern part of the NEGB was subject to a period of uplift and non-deposition lasting from Middle Jurassic to Early Cretaceous (Ziegler, 1990; Underhill, 1998). As a result of this uplift, parts of the Lower Jurassic and Upper Triassic sedimentary sequences were eroded (Kossow et al., 2000; Hansen et al., 2005). Sedimentation resumed towards the end of the Early Cretaceous (Albian) with the deposition of a terrestrial clastic sequence followed by Upper Cretaceous marine marls and carbonates during a period of tectonic quiescence and rising sea level (Kossow & Krawczyk, 2002). A new period of uplift occurred towards the end of the Late Cretaceous and throughout the Palaeogene, during which the NEGB and

surrounding basins were inverted as a result of several inversion pulses related to the Alpine Orogeny (Ziegler, 1990; Krauss, 1994; Bayer et al., 1999; Scheck-Wenderoth & Lamarche, 2005). The basement controlled Grimmen High was inverted with uplift values up to 500 m as a result of this collision (Kossow et al., 2000). The Cenozoic succession in the NEGB shows a facies pattern of terrestrial and shallow-marine clastic sediments deposited under strong influence of halokinesis (Kossow et al., 2000).

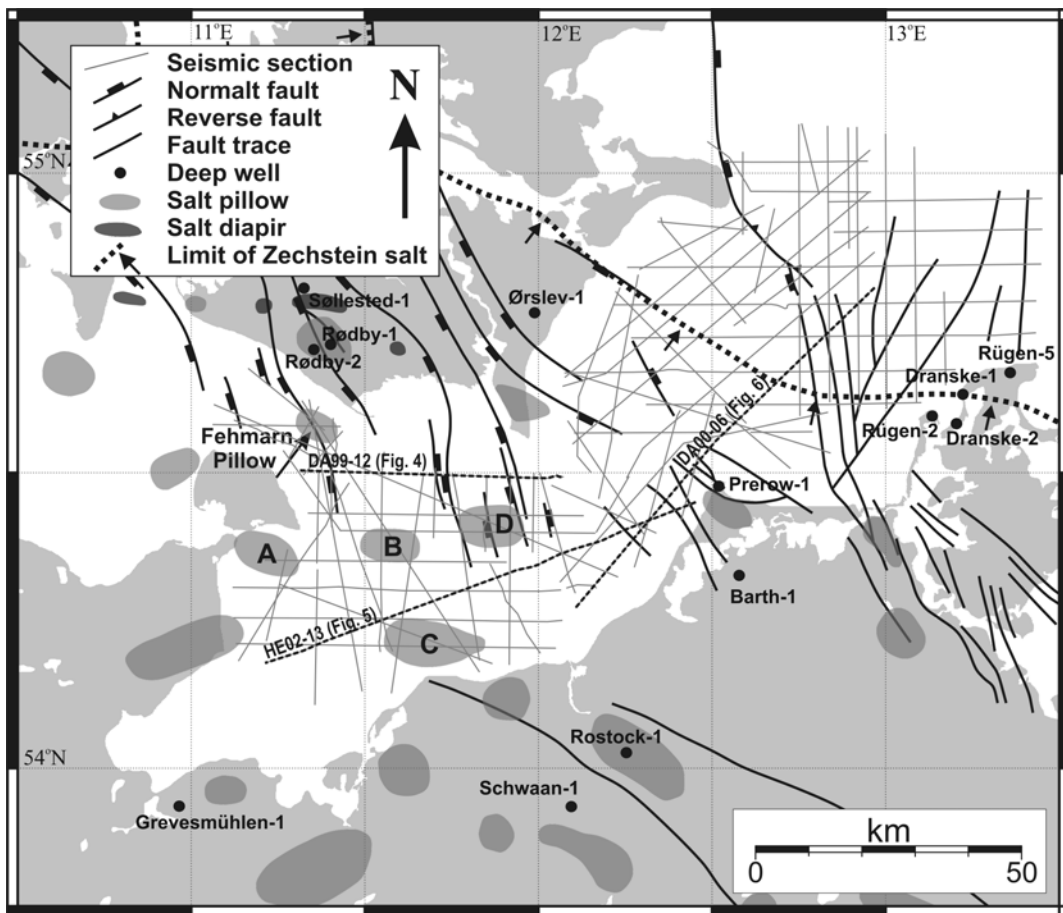


**Fig. 5.2** Map of the study region, revealing the positions of the different seismic lines, and the location of deep exploration wells used for stratigraphic correlation. The positions of the salt structures are based on Vejbæk (1997), Clausen and Pedersen (1999), Scheck et al. (2003) and this study. The positions of the sub-salt faults and fault traces are from Rempel (1992) and Vejbæk (1997). The limit of the Zechstein evaporites is based on Vejbæk and Britze (1994).

## 5.4 Database

### 5.4.1 High-resolution multichannel seismic data

During two research cruises onboard R/V *Dana* in 1999 and 2000 in the Danish territorial waters of the southwestern Baltic Sea, the University of Aarhus (AU) acquired high-resolution multichannel seismic data used in this study as a part of the BaltSeis project (survey names: DA99, DA00). The seismic equipment for these two surveys consisted of a 70 in<sup>3</sup> (~1.1 l) sleeve gun cluster fired at 100 bar air pressure every 12.5 m, and a 48-channel streamer (300 m long) with a hydrophone group spacing of 6.25 m. This configuration resulted in a common mid point distance of 3.125 m. Source and receivers were towed at a depth of 3 m below the water surface.

The University of Hamburg extended the data acquisition into German territorial waters of the southwestern Baltic Sea in cooperation with AU between 2001 and 2004. These cruises took place onboard R/V *Alkor* (cruise names: AL 185; AL 225) and R/V *Heincke* (cruise names: HE 172; HE 217), generating survey datasets AL01, HE02, AL03 and HE04 as a part of the NeoBaltic project. During the HE 172 and HE 217 cruises, the source configuration was the same as on the R/V *Dana* surveys, but this time a 96-channel streamer (600 m long) with the same hydrophone group separation was used. On the 2003 AL 225 cruise, a single 105 in<sup>3</sup> (~1.65 l) GI-gun fired at 140 bar air pressure every 12.5 m was deployed, along with a 96-channel streamer. On all the above-mentioned surveys, the data were recorded digitally and sampled every 1 ms, with a record length between 2 and 3 seconds. The overall good penetration is in the order of 1.5-2 s two-way travel time (TWT) for all the profiles. The vertical resolution is in the order of 8-10 m and the horizontal resolution is between 20 m and 25 m.

### 5.4.2 Well data

Several exploration wells provided stratigraphic information for correlating the different interpreted horizons on the seismic profiles (Fig. 5.2). From the northern margin of the study area, information from four Danish onshore wells (Søllested-1, Ørslev-1 and Rødby-1 & 2) (Nielsen & Japsen, 1991) were used, while stratigraphic information from nine German exploration wells (Grevesmühlen-1, Schwaan-1, Rostock-1, Barth-1, Prerow-1, Dranske-1 & 2 and Rügen-2 & 5) (Hoth et al., 1993) located along the southeastern border of the study region were

integrated. Unfortunately none of these exploration wells are located within the seismic survey grid.

### **5.4.3 Stratigraphic interpretation**

Using the interpretation done by Hansen et al. (2005) in the adjacent Bay of Kiel, it was possible to date six major horizons traced across the survey in the Bay of Mecklenburg. These are: Base Middle Triassic (BMT), Base Upper Triassic (BUT), Base Jurassic (BJ), Base Cretaceous Unconformity (BCU), Base Upper Cretaceous (BUC) and Base Cenozoic (BC). In some areas it was also possible to trace the Top Zechstein (TZ) horizon. In addition, some internal reflectors within the Upper Triassic, Jurassic, Upper Cretaceous and the Cenozoic successions supported the structural and depositional interpretation. An overall stratigraphic table is presented in Figure 5.3.

### **5.4.4 Sedimentary sequences (Fig. 5.3)**

#### **Lower Triassic (Buntsandstein)**

The Lower Triassic succession, bounded by the interpreted TZ and BMT horizons, consists of fluvial to lacustrine sediments and playa-lake deposits (Scheck & Bayer, 1999). Due to the limited resolution of the seismic data, the TZ reflection at the base of this succession is only traced on a few profiles.

#### **Middle Triassic (Muschelkalk)**

This sequence comprises of carbonates deposited during a transgressive period from terrestrial to shallow-marine conditions (Hansen et al., 2005 and references herein), bounded by the BMT and BUT horizons.

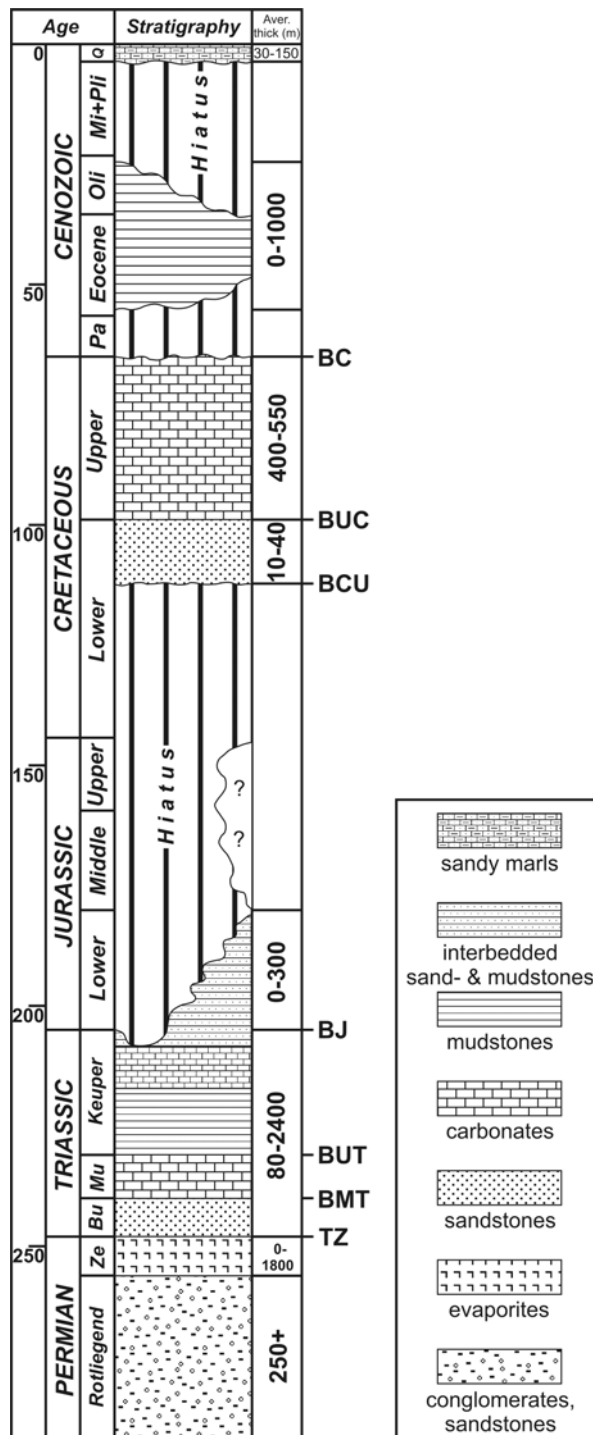


**Fig. 5.3** Stratigraphic table (modified after Kossow et al., 2000) showing the dominant lithologies, average thicknesses and the ages of the major horizons interpreted in the northern margin of the Northeast German Basin. The thickness data are from Nielsen & Japsen (1991) and Hoth et al. (1993). TZ: Top Zechstein, BMT: Base Middle Triassic, BUT: Base Upper Triassic, BJ: Base Jurassic, BCU: Base Cretaceous Unconformity, BUC: Base Upper Cretaceous, BC: Base Cenozoic.

### **Upper Triassic (Keuper)**

This sequence consists of limnic-fluvial and playa-type sediments (Scheck & Bayer, 1999), indicating a sea level drop from the Middle Triassic. The base of this succession is defined by the BUT horizon and the top by the BJ reflector. In some parts of the study area, the Upper Triassic sequence truncates at the BCU horizon as a result of later uplift and erosion. In addition, an angular unconformity has been interpreted on the seismic sections from the eastern part of the study (Fig. 5.4 + 5.5). This reflector corresponds to the 'Late Triassic unconformity' described by Clausen & Pedersen (1999).

### **Jurassic**

The Jurassic succession is bounded at the base by the BJ horizon and is upwardly truncated by the BCU reflector. According to Kossow et al. (2000), the Jurassic sequence in the Northeast German Basin consists of interbedded marine mud and sandstones.

### **Lower Cretaceous**

A thin succession of homogenous thickness, traceable over the entire study area. The BCU and BUC reflectors bound this sequence. The base marks a major transgression of Albian age from non-deposition to shallow marine conditions (Kossow et al., 2000; Hansen et al., 2005). This sequence consists of calcareous sediments, primarily red marls.

### **Upper Cretaceous**

The BUC and BC reflectors mark the base and the top of this sequence respectively. The succession consists of chalk sediments deposited during shallow marine condition developing into open marine conditions. According to Hoth et al. (1993), the upper boundary of this sequence is an unconformity in the Bay of Mecklenburg.

### **Cenozoic**

This sequence, which is basally bound by the BC reflector and upwards by the seafloor, consists of brackish marine clay-silt sediments of Cenozoic age (Scheck & Bayer, 1999), deposited under influence of salt movement (Kossow et al. 2000; Hansen et al. 2005). The top of the succession contains Quaternary glacial and post-glacial deposits.

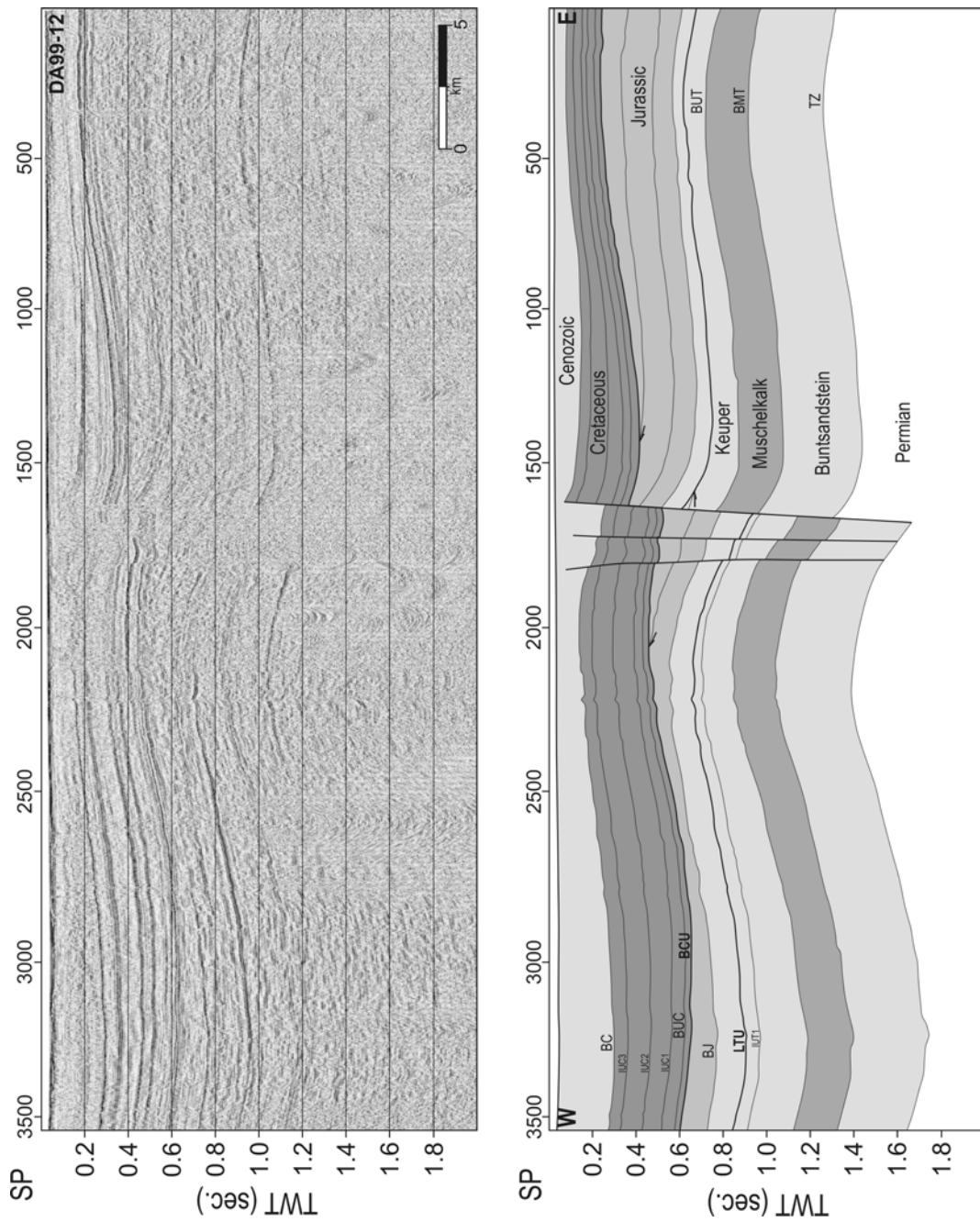


**Fig. 5.4** Time-migrated seismic section DA99-12 (see Fig. 5.2 for location) and interpreted section crossing the N-S striking fault system in the southwestern part of the Bay of Mecklenburg. The section reveals a fault system believed to have developed thin-skinned on top of a salt roller, as active faulting is only observed during periods of accelerated halokinesis. TZ: Top Zechstein, BMT: Base Middle Triassic, BUT: Base Upper Triassic, IUT1: Internal Upper Triassic 1, LTU: Late Triassic Unconformity, BJ: Base Jurassic, BCU: Base Cretaceous Unconformity, BUC: Base Upper Cretaceous, IUC 1, 2 & 3: Internal Upper Cretaceous 1, 2 & 3, BC: Base Cenozoic.

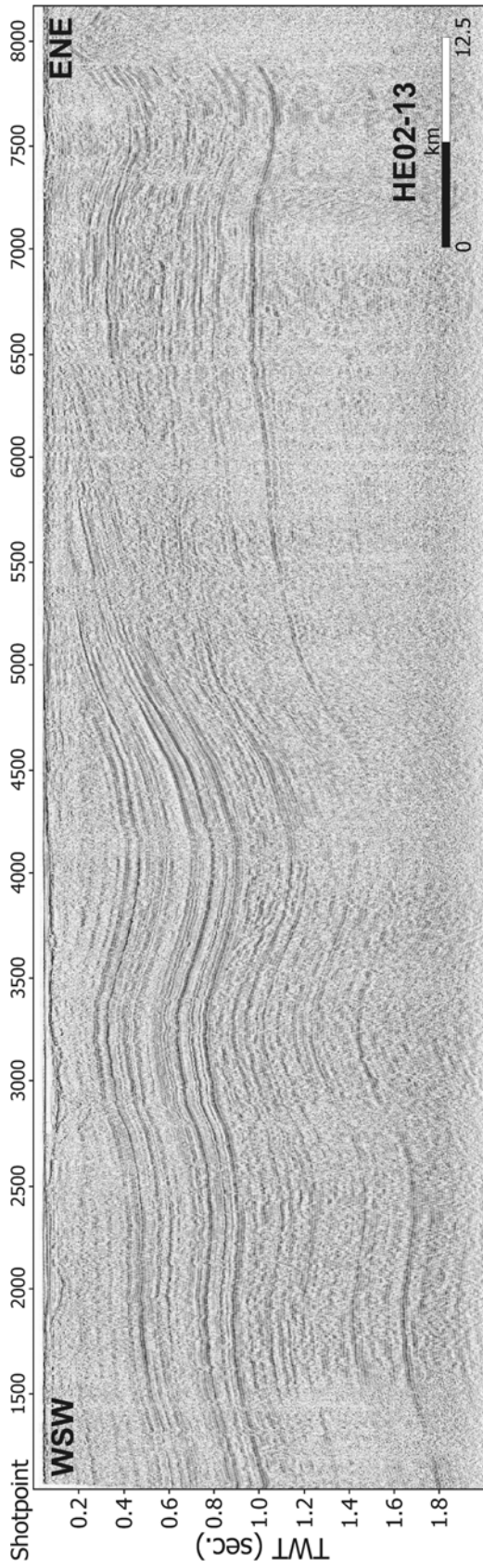
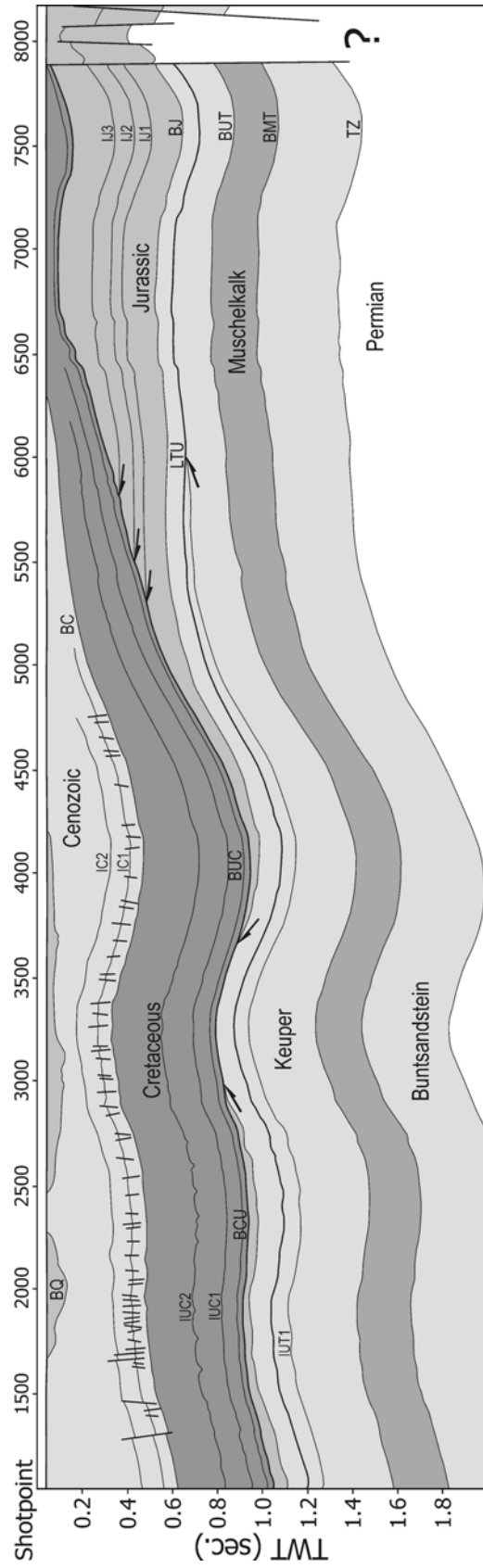


Fig. 5.5



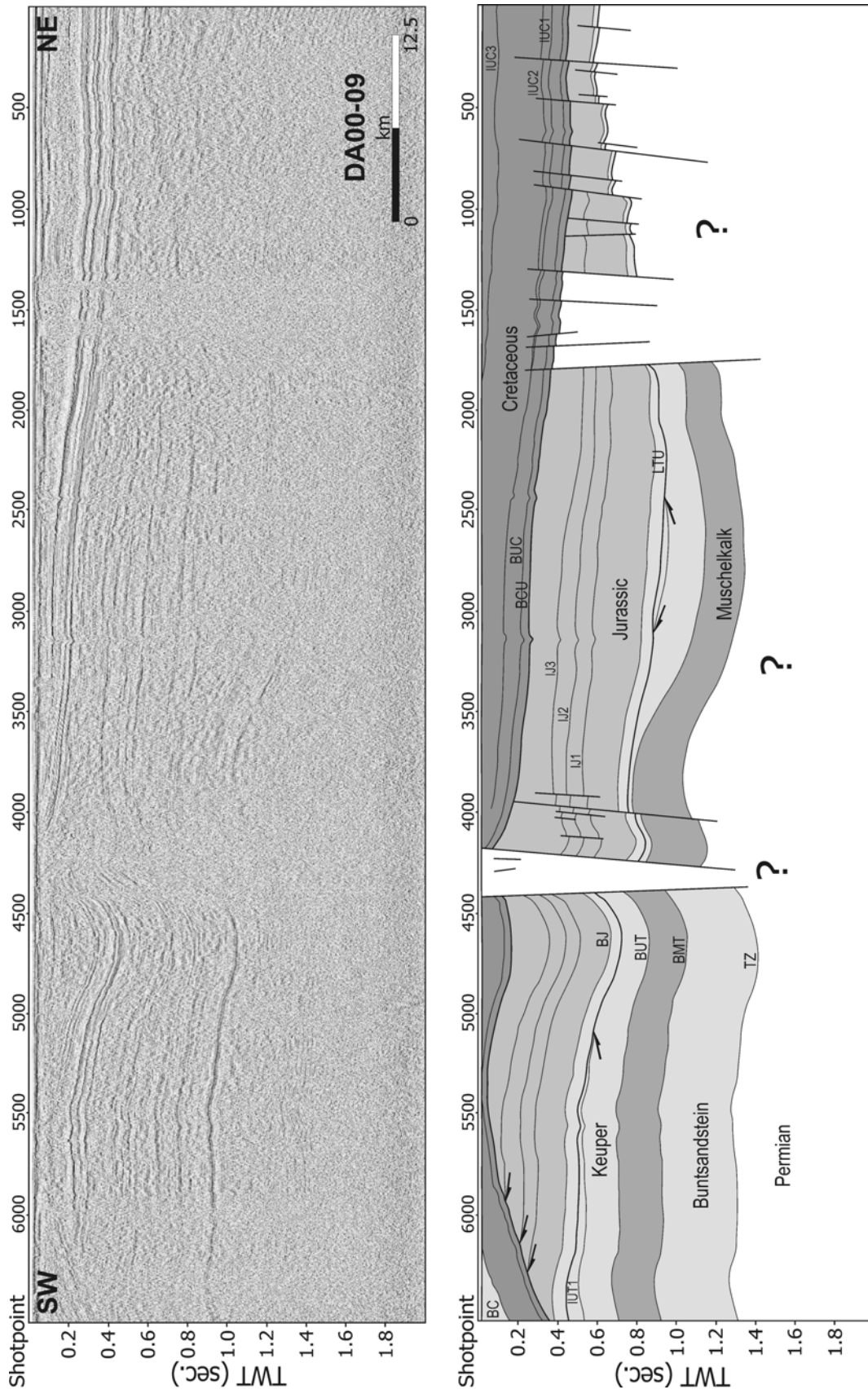


Fig. 5.6

---

**Fig. 5.5** (Page 61) Time-migrated seismic section HE02-13 (see Fig. 5.2 for location) and interpreted section running through the southernmost part of the study area. The general distribution reveals how the angular Base Cretaceous Unconformity (BUC) separates the Triassic and Jurassic successions from the Cretaceous and Cenozoic succession. The stratigraphic thickening of the Jurassic sequence in the eastern part is interpreted to be the result of differential subsidence between the Grimmen High and surrounding areas. TZ: Top Zechstein, BMT: Base Middle Triassic, BUT: Base Upper Triassic, IUT1: Internal Upper Triassic 1, LTU: Late Triassic Unconformity, BJ: Base Jurassic, IJ1, 2 & 3: Internal Jurassic 1, 2 & 3, BCU: Base Cretaceous Unconformity, BUC: Base Upper Cretaceous, IUC1 & 2: Internal Upper Cretaceous 1 & 2, BC: Base Cenozoic, IC1 & 2: Internal Cenozoic 1 & 2.

---

**Fig. 5.6** (Page 62) Time-migrated seismic section DA00-09 (see Fig. 5.2 for location) and interpreted section running through the northeastern part of the Bay of Mecklenburg. Two angular unconformities are recognized within the section. The internal Keuper Late Triassic Unconformity (LTU), and the Base Cretaceous Unconformity (BUC), separating Triassic and Jurassic sediments from Cretaceous sediments. TZ: Top Zechstein, BMT: Base Middle Triassic, BUT: Base Upper Triassic, IUT1: Internal Upper Triassic 1, LTU: Late Triassic Unconformity, BJ: Base Jurassic, IJ1, 2 & 3: Internal Jurassic 1, 2 & 3, BCU: Base Cretaceous Unconformity, BUC: Base Upper Cretaceous, IUC1 & 2: Internal Upper Cretaceous 1 & 2, BC: Base Cenozoic, IC1, 2 & 3: Internal Cenozoic 1, 2 & 3.

---

#### **5.4.5 Seismic stratigraphy**

Examples of interpreted seismic sections from the Bay of Mecklenburg are shown in Figures 5.4, 5.5 and 5.6 (for location see Fig. 5.2). All three profiles reveal that the Mesozoic and Cenozoic strata were deposited under the influence of halokinesis observed from the wavy distribution of the different successions. Furthermore, the Cretaceous and Cenozoic successions are separated from older sequences by an angular unconformity (BCU). Another angular unconformity is located in the northeastern part of the study area within the Upper Triassic succession. Finally, the profiles reveal that Cenozoic sediments only exist in the western part of the Bay of Mecklenburg (Fig. 5.4 and 5.6), whilst a thick Jurassic sequence is preserved in the eastern part (Fig. 5.4 and 5.5).

## **5.5 Structural evolution**

### **5.5.1 Methods**

The interpretation of the structural and depositional evolution of the northern part of the NEGB is based on the created geological maps (Fig. 5.7 – 5.12) and the two restored sections of profile DA99-12 (Fig. 5.13) and profile HE02-13 (Fig. 5.14). The time-structure map presented in Figure 5.7 shows the present day vertical depth in two-way travel time (TWT) to the Base Jurassic surface. This map reveals the position of the different salt structures and the trends of fault systems. The time-isochore maps (Fig. 5.8 – 5.12) show the present day vertical thicknesses of specific stratigraphic sequences bounded by two interpreted surfaces. From these maps it is possible to determine periods of active faulting and halokinesis and the position and trend of local palaeo-depocentres. Only faults that can be traced from line to line across the survey have been included in the geological maps.

The restoring method used in Figure 5.13 and 5.14 is a simple 2D horizon flattening made with the assumption that all sedimentary layers are deposited more or less horizontal. This model does not take volumetric proportions, or decompaction into consideration.

Due to the limited penetration depth of the seismic data, it was not possible to map the Base Zechstein surface underneath the evaporites (Fig. 5.4 – 5.6). For the same reason the Top Zechstein (TZ) surface has only been traceable on a few seismic sections. Thus, it has not been possible to give any volumetric estimation of the amount of halokinesis in the Bay of Mecklenburg.

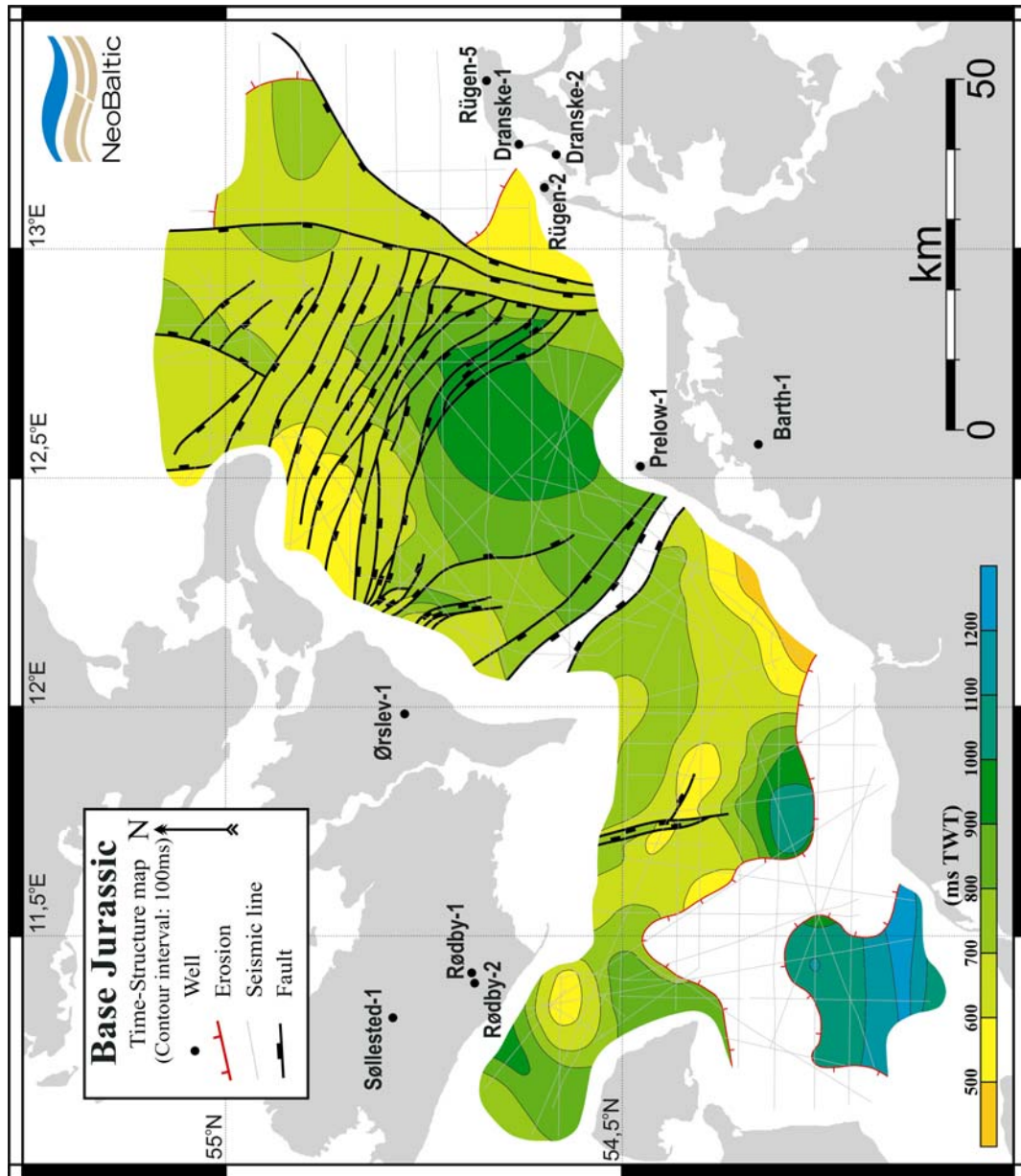


**Fig. 5.7** Time-structure map of the Base Jurassic surface in ms TWT. Contour interval is 100 ms. The locations of the wells referred to in the text are also shown. The orange-yellow colours show the shallowest parts of the surface, whereas the blue-green colour shows the deepest part in the southwestern corner. The red lines show where the surface has been exposed to later erosion.

### 5.5.2 Structural framework

The Base Jurassic (BJ) surface (Fig. 5.7) exhibits two topographic lows: one in the southwestern corner, where the surface has not been exposed to later erosion; and one in the area north of the Prerow-1 well. The low to the southwest is interpreted to be the result of a higher degree of subsidence towards the centre of the NEGB, while the depocenter north of the Prerow-1 is of local origin (Fig. 5.6). Two shallow anomalies are found above the Fehmarn Pillow and Salt Pillow D. A third shallow anomaly is seen west of the Barth-1 well, but, unlike the two other anomalies, this has not been interpreted to be the result of halokinesis. This structure presumably marks the western limit of the Grimmen High inversion structure.

Several fault traces are cutting the BJ surface. In the northeastern corner of the Bay of Mecklenburg, a group of WNW-ESE striking normal faults is located, with a displacement throw towards SSW. Figure 5.1 reveals that this group of fault traces follow the trend of the CDF. Thus, it is interpreted that the traces mark the northern limit of the NEGB and the transition towards the Baltic Shield (Fig. 5.6). To the east, this fault system terminates at a N-S running normal fault. This fault trace, along with the easternmost NE-SW trending fault, is considered to mark the western boundary of the Arkona High (Kossow et al., 2000), an eastward prolongation of the RFH. A NW-SE trending graben structure is located between the Ørslev-1 and the Barth-1 wells, which corresponds to the structure displayed around shotpoint (SP) 8000 on the HE02-13 profile (Fig. 5.5) and around SP 4300 on DA00-09 (Fig. 5.6). Finally a N-S trending fault system is detected west of Salt Pillow D. The main fault in this system is the eastern one with a westerly-directed throw (Fig. 5.4). Figure 5.2 reveals that this fault system is located above a basement fault with the same strike and throw. Despite of the presence of an evaporitic layer acting as a decoupling layer, it is reasonable to presume that this fault system is basement controlled.

### **5.5.3 Early – Middle Triassic (Buntsandstein – Muschelkalk)**

Owing to the limited resolution of the seismic data, the TZ has only been interpreted on a few profiles, so it is difficult to make conclusions about the general distribution of the Buntsandstein sequence in the northern part of the NEGB. On the BUT flattened sections (Fig. 5.13a and 5.14a) both the Buntsandstein and the Muschelkalk successions are observed to be homogenous in thickness, indicating a relatively quiet depositional environment. This observation is confirmed on the Middle Triassic isochore map (Fig. 5.8), where the sequence slightly thickens toward the centre of the basin, caused by the higher degree of subsidence away from the basin margins.

### **5.5.4 Late Triassic (Keuper)**

The Keuper sequence (Fig. 5.9) reveals a general thickening trend towards the south, with thicknesses achieving more than 500 ms TWT. The exception of this general trend is the local depocenter to the north of the Prerow-1 well, where the Upper Triassic succession is little more than 300 ms TWT in thickness. Stratigraphic thinning of the sequence is observed above the Fehmarn Pillow and Salt Pillows A and C, indicating that the initial salt movement into these structures took place during this period. The more abrupt thickness variations of the succession around the N-S striking fault indicate that this fault system was active during the Late Triassic. Because of the disrupted reflection pattern within NW-SE striking fault system, it cannot be determined if displacement took place within this system. Both BJ flattened sections (Fig. 5.13b and 5.14b) reveals that older strata truncates the LTU horizon in the western part of both profiles. This area corresponds to an elongated area with a thickness less than 150 ms TWT southwest of the NW-SE striking fault system. Thus, suggesting that relative uplift only occurred in this local area.

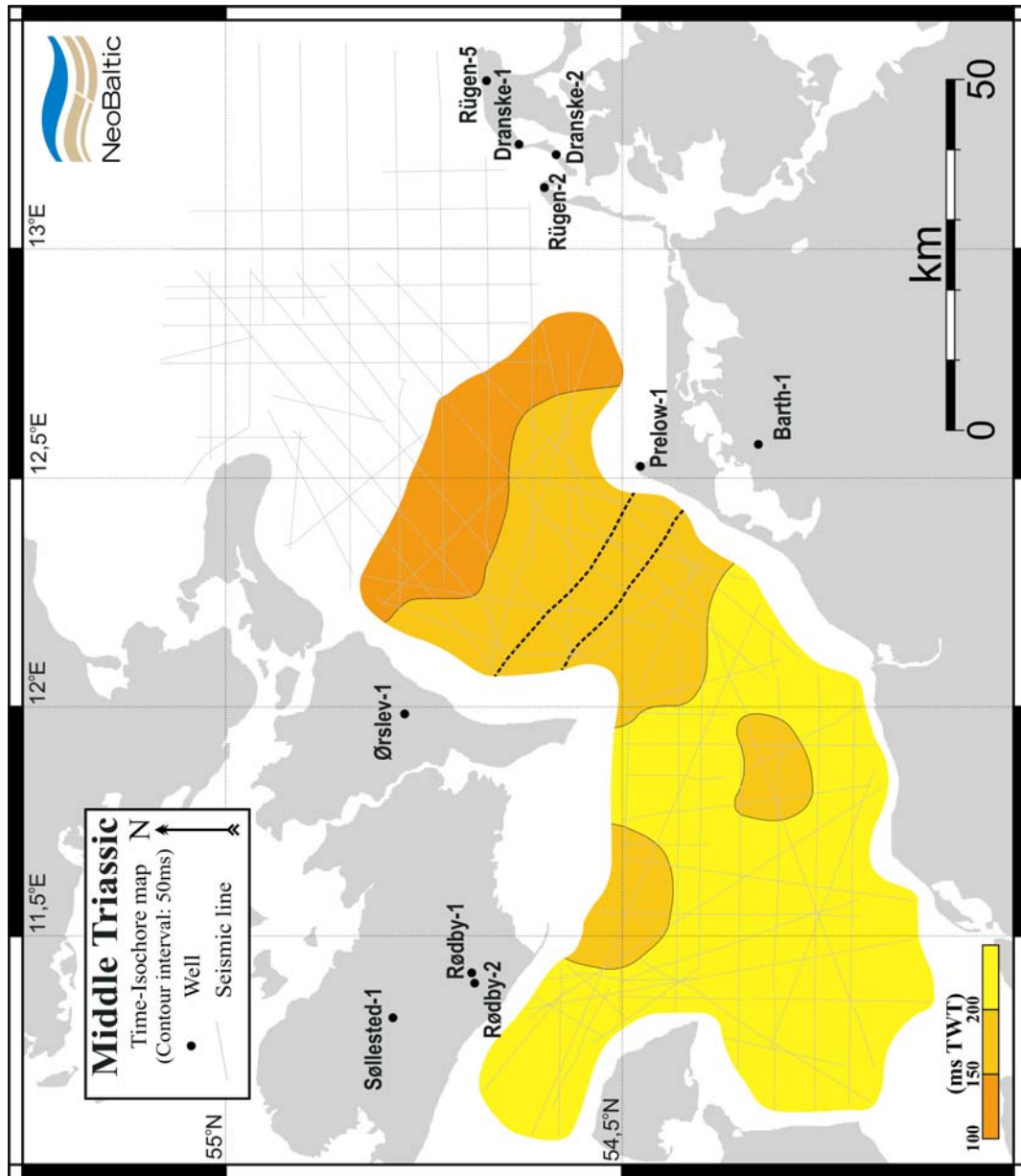


**Fig. 5.8** Time-isochores map of the Middle Triassic (Muschelkalk) succession in ms TWT. Contour interval is 50 ms. The locations of deep wells used in this study are also shown. The orange colour shows the thinnest part, while the yellow colour reflects the thickest part. Because of resolution problems, it has not been possible to map this succession in the northeastern part of the study area.

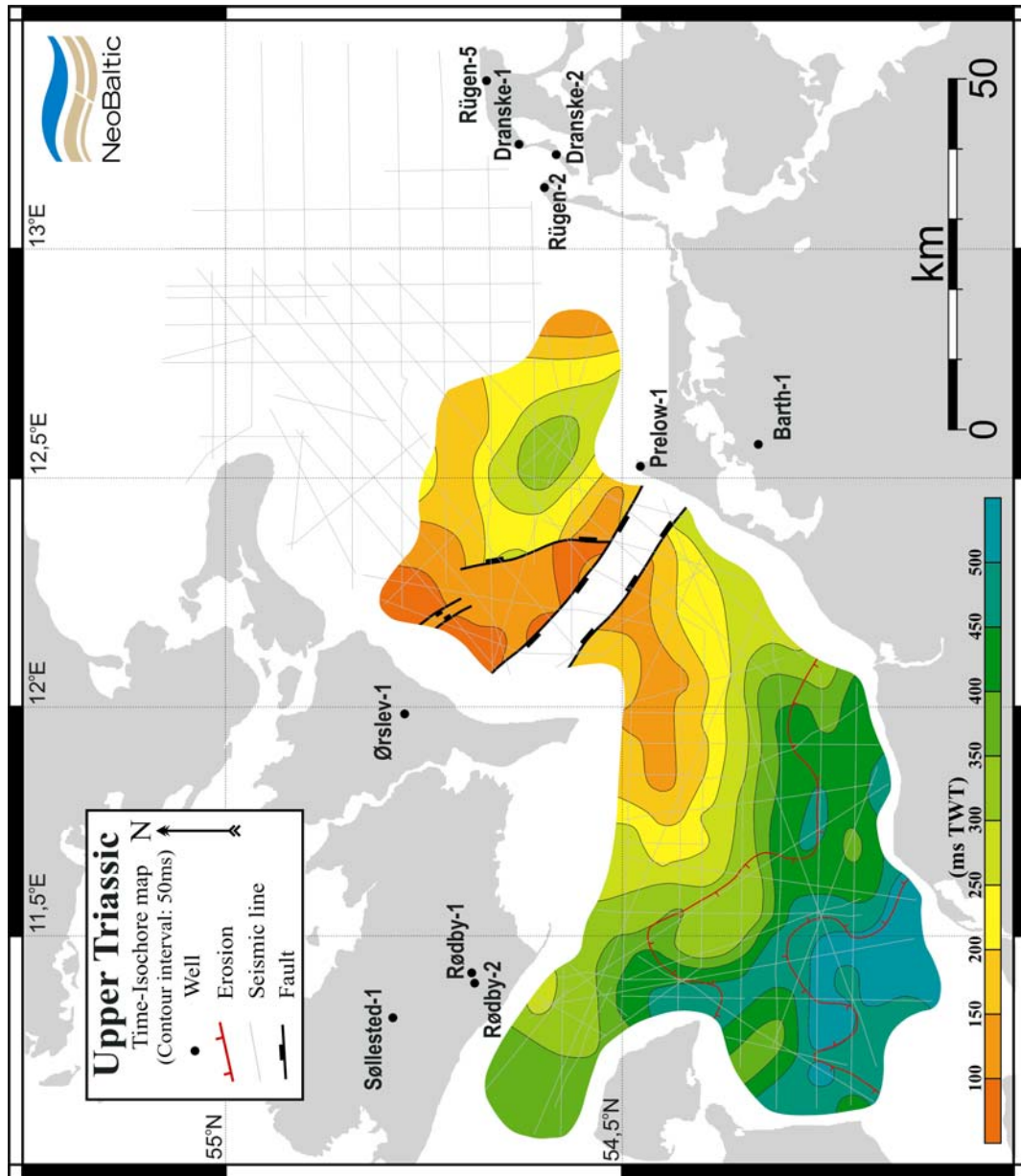


**Fig. 5.9** Time-isochore map of the Upper Triassic (Keuper) succession in ms TWT. Contour interval is 50 ms. The locations of deep wells used in this study are also shown. The red-orange colours show the thinnest parts of the sequence, whereas the thickest part is marked by the blue-green colour in the southwestern part. The red lines show where parts of the succession have been eroded. Due to resolution problems, it has not been possible to map this succession in the northeastern part of the study area.

### **5.5.5 Jurassic**

The Jurassic sediments generally comprise the oldest succession that has been mapped in the study region (in some areas these sediments are absent) (Fig. 5.10). The thickest sequence is to be found in the area northwest of the Prerow-1 well. A stratigraphic thinning over the Fehmarn Pillow suggests that salt movement into this structure continued during the Jurassic. The abrupt thickness variations around all the previous described fault traces show that active faulting took place in Jurassic times. The N-S striking fault system in the western part of the study region is presented on Figure 5.13c, exhibiting an almost vertical westerly throw. The Base Albian flattened sections (Fig. 5.13c and 5.14c) reveal that the thick Jurassic sequence described above was deposited in the area of the Late Triassic uplift.

At some point during the Jurassic, the entire area was uplifted and considerable amounts of Jurassic, and in some parts Upper Triassic, sediments were eroded away. This event is marked by the distinct unconformity, BCU, on all the seismic profiles in the study area. The exact timing of this erosional event is difficult to determine. Jurassic sediments are preserved in all the wells used in this study and are, in all cases, of Liassic age (Nielsen & Japsen, 1991; Hoth et al., 1993). The transgression that marks the renewed sedimentation after the uplift is of Albian age in all the wells, with the exception of the Prerow-1 well. Thus, it can only be concluded that this event took place sometime between the Liassic and the Albian.

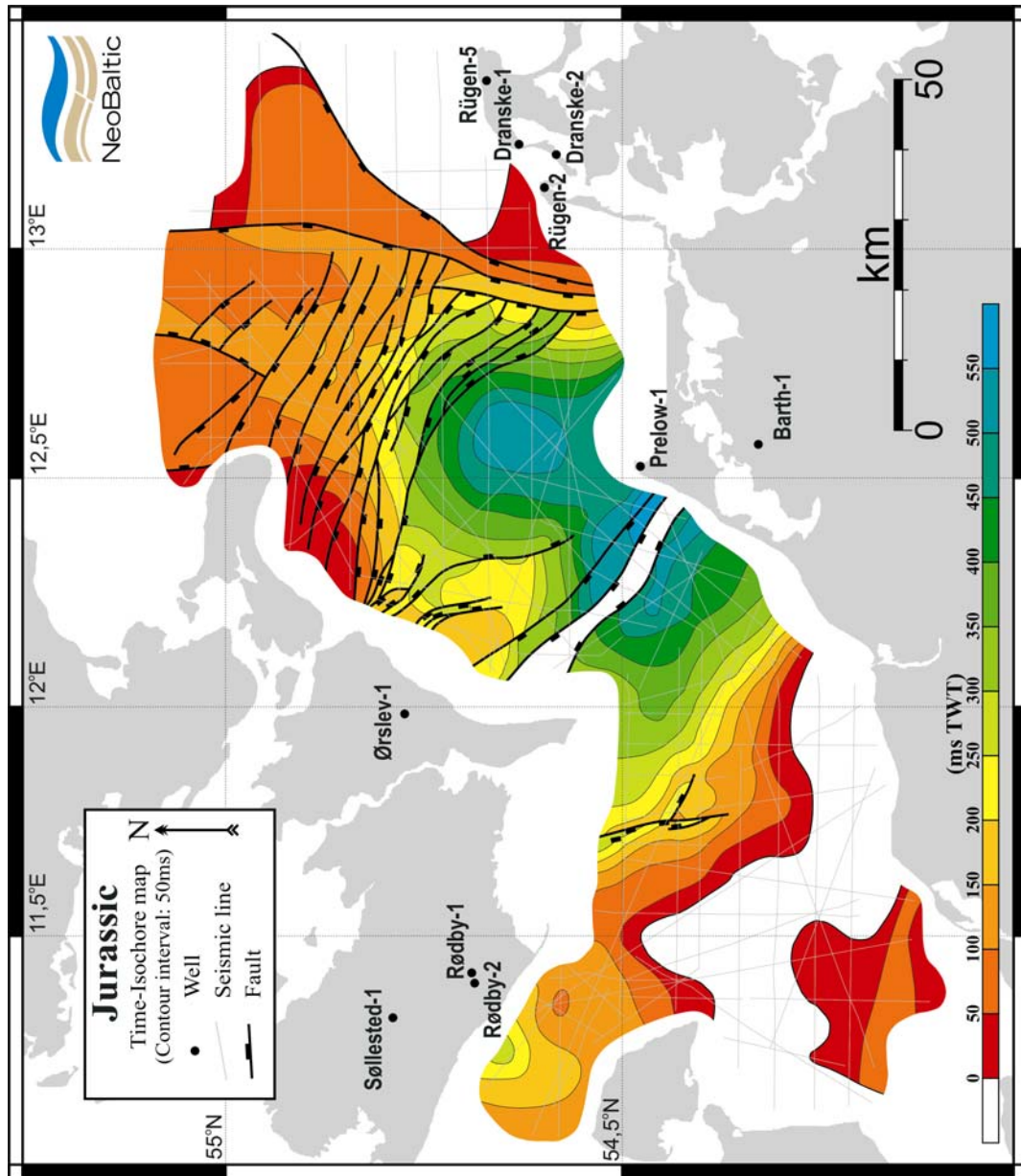


**Fig. 5.10** Time-isochores map of the Jurassic sequence in ms TWT. Contour interval is 50 ms. The locations of deep wells used in this study are also shown. The blank areas reveal where the entire sequence was eroded, whereas the blue-green colours reflect the thickest part around the Prerow-1 well.

### **5.5.6 Cretaceous**

Cretaceous sediments are present throughout the entire study region. The thinnest sequence is located in the centre of the study area, west of the Barth-1 well, with a general thickening trend towards the northeast and the southwest (Fig. 5.11). The red line on Figure 5.11 shows where the sequence has been exposed to later erosion. Thus, it cannot be determined whether the thickening trend towards the northeast reflects the real depositional pattern throughout the Cretaceous. For the same reason, it cannot be concluded if the displacement in the fault traces in the northeastern part of the study area took place in Cretaceous or post-Cretaceous times. Only minor displacement in the N-S trending fault in the western part of the study region can be dated to Cretaceous times. Minor stratigraphic thinning observed on top of the Fehmarn Pillow and Salt Pillow D reveal that salt movement into these structures occurred during this period. On all the interpreted seismic sections (Fig. 5.4, 5.5 and 5.6), it is seen that the thin Lower Cretaceous succession was deposited with a very uniform thickness throughout the Bay of Mecklenburg. This observation is supported by the Base Cenozoic flattened sections (Fig. 5.13d + 5.14d). This suggests that the sedimentation resumed in the study area during a period of tectonic quiescence. The pattern of the internal reflectors in the Upper Cretaceous in Figure 5.13d shows that the thinning is not only the result of later erosion (Fig. 5.14d), but also the result of a minor degree of subsidence over this structure throughout the remaining part of this period.

### **5.5.7 Cenozoic**

Cenozoic sediments are only preserved in the southwestern part of the study area (Fig. 5.12). The sequence general thickens towards the centre of NEGB in the south. Several thickness anomalies are observed on top of all the previously described salt structures, suggesting a period of accelerated halokinesis. On the very top of the Fehmarn Pillow and Salt Pillow D, the Cenozoic succession is absent. More abrupt thickness variations are detected in the fault system west of Salt Pillow D, indicating that active faulting took place during the Cenozoic. This is also observed on the restored profile of line DA99-12 (Fig. 5.13e). The isochore map of the Cenozoic sequence (Fig. 5.12) reveals, that the depocentres in the rim synclines between the salt structures reflect a WNW-ESE striking trend. This trend suggests that the main stress direction at this time was SSW-NNE. Due to the poorly defined reflection pattern within the Cenozoic succession, it cannot be determined if the halokinesis is still ongoing at the present day.

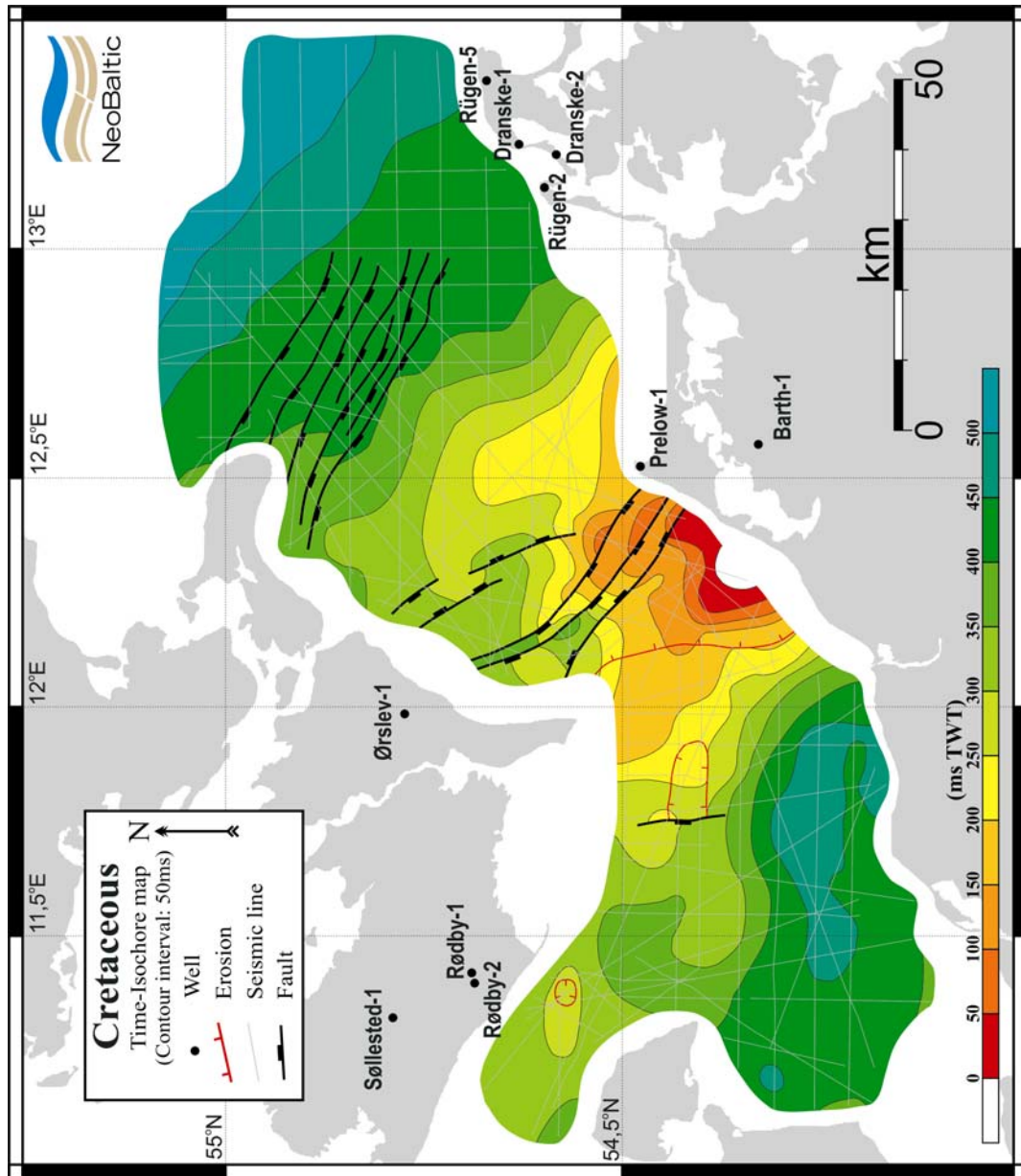


**Fig. 5.11** Time-isochores map of the Cretaceous succession in ms TWT. Contour interval is 50 ms. The locations of deep wells used in this study are also shown. The blank area shows where the entire sequence is absent. The blue-green colours show the areas where the sequence is thickest. The red lines show where parts of the succession have been eroded.

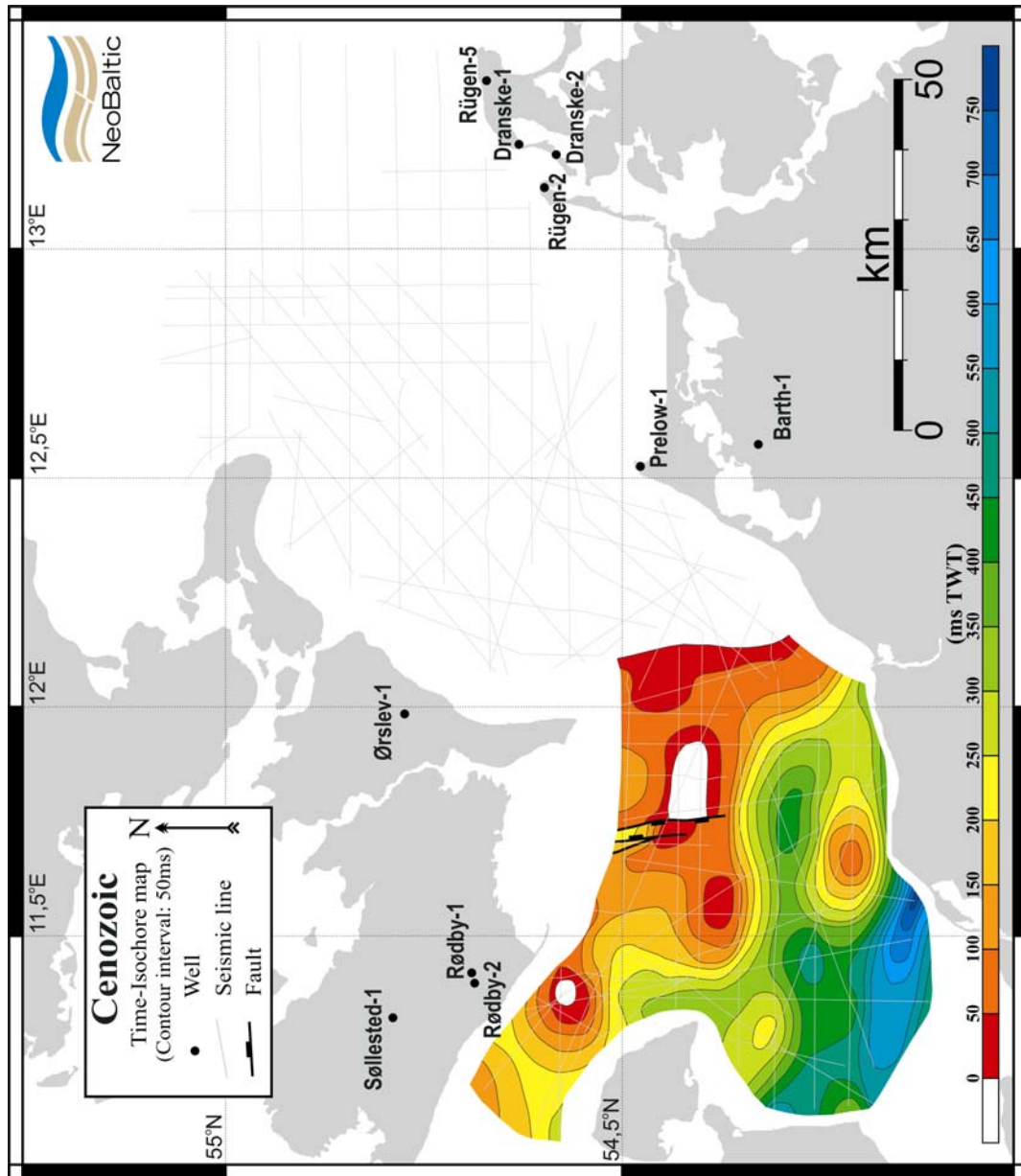
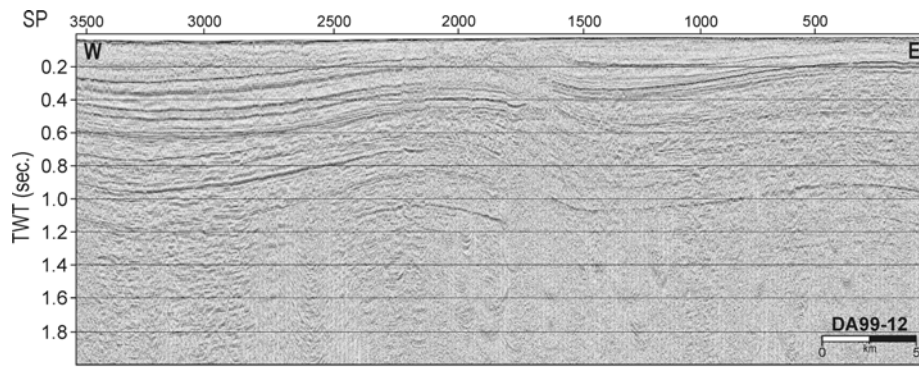
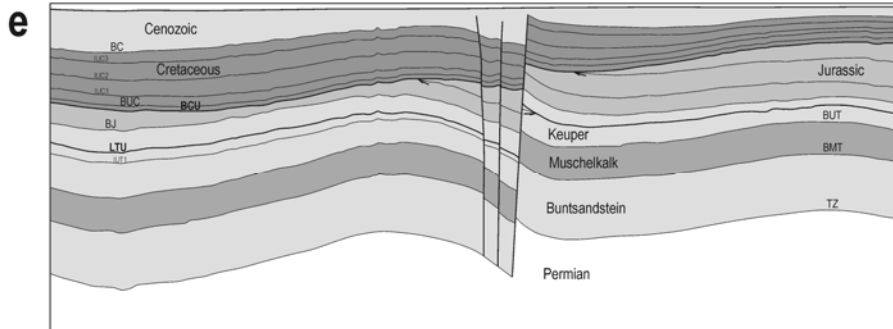


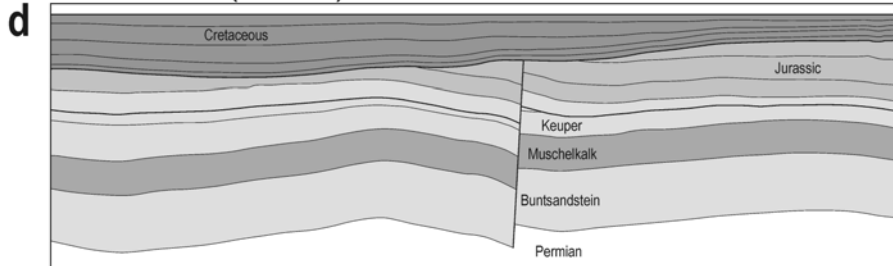
**Fig. 5.12** Time-isochore map of the Cenozoic sequence in ms TWT. Contour interval is 50 ms. The locations of deep wells used in this study are also shown. The blank areas in the northeastern part of the study area and on top of the Fehmarn Pillow and Salt Pillow D reveal where the entire sequence is absent. The Purple colour shows the thickest part of the succession in the southernmost part of the study area.



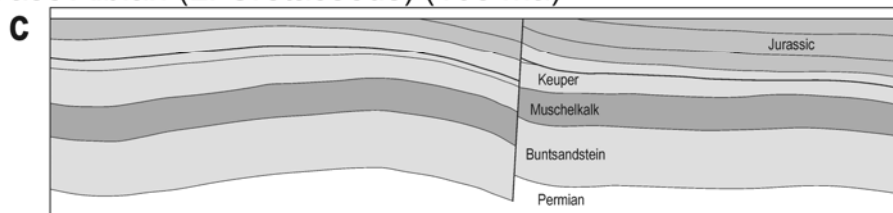
Present



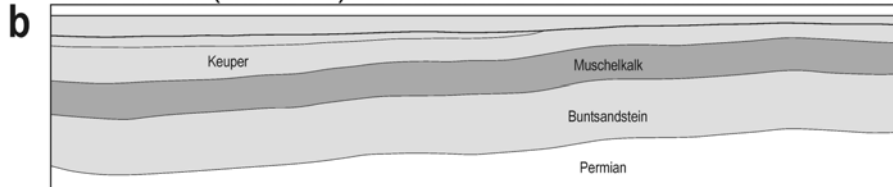
Base Cenozoic (65 ma)



Base Albian (L. Cretaceous) (108 ma)

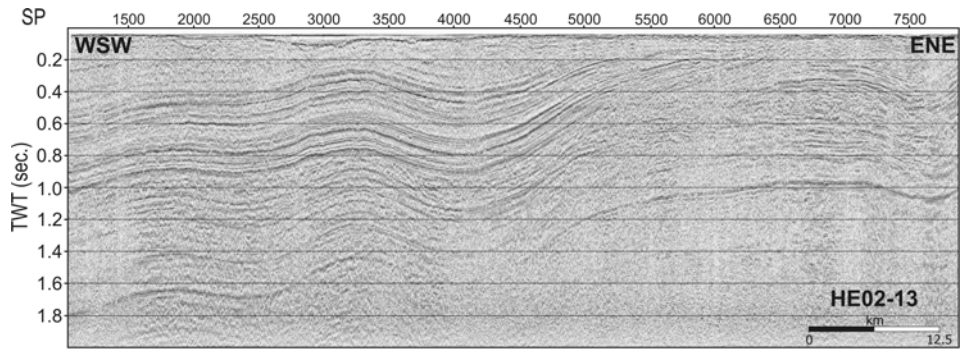


Base Jurassic (203 ma)

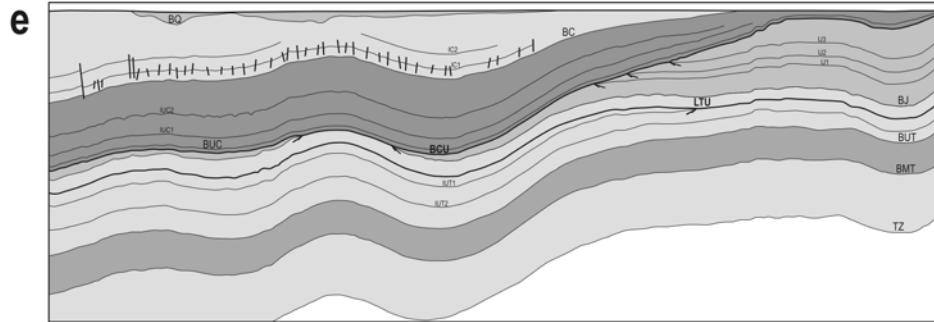


Base Upper Triassic (230 ma)

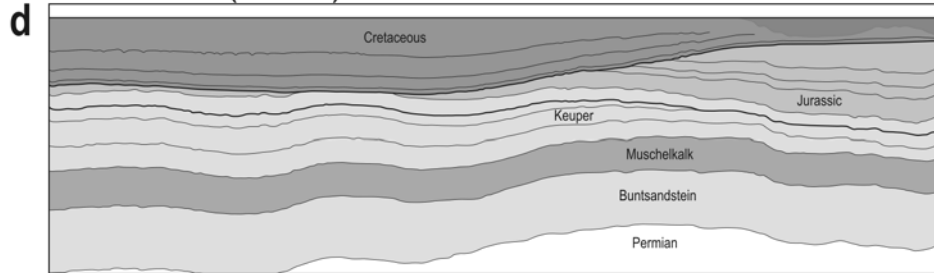




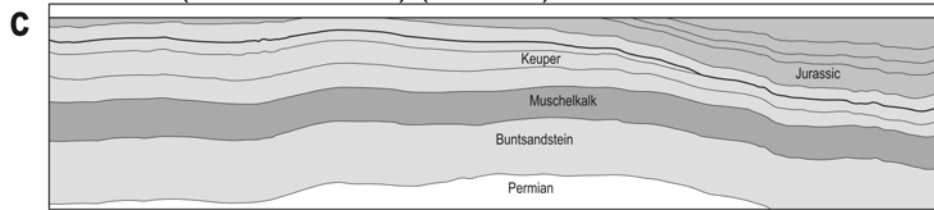
Present



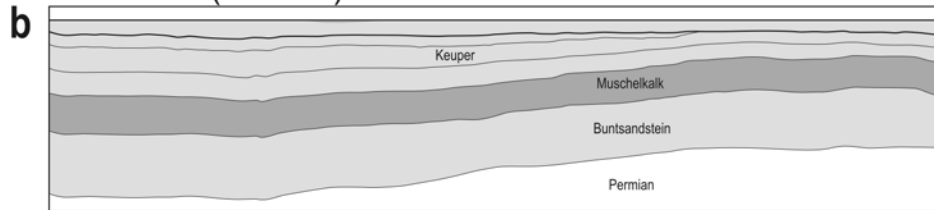
Base Cenozoic (65 ma)



Base Albian (L. Cretaceous) (108 ma)



Base Jurassic (203 ma)



Base Upper Triassic (230 ma)



---

**Fig. 5.13** (Page 75) Horizon flattening of the seismic line DA99-12 (Fig. 5.4) (see Fig. 5.2 for location). (a)-(e) shows the structural reconstruction of the section. (b) demonstrates how the eastern part of the profile was uplifted and eroded during the Late Triassic. This event is marked by the angular unconformity. (c) reveals that the initial displacement within the N-S striking fault system took place sometime during the Jurassic or Early Cretaceous.

---

**Fig. 5.14** (Page 76) Horizon flattening of the seismic profile HE02-13 (Fig. 5.5) (see Fig. 5.2 for location). (a)-(e) shows the structural reconstruction of the section. (b) reveals how the Late Triassic Unconformity (LTU) developed as a result of differential subsidence between the Grimmen High and the surrounding areas. (c) shows how the former "subsidence resisting" area in the eastern part developed into a local basin with the deposition of a great succession of Lower Jurassic sediments. (d) sedimentation resumed in Albian after a period of uplift and erosion marked by the angular Base Cretaceous Unconformity (BCU). Like in the Keuper times, the Grimmen High area was subject to less subsidence than the adjacent areas. (e) the invasion at the Cretaceous/Cenozoic transition is seen on the uplift of the Grimmen High and the erosion of Upper Cretaceous sediments. Furthermore, this compressional event reactivated the halokinesis in the area.

---

## 5.6 Discussion and conclusions

The results of the seismic study in the Bay of Mecklenburg area provide a better insight of the structural framework and the distribution of sediments from the different post-Permian geological periods in the northern part of the Northeast German Basin. In general the Mesozoic-Cenozoic sedimentary deposition in the basin can be subdivided into two distinct periods separated by a period of uplift and erosion lasting from the Middle Jurassic and until Albian towards the end of the Early Cretaceous. The deposition in the southwestern part of the study area took place under the influence of halokinesis, whilst brittle deformation occurred in the northeastern part. The reason for this brittle deformation can be explained by the lack of mobile evaporites underneath acting as a decoupling zone. By comparing the limit of the Zechstein deposits mapped out by Vejbæk and Britze (1994) and Kossow et al. (2000) (Fig. 5.2) with the southwesterly limit of the WNW-ESE striking fault group (Fig. 5.7) it is observed that they share the position and the strike, enhancing this statement. Furthermore, the fault group is located in the same area with the same strike and dip as where Lassen et al. (2001)

and Krawczyk et al. (2002) found seismic evidence for a post-Caledonian collapse. From the isochoremap of the Jurassic succession (Fig. 5.10) it can be concluded that this displacement occurred in the Early Jurassic and to a minor extent during the Cretaceous (or Cenozoic) (Fig. 5.11). Whether this brittle deformation took place in pre-Jurassic times cannot be determined, due to the lack of deeper resolution of the data used in this study.

The interpreted tectonic quiescence during the deposition of the Lower and Middle Triassic sequences (Buntsandstein and Muschelkalk), as these layers only show post-depositional deformation (Fig. 5.10; 5.13a; 5.14a), is in agreement with the observations done by others in the adjacent part of the Northeast German Basin (e.g. Kossow et al., 2000; Kossow and Krawczyk, 2002; Scheck et al. 2003a; Scheck et al., 2003b; Hansen et al., 2005; Maystrenko et al., 2005b). During these times the basin experienced a rapidly tectonic subsidence, with an increasing thickness of the sequences towards the centre of basin.

Continued sedimentation during the Late Triassic and Early Jurassic is evident for the sedimentary record found in the study area from this period (Fig. 5.9; 5.10) But the relatively uniform subsidence and deposition pattern known from the Early and Middle Triassic was interrupted by extensional deformation in the Late Triassic (Keuper). Beside from an accelerated subsidence and basement-affecting normal faulting, creating several N-S trending graben structures within the CEBS (e.g. the Central Graben, Horn Graben and Glückstadt Graben), the extensional event is also believed to have triggered the initial phase of salt movement in the NEGB (Ziegler, 1990; Fisher and Mudge, 1998; Scheck et al., 2003a; Hansen et al., 2005). The growth of salt pillows is indicated from the thinning of the Upper Triassic succession above the Fehmarn Pillow and Salt Pillow A and C (Fig. 5.9). Another stratigraphic thinning is observed directly southwest of the NW-SE fault system, forming an E-W elongated structure. The low angle “Late Triassic Unconformity” observed in this particular area (Fig. 5.13b and Fig. 5.14b) correspond to the unconformity with the same name described by Clausen and Pedersen (1999) on the southern flank on the Ringkøbing-Fyn High north of the study area. They explained this unconformity to be the result of relative uplift of the eastern part of the Ringkøbing-Fyn High, because of differential subsidence during this period between the different structural basement highs and the surrounding basins. The same theory can be adapted to the E-W elongated structure. This structure is believed to have experienced a basement controlled relative uplift compared to the surroundings, due to the heterogeneous subsidence pattern in the Late Triassic. This furthermore explains why a local basin developed, characterized from the stratigraphic thickening of the succession north of the Prelow-1 well, in the eastern part of the study region. This subsidence

“resisting” area supports the statement, that the Avalonia-Baltica Suture zone is more complex than a normal abrupt transition zone (Poprawa et al., 1999; Gregersen et al., 2002; Plomerová et al., 2002).

The area, which experienced relative uplift in Late Triassic times, was subject to a great amount of subsidence during the Early Jurassic (Liassic) (Fig. 5.10). In this particular area Lower Jurassic sediments with a thickness of more than 500 ms are found. Halokinesis in this period is only seen on the minor stratigraphic thinning over the Fehmarn Pillow. The Lower Jurassic sequence is upward bounded by the Base Cretaceous Unconformity. This unconformity marks an uplift and erosional event that occurred sometimes between the Liassic and the Albian. A more specific timing of this event is still debated. Some (Kossow et al., 2000; Kossow and Krawczyk, 2002) argue that it took place on the Jurassic/Cretaceous transition, due to a fundamental reorganisation of the stress field in the region, controlled by the continued crustal extension in the Arctic-North Atlantic domain and the opening of the Alpine Tethys. Since the youngest sediments underneath the Base Cretaceous Unconformity, even in salt rimsynclines, are of Liassic age, it is believed that the initiating event is of an older age. Both in this study area and the adjacent Bay of Kiel (Hansen et al., 2005) an increasing amount of erosion is observed in the westward direction, which correlates well with the Central North Sea doming event (Ziegler, 1990; Underhill, 1998). As a result of the continued E-W directed stretching of the entire CEBS during the Late Triassic and Early Jurassic a plutonic plume developed underneath what became the North Sea triple junction (Underhill, 1998). The crustal thinning involved uplift and erosion in several parts of the CEBS including the entire northern part of the Northeast German Basin (Ziegler, 1990). The reorganisation of the stress field in the region at the Jurassic/Cretaceous transition (Kossow et al., 2000) probably then had a continuing effect, so the study region remained uplifted until the Albian. As a stand-alone example, the stratigraphic record from the Prelow-1 well (Hoth et al., 1993) argues against this scenario. According to the well report there are almost 300 meters of pre-Albian, Lower Cretaceous sediments and no record of the Base Cretaceous Unconformity in this area, which is in contrast to the results of this study. This sedimentary record is believed to be a very isolated example or more likely the result of a wrong dating for two specific reasons. Firstly, none of the other wells in the region holds a record of any pre-Albian Lower Cretaceous sediments (Nielsen and Japsen, 1991; Hoth et al., 1993). Secondly, the angular Base Cretaceous Unconformity, which also marks the Albian transgression in the area (Kossow et al., 2000; Hansen et al., 2005; Maystrenko et al., 2005a; 2005b), is traceable on all seismic lines of the survey (Fig. 5.5 and 5.6).

The sedimentation resumed with the Albian transgression and continued throughout the Cretaceous in most parts of the study region. Only little growth of salt pillows and minor faulting are observed in the areas that did not undergo later Cenozoic erosion (Fig. 5.11; 5.13d and 5.14d). This reveals that the Cretaceous was a period of tectonic quiescence, which is confirmed by studies from the entire Northeast German Basin (e.g. Scheck and Bayer, 1999; Kossow et al., 2000; Kossow and Krawczyk, 2002; Hansen et al., 2005; Maystrenko et al., 2005a; 2005b). The subsidence pattern for the Cretaceous differs from the ones of the previously described periods. The area around Darss, where the greatest amount of Jurassic sediments was found, is located where the Cretaceous succession is thinnest or absent (Fig. 11). The stratigraphic thinning, observed on the internal Cretaceous reflections of both flattened sections (Fig. 5.13d and 5.14d) indicates that this thinning is not just due to later erosion. The Cretaceous sequence is furthermore seen to thicken in the northeasterly and southwesterly directions from this area confirming that the entire regional stress field changed some times between the Early Jurassic and Late Cretaceous as suggested by others (Kossow et al, 2000; Kossow and Krawczyk, 2002 and references herein). The entire northeastern part of the study area experienced later erosion as Cretaceous sediments are found underneath the Quaternary deposits (Fig. 5.5 and 5.6). Whether this is due to the Alpine Orogeny or the later Holocene glaciations or a combination of both cannot be determined completely. Kossow and Krawczyk (2002) estimated the uplift around the Grimmen High obtaining values of around 500 m at the Cretaceous/Cenozoic transition. As the area with the thinnest sequence of Cretaceous sediments represent the western prolongation of the Grimmen High, it is believed that the Alpine Collision is responsible for the main part of inversion observed on the seismic profiles.

The thickness distribution of the Cenozoic sediments (Fig. 5.12) reveals that salt movement had influence on the deposition of the succession. This resumed halokinesis in the area (Fig. 5.13e and 5.14e) is presumably the result of a change in the regional stress field from extensional to compressional owing to the Alpine Orogeny (Ziegler, 1990; Gemmer et al., 2003). This explains why the rimsynclines, which holds the thickest succession of Cenozoic sediments, are orientated with a WNW-ESE striking long axial trend, perpendicular to the main compressional direction from the S (SSW) (Marotta et al., 2000; 2001; 2002; Marotta and Sabadini 2003; Kaiser et al., 2005). Furthermore, the accelerated salt movement caused the reactivation of the fault system found on the western flank of Salt Pillow D (Fig. 5.13e). Later Quaternary erosion is observed on parts of the interpreted seismic sections (Fig. 5.14e).

## **5.7 Acknowledgements**

The authors would like to thank Per Trinhammer for his technical assistance during the acquisition cruises, Egon Nørmark for the processing of the Baltseis surveys and his assistance during the processing of the NeoBaltic surveys and Kathryn Brookes for her constructive comments and corrections. The Baltseis project was founded by the Danish Natural Science Research Council (grant no. 970176, 9802129 and 9901810). The NeoBaltic project is funded by the German Research Foundation (DFG) (grant no. HU698/7-1 and -2) in the frame of the Special Research Project 1135.



## **6. Basin evolution of the northern part of the Northeast German Basin – insights from a 3D structural model**

by Martin Bak Hansen, Magdalena Scheck-Wenderoth, Christian Hübscher, Holger Lykke-Andersen, Ali Dehghani, Benjamin Hell and Dirk Gajewski.

Submitted to *Tectonophysics*, 01/2006

### **6.1 Abstract**

A 3D structural model for the entire southwestern Baltic Sea and the adjacent onshore areas was created with the purpose to analyze the structural framework and the sediment distribution in the area. The model was compiled with information from several geological time-isochore maps and digital depth maps from the area and consists of six post-Rotliegend successions: The Upper Permian Zechstein; Lower Triassic; Middle Triassic; Upper Triassic – Jurassic; Cretaceous and Cenozoic. This structural model was the basis for a 3D backstripping approach, considering salt flow as a consequence of spatially changing overburden load distribution, isostatic rebound and sedimentary compaction for each backstripping step in order to reconstruct the subsidence history in the region. This method allows determining of the amount of tectonic subsidence or uplifting as a consequence of the regional stress field acting on the basin and was followed by a correlation with periods of active salt movement. In general, the successions above the highly deformed Zechstein evaporites reveal a thickening trend towards the Glückstadt Graben, which also experienced the highest amount of tectonic subsidence during the Mesozoic and Cenozoic. Two periods of accelerating salt movement in the area has been correlated with the E-W directed extension during the Late Triassic – Early Jurassic and later by the Late Cretaceous – Early Cenozoic inversion, suggesting that the regional stress field plays a key role in halokinesis. The final part of this work dealt with a neotectonic forward modelling in an attempt to predict the future topography when the system is in a tectonic equilibrium. The result reveals that many of the salt structures in the region are still active and that future coastline will run with a WNW-ESE trend, arguing that the compressional stresses related to the Alpine collision are the prime factor for the present day landscape evolution.

*Key words: Basin modelling, backstripping, Central European Basin System, Northeast German Basin, Mesozoic and Cenozoic evolution, Neotectonic*

## 6.2 Introduction

The Northeast German Basin (NEGB) (Fig. 6.1) is a subbasin of the Central European Basin System (CEBS). This is one of the most intensive researched areas in the world, not just in terms of hydrocarbon exploration, but also for scientific purposes. Several projects were carried out to obtain a better understanding of the deep-rooted tectonic structure of the region, for example the EUGENO-S (EUGENO-S working group, 1998), BABEL (BABEL working group, 1991; 1993), DEKORP-BASIN (e.g. Meissner and Krawczyk, 1999; Krawczyk et al., 1999; DEKORP-BASIN research group, 1999), and POLONAISE '97 (e.g. Guterch et al., 1999; Grad et al., 1999) projects. Seismic stratigraphic studies in the southwestern Baltic Sea revealed evidence for Caledonian deformed younger sediments (Lassen et al., 2001; Krawczyk et al., 2002; Hansen et al., 2006), while Poprawa et al. (1999) provided a subsidence analysis of the Baltic Basin based on borehole information. Numerous detailed studies of the structural framework and the sedimentary cover have been carried out in the onshore parts of the NEGB (Scheck and Bayer, 1999; Bayer et al., 1999; Kossow et al., 2000; Kossow and Krawczyk, 2002; Scheck et al., 2003a; 2003b) and the offshore parts (Clausen and Pedersen, 1999; Hansen et al., 2005; 2006) and in the adjacent Northwest Germany and German North Sea sector (e.g. Baldschuhn et al., 2001; Maystrenko et al., 2005b). Studies of the paleo- and present-day stress fields of North German Basin are presented in several publications (e.g. Marotta et al., 2000; 2001; 2002; Marotta and Sabadini 2003; Kaiser et al., 2005; Kaiser 2005).

Despite several 3D geodynamic models being built for the different parts of the North German Basin, for example in the North Sea area (Gemmer et al., 2002a; 2002b; 2003), the Glückstadt Graben (Maystrenko et al. 2005a; 2005b), the southern and central parts of the NEGB (Bayer et al., 1997; Scheck and Bayer, 1999; Scheck et al., 1999; Scheck et al., 2003a; 2003b) and the adjacent Polish Basin (Lamarche et al., 2003; Lamarche and Scheck-Wenderoth, 2005), the northern part of the NEGB has until now never been included in such a model. This paper presents a 3D structural model and a 3D backstripping of this area based on the seismic studies by Britze (1989) on the islands of Lolland and FASTER in Denmark, and Hansen et al. (2005; 2006) in the southwestern Baltic Sea, combined with parts of the 3D structural models by Scheck and Bayer (1999) and Maystrenko et al. (2005a; 2005b). This work is a part of the NeoBaltic project (Hübscher et al., 2004) in the frame of the Special Research Project (SPP) 1135 (Littke et al., 2005) of the German Research Foundation (DFG).

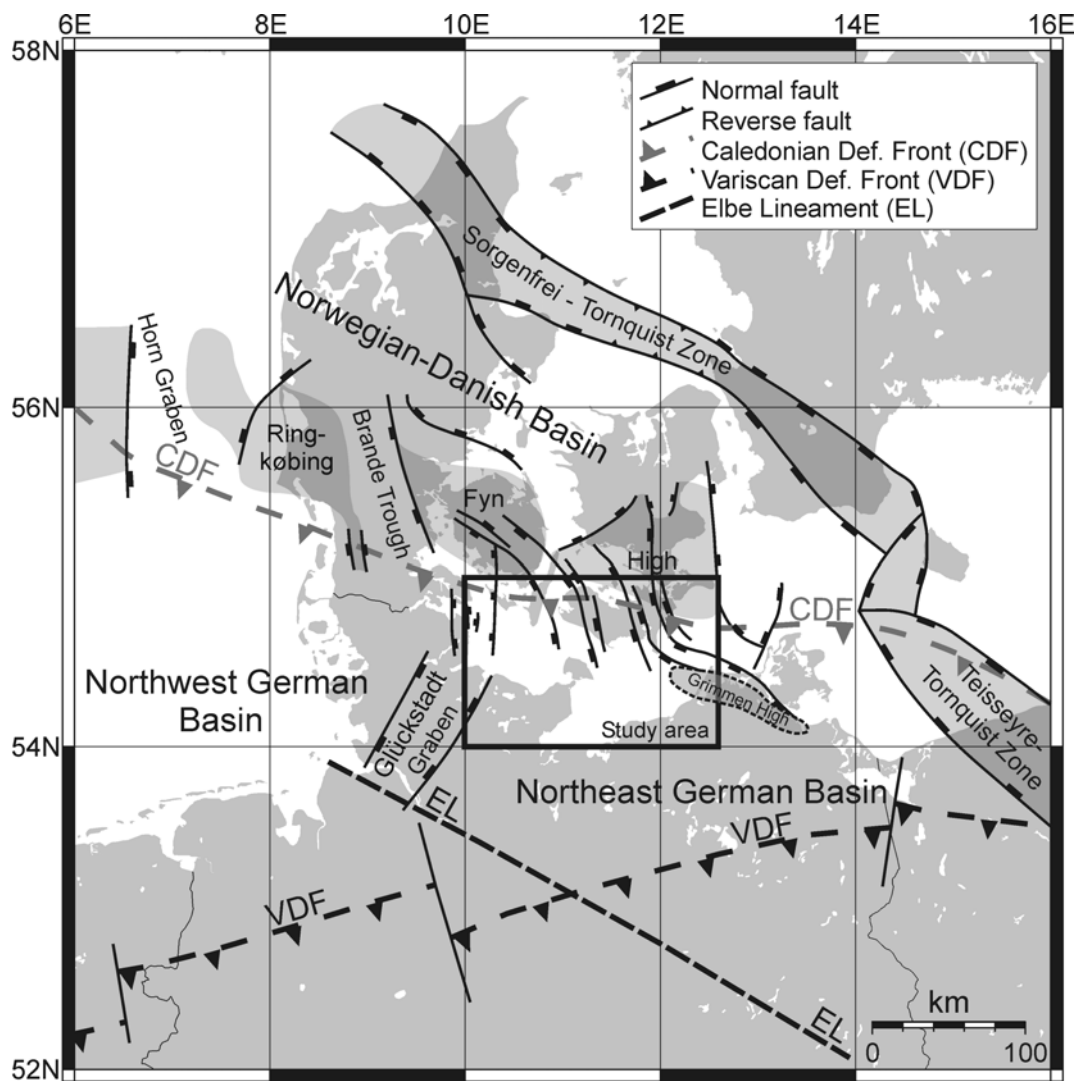


**Fig. 6.1** Location of the study area and the important structural elements of the region around the study area (compiled from Krauss, 1994; Vejrbæk, 1997; Bayer et al., 1999; Clausen and Pedersen, 1999; Kossow et al. 2000).

### 6.3 Geological Settings

The North German Basin (NGB) is the largest basin within the CEBS, covering an area extending from the southern North Sea across Denmark, the Netherlands and northern Germany to Poland. The CEBS comprises a series of subbasins that were initiated after the Variscan Orogeny. All the subbasins of the CEBS developed as intra-continental basins to the south and southeast of the Sorgenfrei-Tornquist Zone (STZ) and the Teisseyre-Tornquist Zone (TTZ) and north of the Variscan Deformation Front (VDF) (Scheck-Wenderoth and Lamarche, 2005). Other major

subbasins of the CEBS are (1) the Norwegian-Danish Basin and (2) the Polish Basin. The Northeast German Basin (NEGB) (Fig. 6.1) comprises the eastern part of the NGB and is bounded by the Ringkøbing-Fyn High to the north and to the south by parts of the VDF and the Elbe Lineament. To the west, the Glückstadt Graben separates the NEGB from the Northwest German Basin. Sediments in the NEGB range in age from Permian to present and have a thickness of 10-12 km in the central parts (Scheck et al., 1996; Benek et al., 1996).

The initial phase of thermal subsidence in the NEGB began in the Early Permian and continued until the end of the Middle Triassic (van Wees et al., 2000; Kossow et al., 2000). The oldest deposits in the basin consist of Carboniferous-Permian volcanics overlain by aeolian, fluvial and shallow-lake sediments of Lower Permian age. These sediments are followed by a sequence of Upper Permian (Zechstein) evaporites (Scheck and Bayer, 1999). This succession of evaporites was deposited as the result of a series of marine transgressions, primarily from the north, into the basin after a period of terrestrial conditions (Ziegler, 1990; Taylor, 1998). The following Triassic succession consists of a terrestrial Lower Triassic clastic red-bed sequence (Buntsandstein), overlain by marine carbonates of Middle Triassic age (Muschelkalk) (Kossow and Krawczyk, 2002). A eustatic sea-level drop at the Middle-Late Triassic transition led to renewed terrestrial sedimentation (Keuper) (Nöldeke and Schwab, 1976). The Triassic succession is overlain by a Lower Jurassic sequence, deposited under shallow-marine conditions (Underhill, 1998). From the Late Triassic and throughout the Early Jurassic, the basin evolution was influenced by a regional east-west directed extension. This extension resulted in accelerated faulting in the north-south trending graben structures in the CEBS (Central Graben, Horn Graben, Glückstadt Graben and the Brande Trough) (Ziegler, 1990). The regional extension furthermore initiated the first period of strong halokinesis in the NEGB (Jaritz, 1987; Hansen et al., 2005; 2006). The long period of subsidence and deposition in the NEGB was interrupted by a period of uplift and non-deposition lasting from Middle Triassic to Early Cretaceous (Ziegler, 1990; Underhill, 1998). The uplift caused the erosion of parts of the Lower Jurassic and Upper Triassic successions in the NEGB (Kossow et al., 2000; Hansen et al., 2005; 2006). The strong halokinesis in the central parts of the basin has resulted in younger Jurassic sediments being preserved in the rim synclines between salt structures (e.g. The Eastholstein Trough) (Maystrenko et al., 2005b). Sedimentation in the entire NEGB resumed towards the end of the Early Cretaceous (Albian) with the deposition of a terrestrial clastic sequence, followed by Upper Cretaceous marine marls and carbonates during a period of tectonic quiescence and rising eustatic sea level (Kossow and Krawczyk, 2002). Several pulses related to the Alpine Orogeny

inverted the NEGB and surrounding basins towards the end of the Late Cretaceous and during the Palaeogene (Ziegler, 1990; Krauss, 1994; Bayer et al., 1999; Scheck-Wenderoth and Lamarche, 2005). This N-S directed compressional stress-regime furthermore caused the reactivation of salt movement into existing structures in the northern part of the NEGB (Hansen et al., 2005; 2006). The Cenozoic succession in the NEGB shows a facies pattern of terrestrial and shallow-marine sediments deposited under the influence of salt movement (Kossow et al., 2000).

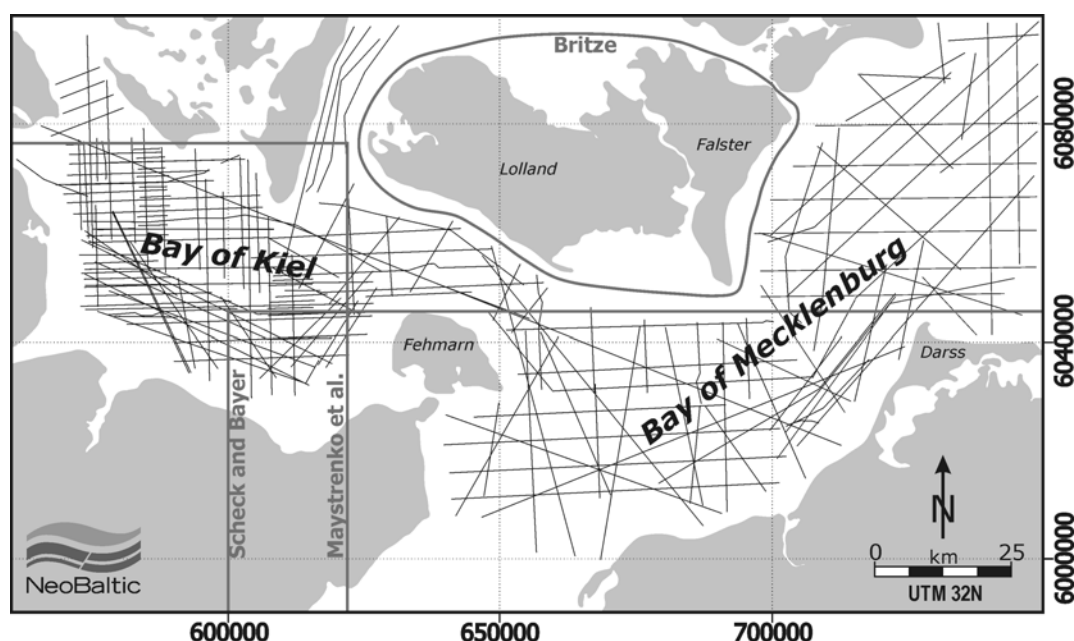


**Fig. 6.2** Modelling area with the geographical names referred to in the text. Furthermore, the grid of the seismic lines used for the mapping of the different horizons in the western Baltic Sea is shown along with the working areas of Britze (1989), Scheck and Bayer (1999) and Maystrenko et al. (2005a).

## 6.4 Methods

The 3D structure of the northern part of the Northeast German Basin has been modelled using the GeoModelling System developed at the GeoForschungs-Zentrum Potsdam, Germany (Bayer et al., 1996; 1997; 1999; Lewerenz, 1996; Scheck, 1997a; 1997b; Scheck and Bayer 1999). The method has previously been applied to the Northeast German Basin (Bayer et al., 1996; 1997; 1999; Lewerenz, 1996; Scheck, 1997a; 1997b; Scheck and Bayer, 1999; Scheck et al., 1999; 2002;

2003a; 2003b), the Glückstadt Graben (Maystrenko et al., 2005a; 2005b), the Polish Basin (Lamarche and Scheck-Wenderoth, 2005) and the entire CEBS (Scheck-Wenderoth and Lamarche, 2005).

The input datasets for the 3D modelling are the present-day time-structure maps from the NeoBaltic study of the southwestern Baltic Sea (Hansen et al., 2005; 2006) and from a seismic study in the Lolland-Falster onshore area (Britze, 1989). Depth information from the northeastern corner of the Glückstadt Graben (Maystrenko et al., 2005a, 2005b), the northern onshore parts of the Northeast German Basin (Scheck, 1997a, 1997b; Scheck and Bayer, 1999; Scheck et al., 1999, 2002) and the CEBS study (Scheck-Wenderoth and Lamarche, 2005) were also incorporated into the final model. The model consists of six layers covering the Permian to Cenozoic. The sedimentary layers represent (1) Cenozoic, (2) Cretaceous, (3) Upper Triassic (Keuper) to Jurassic, (4) Middle Triassic (Muschelkalk), (5) Lower Triassic (Buntsandstein) and (6) Zechstein. There were two depth levels available in the literature: the present-day topography (Institute of Geophysics and Planetary Sciences, 2003; Smith and Sandwell, 1997) and the Moho (Scheck-Wenderoth and Lamarche, 2005 and references therein). The input time-structure maps were digitised and depth converted using interval velocities (Table 6.1) determined by pre-stack depth migration on selected lines from the NeoBaltic Survey (Fig. 6.2). The different data points were interpolated using a minimum tension gridding technique (Earth Version 5.1; Dynamic Graphics). The thicknesses of the different stratigraphic layers are calculated as the difference between the depth levels bounding the sequence. The 2D grids used for the thickness interpolation are integrated into a 3D structural model using the GeoModelling System. The 3D model covers an area of 190×110 km, which comprises the entire southwestern Baltic Sea and the adjacent onshore areas (Fig. 6.2). The horizontal resolution is approximately 600 metres, as the 2D grids are composed of 300×166 cells. The vertical resolution corresponds to the number of layers (six). The coordinates in the model are based on UTM 32N.

Stratigraphic layer	Internal velocity [m/s]
Cenozoic	2000
Cretaceous	2400
Jurassic + U. Triassic	2600
Middle Triassic	3500
Lower Triassic	2800
U. Permian Zechstein	4800

**Table 6.1** Interval velocities used for depth conversion.

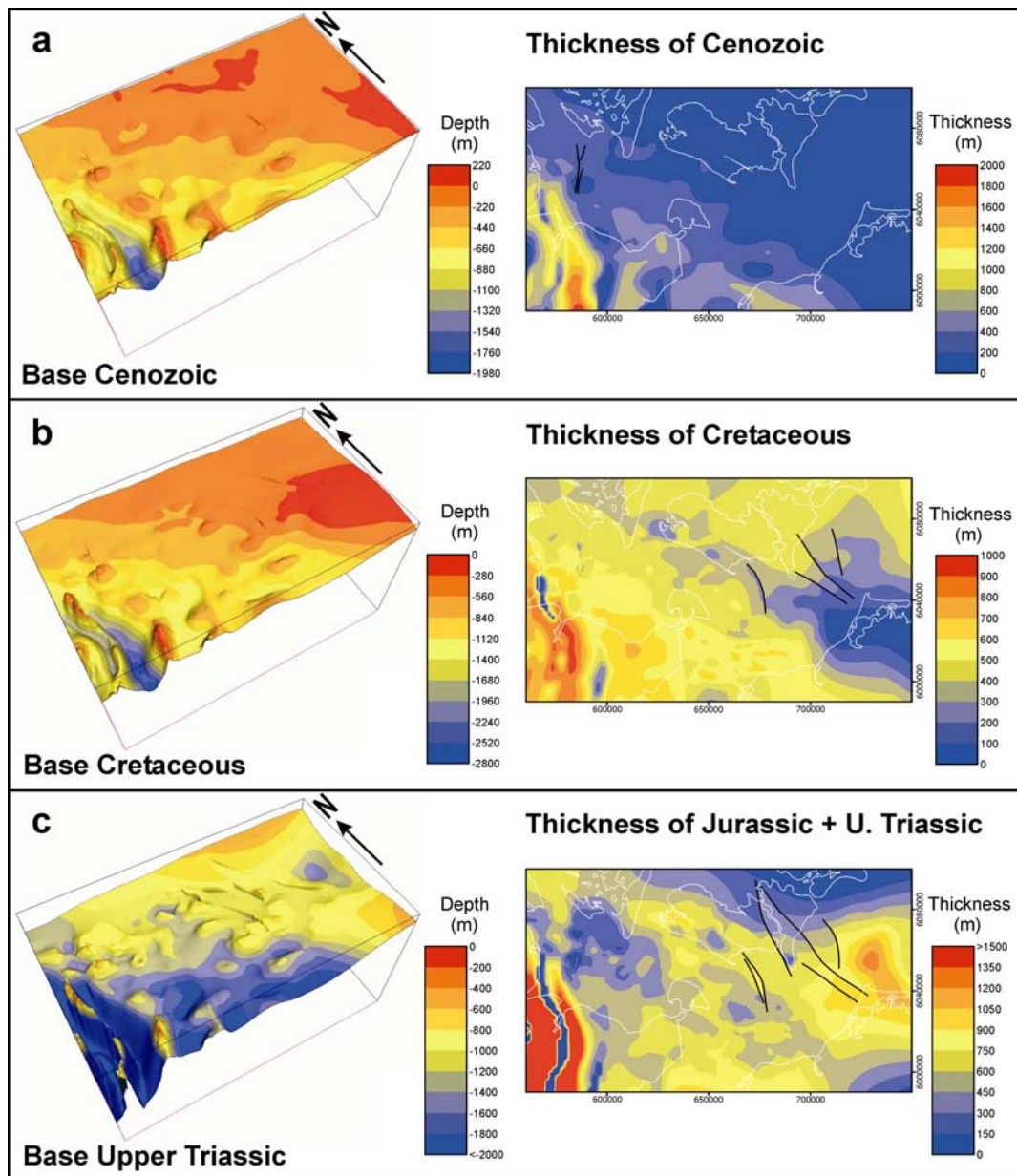


**Fig. 6.3** a-c 3D view of the base (left) and thickness maps (right) of the (a) Cenozoic, (b) Cretaceous and (c) Jurassic + U. Triassic successions. The modelling area is 190 x 110 km. The scale for the shaded relief 3D views is the same as for thickness maps.

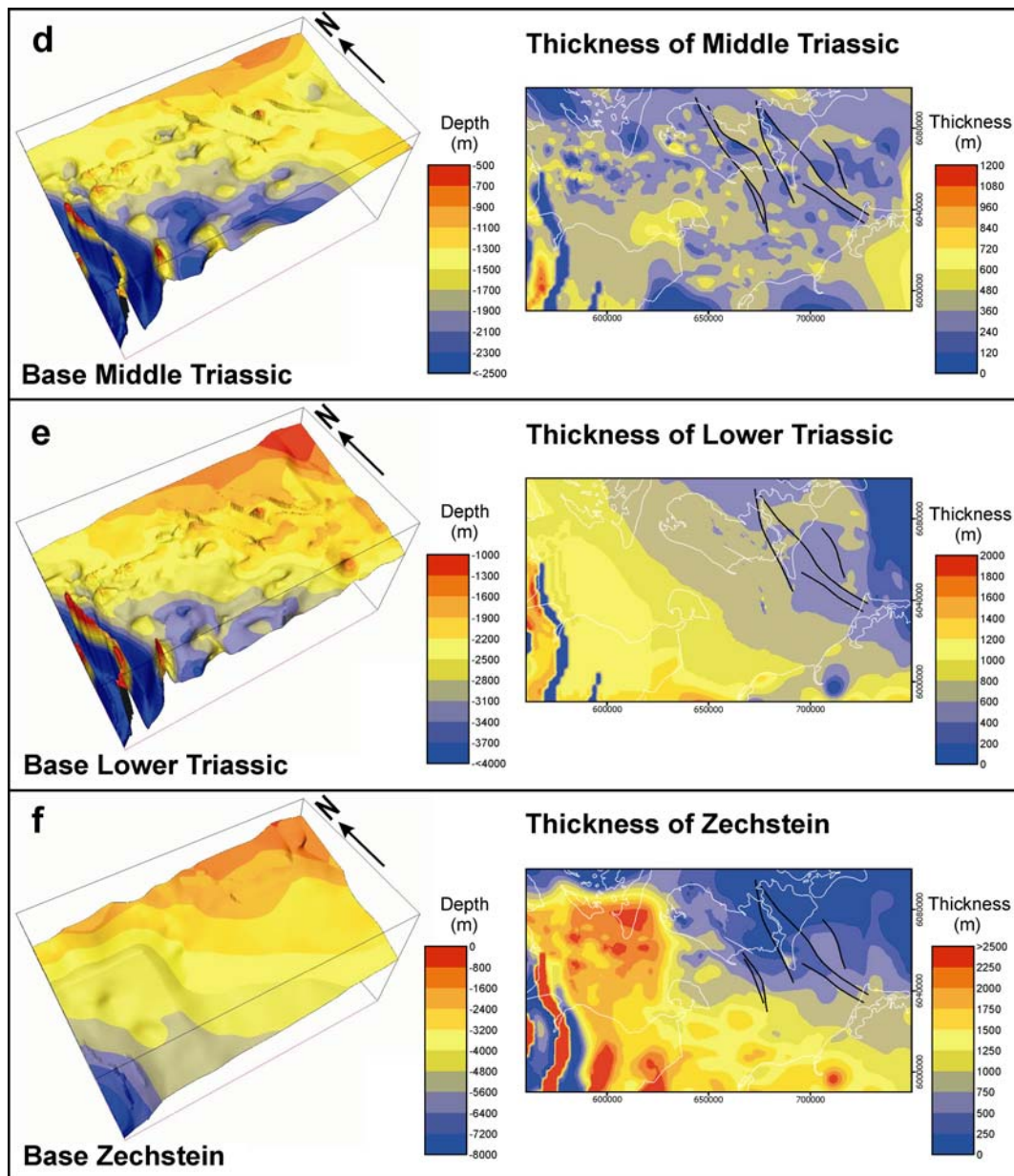


**Fig. 6.3 d-f** 3D view of the base (left) and thickness maps (right) of the (d) Middle Triassic, (e) Lower Triassic and (c) Upper Permian Zechstein successions. The modelling area is 190 x 110 km. The scale for the shaded relief 3D views is the same as for thickness maps.

## **6.5 3D structure of the northern part of the Northeast German Basin**

The results of the 3D structural modelling are displayed as shaded relief 3D views of successive surfaces from the present-day topography down to the base of the Zechstein (Fig. 6.3). Each 3D structure map is coupled with a thickness map of the respective layer. The 3D structure-depth maps provide geometric information on the present-day depths. The thickness maps show the distribution and the thickness of the sediments.

### **6.5.1 Cenozoic (Fig. 6.3a)**

The 3D structure map of the Base Cenozoic reveals the present-day topography of the surface. The surface has a general dip towards the southwest with the deepest part in the southwestern corner, between two updoming N-S oriented elongated structures. Several topographic highs and lows are seen on the surface.

By subtracting the topography values from the depth values of the Base Cenozoic surface, the thickness map of the Cenozoic succession was created. This map reveals that sediments from this geological time period are absent in the northeastern part of the modelling area, whilst a sequence of up to 2000 metres is found in the Glückstadt Graben. The succession thins out on both sides of this thick sequence as a result of accelerated halokinesis during the Cenozoic (Hansen et al., 2005). The N-S trending fault system in the northwestern corner is also a result of salt movement during the Cenozoic as known from the seismic data.

### **6.5.2 Cretaceous (Fig. 6.3b)**

The 3D depth view of the Base Cretaceous surface structure shows the same dipping and topography trends as the Base Cenozoic surface. One exception is the topography high in the southeastern part of the study area. This high represents the western part of the Grimmen High - a basement controlled inversion structure (Kossow et al., 2000; Hansen et al., 2006). Northwest of the Grimmen High, a few NW-SE orientated fault traces are observed.

The thickness map of the Cretaceous succession was made by subtracting the depth values of the Base Cenozoic surface from the ones of the Base Cretaceous. The map reveals thicknesses from 0 to 1000 metres. The thickest sequence is found in the Glückstadt Graben, whilst the succession is absent on top of the

Grimmen High and above two salt structures in the southwestern corner. The absence of the sequence above the two salt structures is presumed to be result of later erosion due to halokinesis as the succession is more than 500 metres thick around these areas. The abrupt displacements around the four fault traces in the eastern part of the area indicate that these systems were active during the Cretaceous.

### **6.5.3 Jurassic and Upper Triassic (Fig. 6.3c)**

The depth of the Base Upper Triassic surface is represented in the interval from 0 to 7000 metres. The surface generally dips toward the Glückstadt Graben in the southwest, with the exception being a local topographic low in the eastern part of the area. Several highs and lows show the positions of salt structures and rim-synclines respectively. In the western part, a N-S orientated fault system is seen above two salt pillows, while several N-S to NW-SE trending fault traces are detected in the northeastern part of the study area.

Subtraction of the Base Cretaceous surface from the Base Upper Triassic surface created the Jurassic – Upper Triassic thickness map. Thicknesses up to 5600 metres are seen in the Glückstadt Graben, whilst the average thickness outside the graben is around 750 metres. A stratigraphic thickening (up to 1350 metres) is observed in the topographic low in the eastern part of the Base Upper Triassic surface. The stratigraphic thinning of the sequence in the northeastern part represents the southern margin of the Ringkøbing-Fyn High, which at the time still separated the Northeast German Basin from the Norwegian-Danish Basin (Vejbæk, 1997). The absence of the succession above the N-S orientated salt walls is due to the piercing of salt body (Maystrenko et al., 2005a, 2005b). Abrupt thickness variations around the fault traces in the eastern part show that active displacement took place in these systems during this period.

### **6.5.4 Middle Triassic (Fig. 6.3d)**

The Base Middle Triassic surface reveals an almost identical topography to the previously described Base Upper Triassic surface. The surface occurs in the depth interval from 500 metres in the northeastern corner down to 7500 metres in the Glückstadt Graben. The throw on the different fault traces in the eastern part of the modelling area is more pronounced on this surface.

The thickness map of the Middle Triassic carbonate sediments was created by subtracting the depth values of the Base Upper Triassic surface from the ones of the Base Middle Triassic surface. The average thickness is around 500 metres with minor variations on top of salt structures and in the rim-synclines between in the central parts of the modelling area, whilst a succession of more than 1100 metres is found in the Glückstadt Graben. The lack of Middle Triassic sediments above the diapiric salt walls to the southwest is due to the later piercing of the mobile evaporate layer underneath.

### **6.5.5 Lower Triassic (Fig. 6.3e)**

The 3D structure map of the Base Lower Triassic reveals the topography of the top of the Zechstein evaporites. This map was created from the results of three other studies (Britze, 1989; Scheck and Bayer, 1999; Maystrenko et al., 2005a), due to the limited deeper resolution of the NeoBaltic data (Hansen et al., 2005; 2006). The surface covers the depth range from 700 metres in the northeastern corner and down to 8000 metres in the centre of the Glückstadt Graben. The map reveals the N-S oriented diapiric salt structures in the southwest, and the geometry of the salt domes and the rim-synclines in the central and eastern parts of the modelling area. Around the fault traces in the eastern part, displacements are detected on the surface. Thus, some of these salt structures must have developed on the flanks of the previously described faults in the region.

By subtracting the depth values of the Base Middle Triassic surface from the depth values of the Base Lower Triassic surface, the thickness map of the Lower Triassic Buntsandstein succession was created. This sequence is absent in the northeastern corner, whilst a thickness of up to 2000 metres is found in the Glückstadt Graben. In general, the succession reveals a thickening trend in the southwesterly direction throughout the entire modelling area. No abrupt thickness differences are seen around the NW-SE orientated fault traces in the eastern part, allowing the conclusion that no active faulting took place in these systems during the Early Triassic.

### **6.5.6 Zechstein (Fig. 6.3f)**

The structure map of the Base Zechstein surface was created with results from the studies by Maystrenko et al. (2005a) and Scheck-Wenderoth and Lamarche (2005). The surface shows a general dip from the northeastern corner towards the

Glückstadt Graben in the southwest. The highest part is shallower than 800 metres below NN, while the deepest part is in more than 8000 metres depth from the present-day surface. No major fault-related displacements are seen on this surface. The thickness map of the Zechstein evaporites was created by subtracting the depth values of the Base Lower Triassic surface from the ones of the Base Zechstein surface. The thickness map reveals thicknesses from 0 to 7500 metres. The thickest successions are found in the three N-S orientated diapiric salt walls in the Glückstadt Graben and in the salt pillows in the northwestern corner of the study region. The sequence is absent along the northern margin of the modelled area, which represents the southern boundary of the Ringkøbing-Fyn High, and in the rim-synclines between the diapiric salt walls in the Glückstadt Graben as a result of halokinesis. The abrupt thickness changes in the eastern part of the study area indicate that the thin-skin developed fault systems had an influence on the distribution of the evaporites throughout the Mesozoic and Cenozoic.

## **6.6 Backstripping method**

### **6.6.1 Basic assumptions**

In this modelling approach, some basic assumptions have to be made. Firstly it has to be assumed that salt behaves like a viscous fluid on a geological time-scale. This is consistent with the results of several studies related to the complexity of salt tectonic deformation (e.g. Vendeville and Jackson, 1992; Schultz-Ela et al., 1993; Davison et al., 1995), with analogue modelling studies (e.g. Koyi et al., 1993; Nalpas and Brun, 1993; Vendeville et al., 1995) and with the results from numerical models (van Keken et al., 1993; Poliakov et al., 1993; Podlachikov et al., 1993). All these studies indicate that the salt reacts as a viscous fluid over geological time spans.

The second assumption is that salt and the overburden are in a near hydrostatic equilibrium at all times, which means that the shape of the salt upper surface is dependent on the load acting upon it. This assumption is in agreement with the observation that there is a relationship between the thickness of diapir peripheral sinks and the amount of salt withdrawn from the corresponding area (e.g. Zirngast, 1996).

The third assumption is that the volume of the salt body is constant, because the salt is treated as an incompressible fluid, and that seismic studies from the

working area indicate that almost no salt has been lost due to solution (Hansen et al., 2005; 2006).

Finally, the observation that the salt in the study area tectonically decouples the deformation is used as an additional constraint. Knowledge that the basement of the salt is virtually undeformed due to this decoupling enables the base of the salt to be considered as a reference surface at which the load pressure must be in equilibrium.

Stratigraphic layer	Dominant lithology	Rock density [kg/m <sup>3</sup> ]	Final porosity [%]	Initial porosity [%]	Porosity depth factor
Cenozoic	Clastics	2670	0	51	6.2
Cretaceous	Chalk	2400	0	67	6.8
Jurassic + U. Triassic	Clastics	2700	0	81	12.0
Middle Triassic	Carbonates	2400	0	20	0.5
Lower Triassic	Sandstone	2670	0	51	6.2
U. Permian Zechstein	Evaporites	2200	0	0	0
Pre-Zechstein crust	Granodiorite	2850	0	0	0
Mantle	Peridotite	3300	0	0	0

**Table 6.2** Rock properties for the different layers used in the backstripping calculations.

## 6.6.2 Modelling concept

Prior to the backstripping, a starting model is defined with assigned physical properties for the sedimentary layers including load-porosity dependent densities and associated compaction determined by the porosity depth factor for each sedimentary succession (Table 6.2). These assigned physical properties have to be assumed homogenous for each layer. Consequently, every layer is characterised by an average dominant lithology with lithology-dependent physical properties.

For this starting model, the sedimentary load is determined using a 3D finite element method (Scheck et al., 2003a). For the resulting model of load distribution, the variation of the crustal density that is in isostatic equilibrium with the sediment load and the position of the Moho is calculated assuming Pratt-Isostasy. This calculates which average density distribution in the crystalline crust would be in isostatic equilibrium with a given Moho position and a given sediment load (Scheck and Bayer, 1999). Subsequently the different stratigraphic layers are removed step-by-step and the salt distribution and the isostatic equilibrium are recalculated for each step according to an Iceberg Model. After

stripping off a layer, load-porosity-dependent densities and associated decompaction are recalculated (Scheck and Bayer, 1999).

Calculations are performed using software developed at the GeoForschungs-Zentrum Potsdam running on UNIX workstations or on LINUX-PCs. In order to handle the backstripping problem in reasonable CPU times or even interactively, certain constraints have to be enforced during the backstripping and the complexity of 3D calculations has to be reduced. Thus, the 3D problem is split into three separate processes (Fig. 6.4). The first step is the stripping off of a sedimentary layer and the decompaction of the remaining layers. The second step deals with the redistribution of the salt according to the new load condition, followed by an adjustment of the compaction distribution. Finally, the entire model is isostatically compensated.

The equilibrium distribution of salt is found for each backstripping step in an iterative process by alternating between salt redistribution and compaction adjustments followed by local isostatic compensations.

Starting with the present-day model, each layer is stripped off step-by-step down to the top of the salt. After several iterations of smoothing the top salt surface and a final isostatic compensation of the model, it is possible to get the salt distribution for each step that is in hydrostatic equilibrium with the load of the overburden. Continued backstripping, followed by salt redistribution down to the top of Zechstein results in an equilibrated salt layer.

## **6.7 Backstripping**

In order to investigate how far the previously described patterns of subsidence were controlled by tectonics, the amount of tectonic subsidence for each of the different geological time periods was calculated. In the backstripping process, each sedimentary sequence is removed successively with decompaction of the underlying layers, followed by salt redistribution and local isostatic compensation. Therefore, the load-induced subsidence is removed in order to determine the amount of subsidence (or uplift) that has taken place since the deposition of each succession in the model. This is done by subtracting the cumulative tectonic subsidence of a specific layer from the cumulative tectonic subsidence of the overlying layer. The result is the real amount of tectonic subsidence or uplift during the deposition of the specific layer.

In this case it should be mentioned that the different results of this exercise reflects the net amount of subsidence or uplift during the different geological periods of interest. Thus, e.g. periods of inversion and associated erosion are

neglected if the amount of subsidence before and after exceeds the amount of uplift. Furthermore, neither periods of glaciations and related isostatic rebounds nor paleo water depth variations have been taken into account. Therefore, some errors might occur in these calculations.

The average amount of subsidence/uplift has been calculated for four geological periods in this study. These are the Middle Triassic (Muschelkalk) (Fig. 6.5a), the Keuper and Jurassic (Fig. 6.5b), the Cretaceous (Fig. 6.5c) and the Cenozoic (Fig. 6.5d). On these figures the positive values reflect the amount of subsidence, while the negative values reveal uplift. Compared to the previous described 3D structural model the Upper Permian Zechstein and the Lower Triassic have not been included in these calculations. The reason for this is, that the values for these successions used in this study are based on interpolations of the results done by others outside the NeoBaltic project. Finally, the result of an approach to model the neotectonic activity is shown and compared to the present day surface in Figure 6.6.

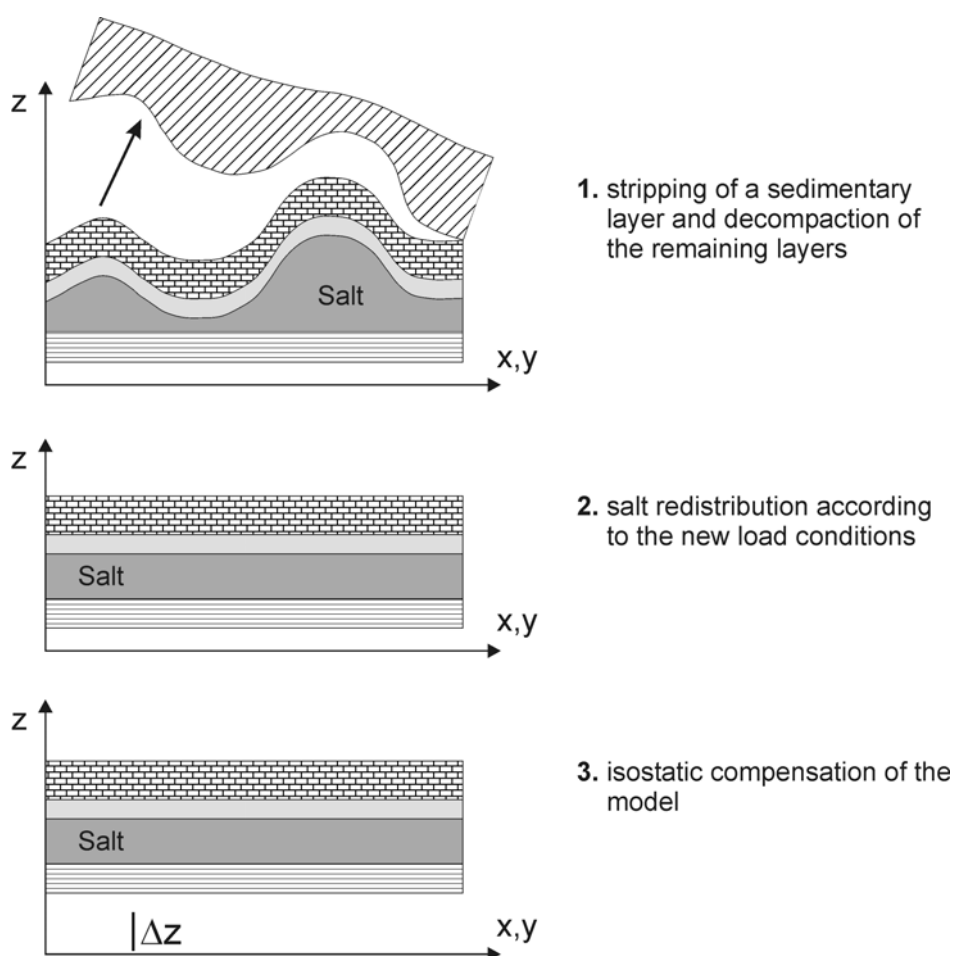
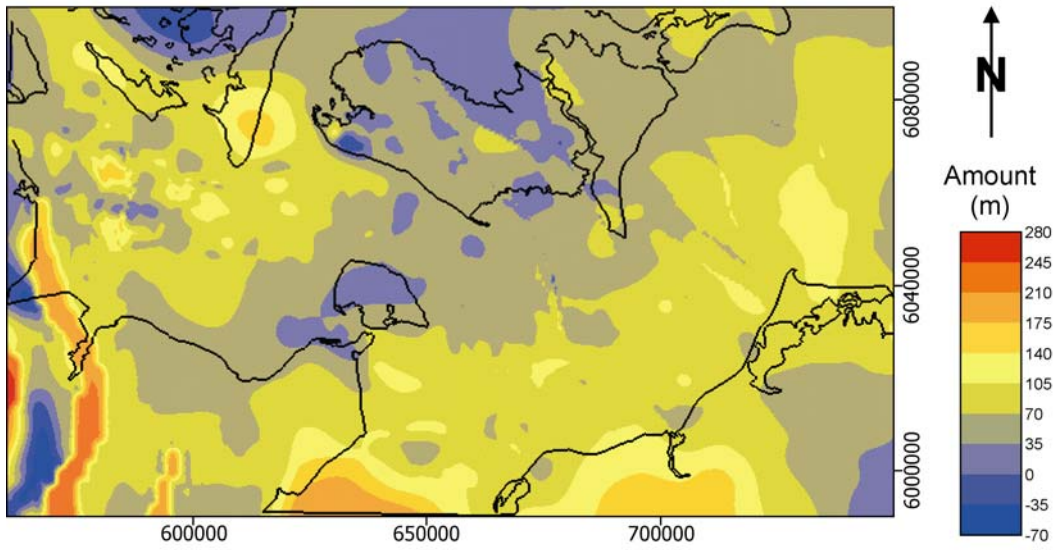


**Fig. 6.4** Simplified scheme of the modelling concept to perform backstripping with salt redistribution (from Scheck et al., 2003b).

### A. Middle Triassic



### B. Upper Triassic + Jurassic

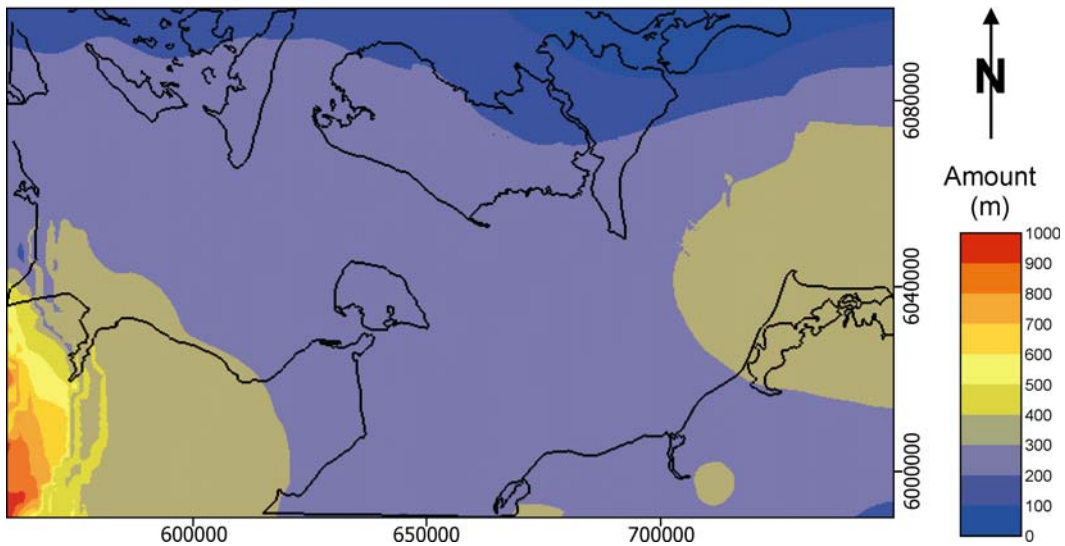
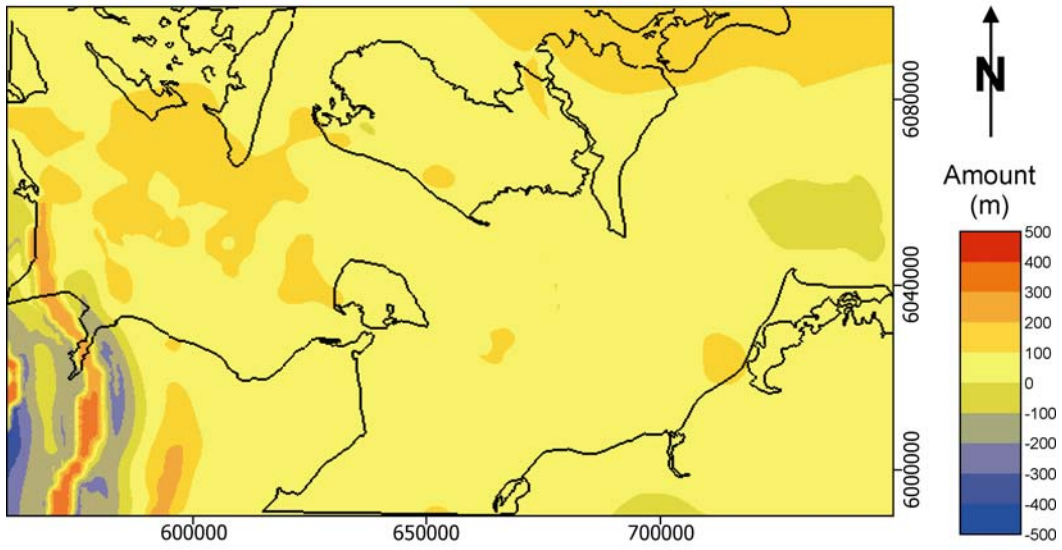


**Fig. 6.5 a-b** Distribution of the calculated vertical tectonic movement for (a) the Middle Triassic and (b) the Upper Triassic and Jurassic. Positive values indicate tectonic subsidence and negative values uplift.

### C. Cretaceous



### D. Cenozoic

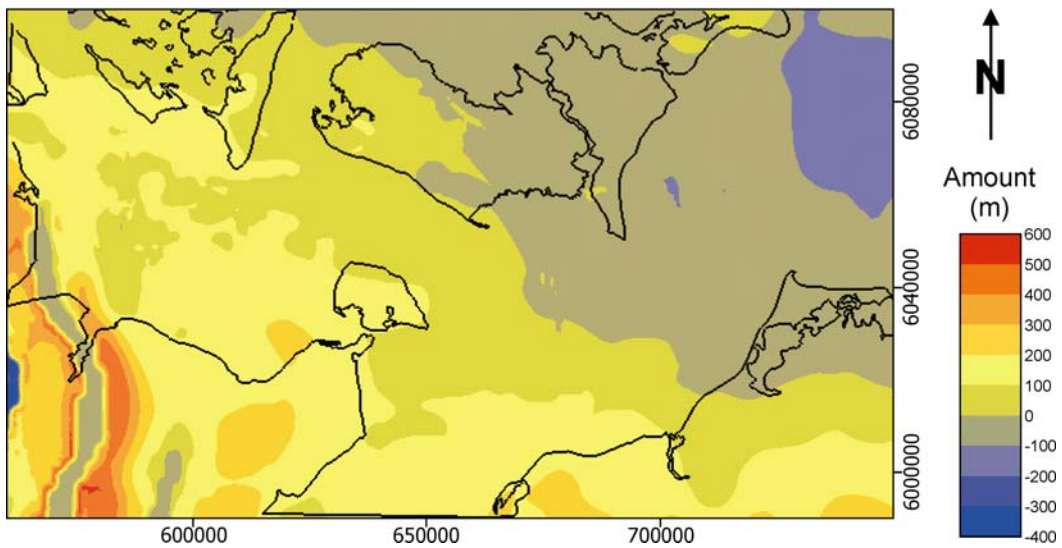


**Fig. 6.5 c-d** Distribution of the calculated vertical tectonic movement for (c) the Cretaceous and (d) the Cenozoic. Positive values indicate tectonic subsidence and negative values uplift.

### **6.7.1 Subsidence and uplift patterns**

The distribution of the tectonic movements of the Middle Triassic (Muschelkalk) (Fig. 6.5a) reveals a very unequal subsidence pattern throughout the western Baltic Sea. The largest amount of tectonic subsidence with more than 140 m is found in the southern part of the study area. The abrupt changes between areas with an average subsidence and areas with uplift in the Glückstadt Graben in the southwestern corner will be discussed in the following chapter.

The tectonic subsidence distribution pattern for the Upper Triassic (Keuper) and the Jurassic (Fig. 6.5b) shows that the smallest amount of subsidence occurred in the northern part of the study area, towards the Ringkøbing-Fyn High (less than 100 m), with an incensement in the southwesterly direction towards the Glückstadt Graben (up to 1000 m). An exception of this general pattern is the greater amount of subsidence observed in the eastern part during this time.

The pattern of tectonic subsidence for the Cretaceous (Fig. 6.5c) reveals a uniform distribution with values up to 100 m in most parts of the region. An area north of Darss in the eastern part of the study area shows a little uplift, while some parts of the Bay of Kiel reveals subsidence values between 100 and 200 m. Like in the case with the tectonic movement map of the Middle Triassic (Fig. 6.5a), the abrupt changes between areas with uplift and subsidence in the Glückstadt Graben will be discussed later.

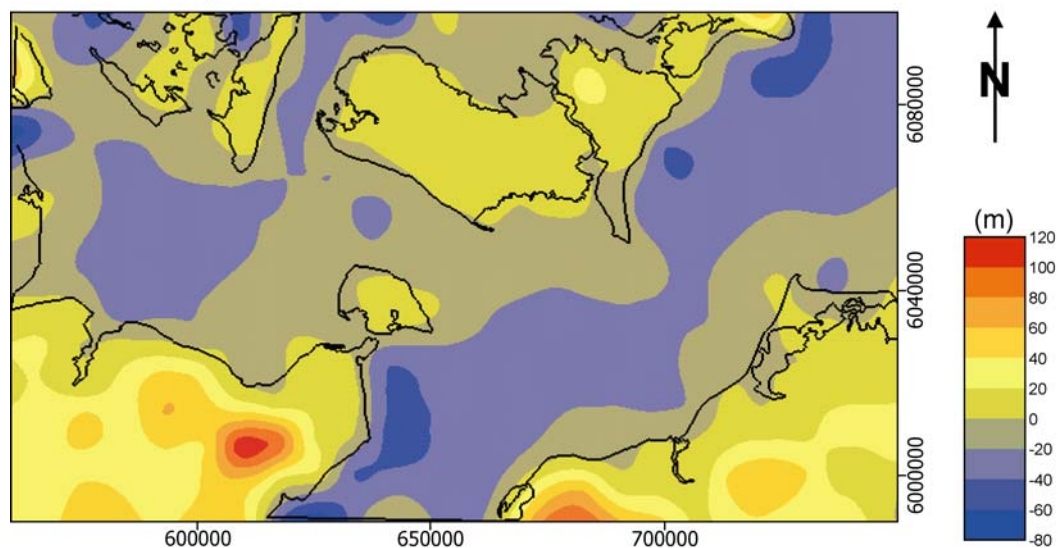
The Cenozoic tectonic movement map (Fig. 6.5d) indicates uplift (up to 200 m) in the northeastern part of the study area and subsidence with an increasing trend towards the southwest. In parts of the Glückstadt Graben the subsidence values exceeds 500 m. The areas on top of the diapiric salt walls in the southwestern corner reveal uplift, which is interpreted to be the result of an accelerated movement of the evaporitic structures underneath in the Cenozoic.

### **6.7.2 Neotectonic modelling**

A forward modelling was completed in order to determine the neotectonic vertical movement in the southwestern Baltic Sea. The surface (Fig. 6.6a) shows where the coastline would be running when the entire tectonic system is in equilibrium. For comparison the present-day topography surface used in this modelling is presented in Figure 6.6b. If the present-day load regime would continue towards equilibrium, the area around the western Baltic Sea would be more or less equally subdivided in one land and one sea area. The coastline would run from the northwestern corner in a WNW-ESE trend towards the southeast. In the Bay of

Kiel three islands are seen on top of the salt pillows previously described by Hansen et al. (2005). The same is seen to be the case in the area on top of the salt structures in the northeastern part of the Glückstadt Graben. This suggests that present-day halokinetic movement in these structures is occurring.

### A. Present day surface



### B. Modelled future surface (Tectonic equilibrium)

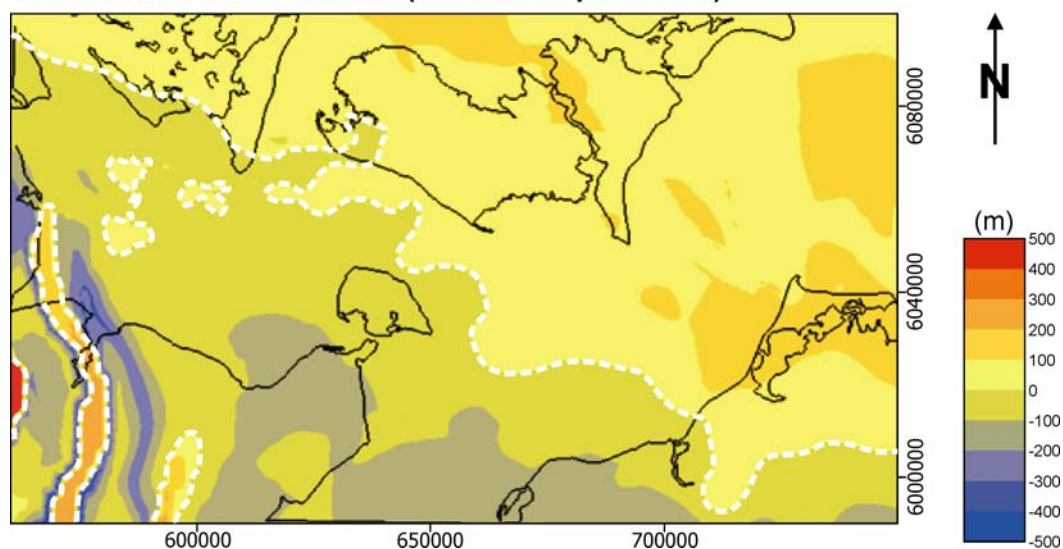


**Fig. 6.6** Present-day surface topography (a) compared to the modelled future surface topography (b) when the system is in tectonic equilibrium. The white dotted lines mark the future coastline.

## **6.8 Discussion and conclusions**

The 3D structural model of the northern part of the Northeast German Basin presented in this work, contributes to a better visualisation of the present-day structural framework of the sedimentary infill (Upper Permian to recent). The structural analysis of the 3D model and the outcome of the backstripping will be compared for each of the steps below and the assumed errors discussed.

### **6.8.1 Late Permian (Zechstein) to Early Triassic**

The thickness map of the Upper Permian Zechstein succession (Fig. 6.5f) reveals the present-day distribution of the sediments after an extensive amount of salt movement. Because the modelling area only covers a part of the entire salt basin, it is difficult to access the initial thickness after deposition. Since it cannot be determined how much salt moved in or out of the area or how much salt was later dissolved. The first is especially the case in the Glückstadt Graben in the southwestern corner. Maystrenko et al. (2005a; 2005b) demonstrates that the graben system experienced a high amount of salt movement into several N-S trending diapiric salt walls. As seen on Figure 6.3f the modelling area in this work only covers parts of the Glückstadt Graben. So far no one has modelled the entire Southern Permian Basin (van Wees et al., 2000) with the emphasis on halokinesis. The Southwesterly thickening trend of the Lower Triassic sequence (Fig. 6.3e) without any abrupt variations around the known salt structures in the area, suggest that no major halokinesis occurred during this period of time. This observation is in agreement with the work done by others in the adjacent areas of the western Baltic Sea (e.g. Scheck and Bayer 1999; Kossow and Krawczyk 2002; Scheck et al. 2003a; Maystrenko et al. 2005a; 2005b; Hansen et al. 2005; 2006). The structural modelling furthermore reveals that the Lower Triassic succession was later pierced by mobile Zechstein salt, revealed from the absence of sediments from this period on top of the N-S trending diapiric walls in the Glückstadt Graben (Fig. 6.3f).

### **6.8.2 Middle Triassic**

The thickness variations of the Middle Triassic sediments around salt structures (Fig. 6.3d) indicate that the movement of the underlying Zechstein evaporites was initiated in this time period. This initiation was caused by a basin wide E-W

extension (Ziegler 1990; Fisher and Mudge 1998; Scheck et al. 2003b), which also created several N-S trending graben structures, including the Glückstadt Graben, in the entire CEBS. This could also explain the thin-skinned (no fault traces on the Base Zechstein surface (Fig. 6.3f)) faulting during the Middle Triassic in the eastern part of the study area. The unequal subsidence pattern modelled for the Middle Triassic (Fig. 6.5a) might be the result of the ongoing salt movement during this period.

### **6.8.3 Late Triassic and Jurassic**

The high amount of tectonic subsidence in the Glückstadt Graben (Fig. 6.5b) throughout the Late Triassic and parts of the Jurassic resulted in a thick sequence of sediments from this period (Fig. 6.3c). This shows that the E-W extension initiated in the Middle Triassic continued throughout the Late Triassic and into the Early Jurassic. This subsidence pattern is believed to have ended at the transition between the Early and Middle Jurassic, because the thick successions of Jurassic sediments in the Glückstadt Graben and in the local subbasin in the eastern part of the modelling area (Fig. 6.3c) are all of Early Jurassic age (Hansen et al. 2005; 2006 and references therein). From the Middle Jurassic and onward the entire CEBS was uplifted due to the mid North Sea doming event and a considerable amount of older sediments were eroded away (Underhill 1998; Gemmer et al. 2003; Hansen et al. 2005; 2006). This uplift event is not detectable in the modelling, as the subsidence during the Late Triassic and Early Jurassic exceeds the amount of uplift.

### **6.8.4 Cretaceous**

The subsidence pattern for the Cretaceous (Fig. 6.5c), do not fit the thickness distribution of the sediments deposited in this time period very well. It reveals an average subsidence of around 100 m in most parts of the modelled region and uplift in the rimsynclines between the diapiric walls in the Glückstadt Graben. The thickness map (Fig. 6.3b) shows that the thickest succession is found in the Glückstadt Graben in an area that should have experienced the highest amount of uplift. Furthermore, the map reveals that Cretaceous sediments are absent in the southeastern corner, which was modelled to have undergone subsidence. The first problem can only be interpreted as a modelling error, whilst the last one could be

explained by the Late Cretaceous inversion of the Grimmen High and later erosion during the Cenozoic (Fig. 6.5d).

### **6.8.5 Cenozoic**

In contrast to the modelling result for the Cretaceous period, the subsidence/uplift pattern of the Cenozoic fits well to the distribution of the sediments from this Era (Fig. 6.3a + 6.5d). The thickest successions of sediments are found in the areas which experienced the highest amount of subsidence and the Cenozoic sequence is absent in the areas with uplift. Furthermore, the uplift is less pronounced on top of the salt structures in the Bay of Kiel and the Glückstadt Graben indicating active salt movement. This is in agreement with the observations by e.g. Hansen et al. (2005) and Maystrenko et al. (2005b). Compared to subsidence pattern for the entire CEBS (Scheck-Wenderoth and Lamarche, 2005) this modelling suggests tectonic subsidence in the Glückstadt Graben. Like earlier, accelerated salt movement could explain this, but since Cenozoic sediments are present in most parts of the Bay of Kiel (Hansen et al., 2005) an additional amount of tectonic subsidence is expected in this case.

### **6.8.6 Neotectonic**

One of the more interesting results of this study is the neotectonic forward modelling (Fig. 6.8a). The future coastline, which also represents the subsidence/uplift boundary, is running in a WNW-ESE direction. This is in very good agreement with the neotectonic studies done by Stackebrandt (2004) and Reicherter et al. (2005). Both these studies are based on analysis of the present-day landscape and the drainage pattern of rivers in the region. These results are numerically proven in this work. Furthermore, the forward modelling also suggests that active salt movement is occurring into the salt pillows in the Bay of Kiel and the diapiric wall in the Glückstadt Graben. Lehné and Sirocko (2005) have also suggested this for the Glückstadt Graben and Hansen et al. (2005) for the Bay of Kiel.

### **6.8.7 Modelling errors**

As mentioned a couple of times in earlier chapters, some of the resulting subsidence and uplift patterns are in contrast to the amount of sediments deposited during the same period. Errors are believed to occur in the modelling process, especially when it includes salt movement. The redistribution of the salt is done at the beginning of each backstripping step followed by isostatic compensation. Thus, these calculations are only performed instantly a number of times determined by the vertical resolution of the model (the number of layers). This is in contrast to the true picture where halokinesis and vertical tectonic movements are continuous processes for a period of time. Other errors can occur if the modelling area includes piercing salt structures. The sequence will appear to be absent in the area of the piercing salt structures in the 3D structural model used for the backstripping. Thus, the salt will flow into these voids during redistribution straight away because of the density contrast. This can be avoided if a restored cover is incorporated into the model and later replaced by the present-day layer at the believed time of piercing. This exercise was completed successfully by Scheck et al. (2003b) for the onshore part of the Northeast German Basin. This is not the case for this study because the western Baltic Sea, the main study area for this project, does not include any piercing salt structures. However, the northeastern corner of the Glückstadt Graben was included into the modelling rectangle. For a detailed modelling of the Glückstadt Graben we refer to Maystrenko et al. (2005a; 2005b), who also showed that some salt was dissolved and redeposited during the mid-Late Triassic times (Keuper). In this study potential volume change for the salt was not considered. Thus, the total volume of initial salt may be slightly underestimated.

### **6.8.8 Concluding remarks**

Despite the modelling errors observed in some parts of this work, the overall result is satisfactory. The general subsidence and uplift pattern fits well with the observations done by others in the region and the neotectonic forward modelling proved numerically the interpretations of other authors. In general it can be concluded that this kind of 3D modelling is suitable for an analysis of the structural evolution of a basin with active salt movement, if the proper precautions are taken into account.

## **6.9 Acknowledgements**

The authors would like to thank Per Trinhammer and Egon Nørmark for their technical assistance during the acquisition and processing of the seismic data from the Baltseis and NeoBaltic surveys. We are grateful to Yuriy Maystrenko for the permission to incorporate the northeastern corner of the digital 3D structural model from the Glückstadt Graben area into this work. Special thanks go to Björn Lewerenz for his tireless technical support during the model build-up and backstripping process. Finally, the authors would like to acknowledge Kathryn Brookes very much for all her constructive comments in order to improve the manuscript. The Baltseis surveys were funded by the Danish Natural Science Research Council (grant no. 970176, 9802129 and 9901810). The NeoBaltic project is funded by the German Research Foundation (DFG) grant no. HU698/7-1 & 2 in the frame of the Special Research Project no. 1135: Dynamics of Sedimentary Systems.

## 7. Summary and Conclusions

During several marine geophysical data acquisition cruises in the western Baltic Sea, for the Baltseis and NeoBaltic projects, a dense grid of 2D high-resolution multichannel seismics and to some extent gravity and magnetic data were acquired in the German and Danish territorial waters of the region. The western Baltic Sea comprises the northern part of the Northeast German Basin on the southern flank of the Ringkøbing-Fyn High. Furthermore, parts of the suture zone between the Avalonia and Baltica plates (the Caledonian Deformation Front) and the Sorgenfrei Tornquist Zone were investigated during these research cruises. Adjacent to the study area two structures are located, which are important for the structural evolution in the region. To the west the N-S trending Glückstadt Graben and in the eastern part the E-W running Grimmen High.

The work presented in this dissertation is based on the seismic data, in terms of processing, interpretation and modelling, as a part of the Special Research Project (SPP) 1135 of the German Research Foundation “Dynamics of sedimentary systems under varying stress regimes: The example of the Central European Basin System”. In the following, the main results of the three scientific articles, presented in the previous three chapters, will be compared and summarised briefly without references.

The depositional and structural evolution for the Bay of Kiel and the southwestern half of the Bay of Mecklenburg are very much alike, as both sub-areas are located within the area of distribution of the Zechstein evaporites. After the deposition of the Upper Permian Zechstein salts the thermal subsidence in the Northeast German Basin continued in during the Early and Middle Triassic, as a result of the cooling of the lithosphere after the Rotliegend (Lower Permian) volcanism. This subsidence pattern provided accommodation space for Lower Triassic clastics (Buntsandstein) and Middle Triassic carbonates (Muschelkalk) in the entire Northeast German Basin. Both sequences reflect a slight thickening trend towards the basin centre in the south-southwesterly direction on the isochore maps produced from the seismic sections interpreted in this study. In the adjacent parts of the basin, both successions also reveal a uniform gradient of increasing thickness toward the centre of the basin suggesting a regional subsidence pattern without any major tectonic activity or halokinesis throughout the Early and Middle Triassic. The 3D backstripping revealed that deposition during the Middle Triassic was determined by an amount of tectonic subsidence up 140 m.

A Late Triassic extensional event affected the entire Central European Basin System, related to the break-up of the Pangea supercontinent, with an accelerated subsidence and normal faulting of the basement. This E-W directed regional extension created several N-S trending graben structures in the region (e.g. the Central Graben, the Horn Graben and the Glückstadt Graben) and initiated vertical salt movement within the basin. Especially in the Bay of Kiel the halokinesis had a syn-sedimentary effect on the Upper Triassic deposits. The different salt pillows and the elongated rim synclines in between are orientated in a N-S trend perpendicular to the direction of the regional extension. The vertical salt movement lead in one case to the development of a thin-skinned crestal graben on top of one of the salt structures in the Bay of Kiel.

A low angle Late Triassic unconformity is observed on the seismic profiles in the area around the Grimmen High, and by other authors on the southern flank of the Ringkøbing-Fyn High. This unconformity is the result of a differential subsidence between the different blocks of the Ringkøbing-Fyn High, the different parts of the Avalonia Plate and the surrounding basins. Another outcome of this Late Triassic differentiated subsidence was the development of a basin between the Grimmen High and the Avalonia/Baltica suture zone in the eastern part of the Bay of Mecklenburg.

The E-W directed extensional regime proceeded into the Early Jurassic with continues halokinesis. In contrast to the tectonic settings for the Late Triassic, the former subsidence-resisting areas underwent a pronounced amount of subsidence during the Early Jurassic. This is seen on the local (Lower) Jurassic basin in the area west and north of Darss. Other evidence for continues stretching is the normal faulting observed in the Avalonia/Baltica suture zone. The reason for this faulting with little throw is the lack of an evaporitic layer underneath acting as a decoupling zone. The tectonic subsidence map for the Upper Triassic and Jurassic shows that the E-W directed extension caused a net amount of tectonic subsidence up to 1000 m in the Glückstadt Graben and more than 300 m in the area around the local Jurassic basin in the eastern part of the modelling region.

The continuing extension and thinning of the lithosphere induced a pronounced rifting in the Central North Sea area. The rifting resulted in a plutonic updoming with comprehensive erosion of the Lower Jurassic and Upper Triassic strata. This erosional event is marked by a clear angular unconformity on all the seismic sections from the western Baltic Sea, with an increasing amount of erosion westward. In most parts of the Bay of Kiel Upper Triassic deposits are

subcropping the unconformity, whilst Lower Jurassic sediments are present in the salt rimsynclines in the Bay of Kiel and in most part of the Bay of Mecklenburg.

The entire northern part of the Northeast German Basin remained uplifted, presumably due to a fundamental structural reorganisation at the Jurassic/Cretaceous boundary. This change in the stress field occurred, according to other authors, due to the opening of the Alpine Tethys Ocean and the continued crustal extension in the Arctic – North Atlantic domain. Sometimes during this period of non-deposition the salt movement ceased in the northern part of the Northeast German Basin.

Sedimentation resumed in the study area in Albian towards the end of the Early Cretaceous with the deposition of continental to shallow marine carbonate rich sandstones. This sequence reveals a very uniform distribution in the entire western Baltic Sea, indicating a tectonically quiet depositional environment.

The sea level kept rising throughout the Late Cretaceous followed by the deposition of shallow marine deep-sea chalk sediments gradually. This occurred in a period of tectonic quiescence, seen on the general uniform distribution with a slight thickening gradient towards the centre of the Northeast German Basin. Only little faulting and minor salt movement around the Fehmarn Pillow are observed in the study area. The net amount of tectonic subsidence throughout the Cretaceous reveals a uniform distribution with values around 100 m in most parts of the modelled area, but in contrast to the previous described periods an increasing amount of subsidence is observed in the northeasterly direction. The reason for this was a change in the regional stress between the Early Jurassic and the Cretaceous, which is also characterized on the gradual thickening of the Upper Cretaceous chinks in the northeasterly direction in the Bay of Mecklenburg away from the Permo-Triassic Northeast German Basin. The internal reflections in the Upper Cretaceous succession reveals that the Grimmen High experienced less subsidence than the surrounding areas, similar to the case during the Late Triassic. Several compressional pulses from the Alpine Orogeny affected the region around the Cretaceous/Cenozoic transition. This caused the intense inversion observed around the Grimmen High, where in some parts Quaternary deposits overlie Lower Jurassic sediments. The central part of the Grimmen High experienced around 500 m uplift as a result of this inversion. In the entire western Baltic Sea, the Top Cretaceous surface is an unconformity, but since it is non-angular in nature, it could only be determined from log information from the surrounding wells.

The overall change in the regional stress field from extensional to compressional between the Cretaceous and the Cenozoic reactivated the vertical salt movement in the area. This is revealed on the pronounced thickness variations between the crest of salt pillows and the rimsynclines in the entire Bay of Kiel and the southwestern part of the Bay of Mecklenburg. On top of three salt structures Cenozoic deposits are absent. The primary indicators for that this renewed halokinesis was triggered by the onset of the Alpine Orogeny are firstly, the long-axis orientation of salt rimsynclines perpendicular to the main compressional stress direction from the S-SSW and secondly, the N-NNE trending thin-skinned crestal graben above two of the salt structures in the Bay of Kiel. Cenozoic deposits are in the Bay of Mecklenburg limited to the southwestern part. The lack of Cenozoic sediments in the northeastern part of the Bay of Mecklenburg can be explained from the calculated vertical tectonic movement map for the Cenozoic. This map reveals that the northeastern part of the modelling area experienced uplift throughout the Cenozoic, which is also observed on the different seismic sections from this region, where Cretaceous sediments truncates the Quaternary deposits or the sea floor. In the southwesterly direction an increasing net amount of tectonic subsidence is calculated with values up to 500 m in the Glückstadt Graben area. In general, it can be concluded that the structural framework and depositional evolution of the northern part of Northeast German Basin were controlled by four major regional tectonic events. Decaying stress due to thermal relaxation after the Rotliegend volcanism superposed by extensional stresses related to the beginning break-up of Pangea during the Triassic – Early Jurassic. The mid North Sea thermal updoming event in Middle Jurassic times. The reorganisation of the regional stress field at the Jurassic/Cretaceous transition, as a result of the opening of the Alpine Tethys Ocean and the North Atlantic. And finally the compressional stresses from the Alpine Orogeny during the Late Cretaceous – Early Cenozoic. It cannot be excluded that other tectonic events on a local scale also influenced the geodynamic evolution of the study area, but they were presumably overprinted by these larger region events.

A neotectonic forward modelling reveals where a future coastline would be running when the present day tectonic stress regime is in equilibrium. It shows a WNW-ESE running trend, subdividing the modelling region into two equally sized areas of land and sea. The overall trend suggests that the compressional stresses related to the Alpine collision are the prime factor for the present day landscape evolution.

In general, this project has provided a better insight into the Mesozoic – Cenozoic structural framework and depositional evolution of the northern part of the Northeast German Basin, which were major milestones for the NeoBaltic project. This was done by creating several geological time-structure and time-isochores maps and from the 3D structural modelling and backstripping. Another milestone for this project was the determination of the neotectonic movement in the region around the western Baltic Sea. The initial idea to trace fault lineaments to the sea floor on the different seismic sections was applied to the thin-skinned crustal graben structure in the Bay of Kiel sub-area, but the analysis revealed that the resolution of the data used were not sufficient enough for this kind of lineament tracing. Instead the neotectonic forward modelling numerically confirmed the work done by other authors.

Following this approach, the data pool, which already is unique in size for academic institutions, should be extended eastward in order to perform a detailed analysis of the structural lineaments in the transition zone towards the Baltic Shield. Furthermore, the existing data also provide an opportunity to complete detailed studies on internal structures, especially in the Upper Cretaceous and Cenozoic strata, to elucidate different depositional environments.

Beside this dissertation, the NeoBaltic project has also been the basis for four master's theses, two completed and one ongoing, at the Department of Earth Sciences, University of Aarhus by Arne Lauridsen, Sheila Piñeiro Triñanes and Anne Camilla Stavnsgaard Nielsen and one completed at the Institute of Geophysics, University of Hamburg by Benjamin Hell.



## References

- BABEL Working Group, 1991.** Deep seismic survey images the structure of the Tornquist Zone beneath the Southern Baltic Sea. *Geophysical Research Letters*, 18, 1091-1094.
- BABEL Working Group, 1993.** Deep seismic reflection/refraction interpretation of crustal structure along BABEL profiles A and B in the southern Baltic Sea. *Geophysical Journal International*, 122, 325-343.
- Bayer, U., Ondrak, R., Wenderoth, F., 1996.** Ansätze zur integrierten Modellierung geothermischer Prozesse. *Mitteilungen der DGG Sonderband II/1996*, 106-109.
- Bayer, U., Scheck, M., Koehler, M., 1997.** Modelling of the 3D thermal field in the northeast German basin. *Geologische Rundschau*, 86, 241-251.
- Bayer, U., Scheck, M., Rabbel, W., Krawczyk, C. M., Götze, H. J., Stiller, M., Beilecke, T., Marotta, A. M., Barrio-Alvers, L., Kuder, J., 1999.** An intergrated study of the NE-German Basin. *Tectonophysics*, 314, 285-307.
- Baldschuhn, R., Binot, F., Fleig, S., Kockel, F., 2001.** Tectonic Atlas of Northwest Germany and the German North Sea Sector. *Geologisches Jahrbuch, Reihe A*, 153, 3-95.
- Benek, R., Kramer, W., McCann, T., Scheck, M., Negendank, J. F. W., Korich, D., Huebscher, H.-D., Bayer, U., 1996.** Permo-Carboniferous magmatism of the Northeast German Basin. *Tectonophysics*, 266, 379-404.
- Britze, P., 1989.** Geological evolution and hydrocarbon potential of the Lolland-Falster area. Unpublished master thesis, University of Copenhagen, 113pp.
- Cartwright, J., 1990.** The structural evolution of the Ringkøbing-Fyn High. In: Blundell, D.J., Gibbs, A.D., *Tectonic evolution of the north sea rifts* (p. 200-216). Oxford: Clarendon Press.

- Clausen, O. R., Pedersen, P. K., 1999.** The Triassic structural evolution of the southern margin of the Ringkøbing-Fyn High, Denmark. *Marine and Petroleum Geology*, 16, 653-665.
- Davison, I., Alsop, G. I., Blundell, D. J., 1995.** Salt tectonics: some aspects of deformation mechanics. In: Alsop, G. I., Blundell, D. J., Davison, I. (Eds). *Salt Tectonics*. Geological Society Special Publication, 100, 1-10.
- DEKORP-BASIN Research Group, 1999.** Deep crustal structure of the Northeast German basin: New DEKORP-BASIN '96 deep-profiling results. *Geology*, 27(1), 55-58.
- Einsele, G., 2000.** *Sedimentary Basins*, 2<sup>nd</sup> edn. Springer Verlag, 792pp.
- EUGENO-S Working Group, 1998.** Crustal structure and tectonic evolution of the transition between the Baltic Shield and the North German Caledonides (the Eugeno-S project). *Tectonophysics*, 150, 253-348.
- Fisher, M. J., Mudge, D. C., 1998.** Triassic. In: Glennie, K. W. (Eds), *Petroleum Geology of the North Sea: Basic Concepts and Recent Advances*, 4<sup>th</sup> edn. Blackwell Science, 656pp.
- Gearhart Geo Consultants, 1985.** Kegnæs-1 well report. Danmark Geologiske Undersøgelser, Denmark, Report file no. 9688
- Gemmer, L., Huuse, M., Clausen, O. R., and Nielsen, S. B., 2002a.** Mid-Paleocene paleogeography of the eastern North Sea basin: integrated geological evidence and 3-D dynamic modelling. *Basin Research*, 14, 329-346.
- Gemmer, L., Nielsen, S.B., L., Huuse, M. and Lykke-Andersen, H., 2002b.** Post-mid-Cretaceous eastern North sea evolution inferred from 3D thermo-mechanical modelling. *Tectonophysics*, 350, 315-342.
- Gemmer, L., Nielsen, S. B., Bayer, U., 2003.** Late Cretaceous - Cenozoic evolution of the North German Basin – results from 3-D geodynamic modelling. *Tectonophysics*, 373, 39-54.

- Grad, M., Janik, T., Yliniemi, J., Guterch, A., Luosto, U., Tiira, T., Komminaho, K., Środa, P., Höing, K., Makris, J., Lund, C. E., 1999.** Crustal structure of the Mid-Polish Trough beneath the Teisseyre-Tornquist Zone seismic profile. *Tectonophysics*, 314, 145-160.
- Gregersen, S., Voss, P., TOR Working Group, 2002.** Summary of project TOR: delineation of a stepwise, sharp, deep lithosphere transition across Germany – Denmark – Sweden. *Tectonophysics*, 360, 61-73.
- Guterch, A., Grad, M., Thybo, H., Keller, G. R., POLONAISE Working Group, 1999.** POLONAISE '97 – an international seismic experiment between Precambrian and Variscan Europe in Poland. *Tectonophysics*, 314, 101-121.
- Hansen, M. B., Lykke-Andersen, H., Dehghani, A., Gajewski, D., Hübscher, C., Olesen, M., Reicherter, K., 2005.** The Mesozoic–Cenozoic structural framework of the Bay of Kiel area, western Baltic Sea. *International Journal of Earth Sciences*, 94, 1070-1082.
- Hansen, M. B., Piñeiro Triñanes, S., Dehghanin, A., Lykke-Andersen, H., Hübscher, C., Gajewski, D., 2006.** Structure and evolution of the northern part of the Northeast German Basin. Submitted to *Marine and Petroleum Geology*.
- Hoth, K., Rusbülu, J., Zagora, K., Beer, H., Hartmann, O., 1993.** Die tiefen Bohrungen im Zentralabschnitt der Mittel-europäischen Senke – Dokumentation für den Zeitabschnitt 1962-1990. *Geowissenschaften*, 2, 145 pp.
- Hübscher, C., Lykke-Andersen, H., Hansen, M.B., Reicherter, K., 2004.** Investigating the Structural Evolution of the Western Baltic, *EOS*, 85(12), 115.
- Jaritz, W., 1987.** The origin and development of salt structures in northwest Germany. In: Lerche, I., O'Brian, J.J. (Eds.), *Dynamical Geology of Salt and Related Structures*. Academic Press, Orlando, FL, 479-493.
- Institute of Geophysics and Planetary Physics, U. C., 2003.** Global seafloor topography from satellite altimetry and ship depth soundings.

- Kaiser, A., Reicherter, K., Hübscher, C., Gajewski, D., 2005.** Variation of the present-day stress field within the North German Basin – insights from thin shell FE modeling based on residual GPS velocities. *Tectonophysics*, 397, 55-72.
- Kaiser, A., 2005.** Neotectonic modelling of the North German Basin and adjacent areas – a tool to understand postglacial landscape evolution? *Zeitschrift der Deutschen Gesellschaft für Geowissenschaften*, 156(2), 357-366.
- Kossow, D., Krawczyk, C., McCann, T., Strecker, M., Negendank, J. F. W., 2000.** Style and evolution of salt pillows and related structures in the northern part of the Northeast German Basin. *International Journal of Earth Sciences*, 89, 652-664.
- Kossow, D., Krawczyk, C. M., 2002.** Structure and quantification of processes controlling the evolution of the inverted NE-German Basin. *Marine and Petroleum Geology*, 19, 601-618.
- Koyi, H., Talbot, C. J., Tørudbakken, B. O. 1993.** Salt diapirs of the southwest Nordkapp Basin: analogue modelling. *Tectonophysics*, 228, 167-187.
- Krauss, M., 1994.** The tectonic structure below the southern Baltic Sea and its evolution. *Zeitschrift für Geologische Wissenschaften*, 22, 19-32.
- Krawczyk, C. M., Stiller, M., DEKORP-BASIN Research Group, 1999.** Reflection seismic constraints on Paleozoic crustal structure and Moho beneath the NE German Basin. *Tectonophysics*, 314, 241-253.
- Krawczyk, C. M., Eilts, F., Lassen, A., Thybo, H., 2002.** Seismic evidence of Caledonian deformed crust and uppermost mantle structures in the northern part of the Trans-European Suture Zone, SW Baltic Sea. *Tectonophysics*, 360, 215-244.
- Lamarche, J., Scheck, M., Lewerenz, B., 2003.** Heterogeneous tectonic inversion of the Mid-Polish Trough related to crustal architecture, sedimentary patterns and structural inheritance. *Tectonophysics*, 373, 75-92.
- Lamarche, J., Scheck-Wenderoth, M., 2005.** 3D structural model of the Polish Basin. *Tectonophysics*, 397, 73-91.

- Lassen, A., Thybo, H., Berthelsen, A., 2001.** Reflection seismic evidence for Caledonian deformed sediments above Sveconorwegian basement in the southwestern Baltic Sea. *Tectonics*, 20(2), 268-276.
- Lehné, R., Sirocko, F., 2005.** Quantification of recent movement potentials in Schleswig-Holstein (Germany) by GIS-based calculation of correlation coefficients. *International Journal of Earth Sciences*, 94, 1094-1102.
- Lewerenz, B., 1996.** Basin modeling, an integrated approach. In: Vereinigung, G. (Eds). *Tagung der Geologischen Vereinigung. Terra Nostra*, Amsterdam, The Netherlands, p. 19.
- Littke, R., Bayer, U., Gajewski, D., 2005.** Dynamics of sedimentary basins: the example of the Central European Basin system. *International Journal of Earth Sciences*, 94, 779-781.
- Marotta, A. M., Bayer, U., Thybo, H., 2000.** The legacy of the NE German Basin – reactivation by compressional buckling. *Terra Nova*, 12(3), 132-140.
- Marotta, A. M., Bayer, U., Scheck, M., Thybo, H., 2001.** The stress field below the NE German Basin: effects induced by the Alpine collision. *Geophysical Journal International*, 144, F8-F12.
- Marotta, A. M., Bayer, U., Thybo, H., Scheck, M., 2002.** Origin of the regional stress in the North German basin: results from numerical modelling. *Tectonophysics*, 360, 245-264.
- Marotta, A. M., Sabadini, R., 2003.** Numerical models of tectonic deformation at the Baltica-Avalonia transition zone during the Paleocene phase of inversion. *Tectonophysics*, 373, 25-37.
- Maystrenko, Y., Bayer, U., Scheck-Wenderoth, M., 2005a.** The Glueckstadt Graben, a sedimentary record between the North and Baltic Sea in north Central Europe. *Tectonophysics*, 397, 113-126.
- Maystrenko, Y., Bayer, U., Scheck-Wenderoth, M., 2005b.** Structure and evolution of the Glueckstadt Graben due to salt movements. *International Journal of Earth Sciences*, 94, 799-814.

- Meissner, R., Krawczyk, C. M., 1999.** Caledonian and Proterozoic terrane accretion in the southwest Baltic Sea. *Tectonophysics*, 314, 255-267.
- Nalpas, T., Brun, J. P., 1993.** Salt flow and diapirism related to extension at crustal scale. *Tectonophysics*, 228, 349-362.
- Nielsen, L. H., Japsen, P., 1991.** Deep wells in Denmark 1935-1990 – lithostratigraphic subdivision. *Danmarks Geologiske Undersøgelser, Denmark*, 223pp.
- Nielsen, A., 1998.** Femer Bælt – geologien under en fast forbindelse, *Geologisk Nyt Danmark*, 6,
- Nöldeke, W., Schwab, G., 1976.** Zur tektonischen entwicklung des tafeldeckgebirges der Norddeutsch-Polnischen Senke unter besonderer berücksichtigung des nordteil der DDR. *Zeitschrift für Angewandte Geologie*, 23, 369-379.
- Plomerová, J., Babuška, V., Vecsey, L., Kouba, D., TOR Working Group, 2002.** Seismic anisotropy of the lithosphere around the Trans-European Suture Zone (TESZ) based on teleseismic body-wave data of the the TOR experiment. *Tectonophysics*, 360, 89-114.
- Podlachikov, Y., Talbot, C., Poliakov, A. N. B., 1993.** Numerical models of complex diapirs. *Tectonophysics*, 228, 189-198.
- Poliakov, A. N. B., Podlachikov, Y., Talbot, C., 1993.** Initiation of salt diapirs with frictional overburdens: numerical experiments. *Tectonophysics*, 228, 199-210.
- Poprawa, P., Šliaupa, S., Stephenson, R., Lazauskienė, J., 1999.** Late Vendian-Early Palæozoic tectonic evolution of the Baltic Basin: regional tectonic implications from subsidence analysis. *Tectonophysics*, 314, 219-239.
- Reicherter, K., Kaiser, A., Stackebrandt, W., 2005.** The post-glacial landscape evolution of the North German Basin: morphology, neotectonics and crustal deformation. *International Journal of Earth Sciences*, 94, 1083-1093.

- Rempel, H., 1992.** Erdölgeologische Bewertung der Arbeiten der Gemeinsamen Organisation "Petrobaltic" im deutschen Schelfbereich. Geologisches Jahrbuch, Reihe D, Heft 99, BGR Hannover, 34 pp.
- Scheck, M., Bayer, U., Lewerenz, B., 1996.** Lithosphere Structure Underneath the Northeast German Basin: Constraints by Gravity Modeling. *Physics and Chemistry of the Earth*, 21(4), 313-318.
- Scheck, M., 1997a.** 3D structural modeling and evolution of the Northeast German Basin. *Terre Nova* 9, 185.
- Scheck, M., 1997b.** Dreidimensionale Strukturmodellierung des Nordost-deutschen Beckens unter Einbeziehung von Krustenmodellen. Unpublished Ph.D. Thesis, Freie Universität Berlin, 126pp.
- Scheck, M., Barrio-Alvers, L., Bayer, U., Götze, H.-J., 1999.** Density Structure of the Northeast German Basin: 3D Modeling along the DEKORP Line BASIN96. *Physics and Chemistry of the Earth*, 24(3), 221-230.
- Scheck, M., Bayer, U., 1999.** Evolution of the Northeast German Basin – inferences from a 3D structural model and subsidence analysis. *Tectonophysics*, 313, 145-169.
- Scheck, M., Bayer, U., Otto, V., Lamarche, J., Banka, D., Pharaoh, T., 2002.** The Elbe Fault System in North Central Europe – a basement controlled zone of crustal weakness. *Tectonophysics*, 360, 281-299.
- Scheck, M., Bayer, U., Lewerenz, B., 2003a.** Salt movements in the Northeast German Basin and its relation to major post-Permian tectonic phases – results from 3D structural modelling, backstripping and reflection seismic data. *Tectonophysics*, 361, 277-299.
- Scheck, M., Bayer, U., Lewerenz, B., 2003b.** Salt redistribution during extension and inversion inferred from 3D backstripping. *Tectonophysics*, 373, 55-73.
- Scheck-Wenderoth, M., Lamarche, J., 2005.** Crustal memory and basin evolution in the Central European Basin System – new insights from a 3D structural model. *Tectonophysics*, 397, 143-165.

- Schultz-Ela, D. D., Jackson, M. P. A., Vendeville, B., 1993.** Mechanics of active salt diapirism. *Tectonophysics* 288, 275-312.
- Smith, W. H. F., Sandwell, D. T., 1997.** Global seafloor topography from satellite altimetry and ship depth soundings. *Science*, 277, 1957-1962.
- Stackebrandt, W., 2004.** Zur Neotektonik in Norddeutschland. *Zeitschrift für Geologische Wissenschaften* 32 (2-4), 85-95.
- Taylor, J. C. M., 1998.** Upper Permian – Zechstein. In: Glennie, K. W. (Eds), *Petroleum Geology of the North Sea: Basic Concepts and Recent Advances*, 4<sup>th</sup> edn. Blackwell Science, 656pp.
- Tucker, M. E., 1991.** *Sedimentary Petrology*, 2<sup>nd</sup> edn. Blackwell Science, 272pp.
- Underhill, J. R., 1998.** Jurassic. In: Glennie, K. W. (Eds), *Petroleum Geology of the North Sea: Basic Concepts and Recent Advances*, 4<sup>th</sup> edn. Blackwell Science, 656pp.
- van Keken, P. E., Spiers, C. J., van den Berg, A. P., Muyzert, E. J., 1993.** The effective viscosity of rocksalt: implementation of steady-state creep laws in numerical models of salt diapirism. *Tectonophysics*, 225, 457-476.
- van Wees, J. D., Stephenson, R. A., Ziegler, P. A., Bayer, U., McCann, T., Dadlez, R., Gaupp, R., Narkiewicz, M., Bitzer, F., Scheck, M., 2000.** On the origin of the Southern Permian Basin, Central Europe. *Marine and Petroleum Geology*, 17, 43-59.
- Vejbæk, O. V., Britze, P., 1994.** Top pre-Zechstein; sub- and supercrop map. DGU Map Series no. 45. Danmarks Geologiske Undersøgelser, Copenhagen.
- Vejbæk, O. V., 1997.** Dybe strukturer i danske sedimentære bassiner. *Dansk Geologisk Forenings Nyheds- og Informationskrift*, 4, 1-31.
- Vendeville, B. C., Jackson, M. P. A., 1992.** The rise of diapirs during thin-skinned extension. *Marine and Petroleum Geology*, 9, 331-353.

- Vendeville, B. C., Hongxing, G., Jackson, M. P. A., 1995.** Scale models of salt tectonics during basement-involved extension. *Petroleum Geoscience*, 1, 179-183.
- Warren, J., 1999.** *Evaporites: Their evolution and economics*. Blackwell Science, 448pp.
- Ziegler, P., 1990.** *Geological atlas of western and central Europe*, 2<sup>nd</sup> edn. Shell International Petroleum Mij Bv (dist by Geol Soc Publ House), 239pp.
- Zirngast, M., 1996.** The development of the Gorleben salt dome (northwest Germany) based on quantitative analysis of peripheral sinks. In: Alsop, G. I., Blundell, D. J., Davison, I. (Eds). *Salt Tectonics*. Geological Society Special Publication, 100, 203-226.



## Acknowledgements

I would like to thank Prof. Dr. Dirk Gajewski and my main supervisor Dr. Christian Hübscher for giving me the opportunity to do this dissertation, for their support and confidence in my work.

Furthermore, I would like to thank Holger Lykke-Andersen and Egon Nørmark for allowing me to do the processing of the raw data at the SeisLab Aarhus and their support during my two stays up there.

I would also like to thank my good friend Magdalena Scheck-Wenderoth for giving me the opportunity to do the 3D modelling and 3D backstripping at the GeoForschungsZentrum in Potsdam. The scientific outcome of my stay in Potsdam would not have been the same without the help from Björn Lewerenz and Yuriy Maystrenko.

I want to express my gratefulness to all the people at the Institute of Geophysics of the University of Hamburg for providing a pleasant working atmosphere. A special thank goes to Gesa Netzeband, Stefan Dümmling, Tina Kaschwich, Kristina Mayer, Klaus Reicherter and Malte Vöge for the daily coffee breaks and good laughs. Many thanks to Christel Mynarik for helping me with the official paper work regarding my three-year stay in Germany and endless stationery supply.

A special thank to Kathryn Brookes for her tireless assistance with the English language and valuable discussions and suggestions.

I want to thank my family for their support through all my years of studying, both in Århus and Hamburg.

Finally, a special thank goes to all those who made my stay in Hamburg a pleasant and rewarding one: Kristian “oldscholl” Larsen, Kirsten Hjorth, Jacob Hasberg, Bjarke Lund, Bella Nielsen, Ole Gabs, Sisse Frandsen and last but not least my wife Inge-Marie Stensen Hansen.